

1 Comparative genomic analysis of 31 *Phytophthora* genomes reveal genome plasticity and horizontal
2 gene transfer

3

4 Brent A. Kronmiller^{a,b}, Nicolas Feau^c, Danyu Shen^d, Javier F. Tabima^e, Shahin S. Alif, Andrew D.
5 Armitage^g, Felipe Arredondo^{a,b}, Bryan A. Bailey^f, Stephanie R. Bollmann^h, Angela Dale^{c, i}, Richard J.
6 Harrison^j, Kelly Hrywkiw^c, Takao Kasuga^k, Rebecca McDougal^l, Charlotte F. Nellist^l, Preeti Panda^m,
7 Sucheta Tripathyⁿ, Nari M. Williams^{l, o}, Wenwu Ye^d, Yuanchao Wang^d, Richard C. Hamelin^{c,p,q}, Niklaus J.
8 Grunwald^r

9

10 ^aCenter for Quantitative Life Sciences, Oregon State University, Corvallis, OR, USA

11 ^bDepartment of Botany and Plant Pathology, Oregon State University, Corvallis, OR, USA

12 ^cDepartment of Forest and Conservation Sciences, The University of British Columbia, Vancouver, British
13 Columbia, Canada

14 ^dDepartment of Plant Pathology, Nanjing Agricultural University, Nanjing, Jiangsu, China

15 ^eDepartment of Biology, Clark University, Worcester, MA, USA

16 ^fSustainable Perennial Crops Laboratory, Northeast Area, USDA/ARS, Beltsville Agricultural Research
17 Center-West, Beltsville, MD, USA

18 ^gNatural Resources Institute, University of Greenwich, Chatham Maritime, Kent, UK

19 ^hDepartment of Integrative Biology, Oregon State University, Corvallis, USA

20 ⁱSC-New Construction Materials, FPInnovations, Vancouver, BC, V6T 1Z4, Canada

21 ^jNIAB EMR, East Malling, United Kingdom.

22 ^kCrops Pathology and Genetics Research Unit, Agricultural Research Service, Davis, United States
23 Department of Agriculture, CA, USA

24 ^lScion (Zealand Forest Research Institute), 49 Sala Street, Te Papa Tipu Innovation Park, Private Bag
25 3020, Rotorua, New Zealand

26 ^mThe New Zealand Institute for Plant and Food Research Ltd, 74 Gerald Street, Lincoln, 7608, New
27 Zealand

28 ⁿCSIR Indian Institute of Chemical Biology, Kolkata, India

29 ^oDepartment of Pathogen Ecology and Control, Plant and Food Research, Private Bag 1401, Havelock
30 North, New Zealand

31 ^pInstitut de Biologie Intégrative et des Systèmes (IBIS), Université Laval, Québec, Canada

32 ^qDépartement des sciences du bois et de la forêt, Faculté de Foresterie et Géographie, Université Laval,
33 Québec, Canada

34 ^rHorticultural Crop Research Unit, United States Department of Agriculture, Agricultural Research
35 Service, Corvallis, Oregon, USA

36

37 Running Head: Comparative genomic analysis of 31 *Phytophthora* genomes

38

39 Address correspondence to Brent Kronmiller, brent.kronmiller@oregonstate.edu

40 Nicolas Feau, Danyu Shen, Javier F. Tabima contributed equally to this work. Author order is
41 alphabetical.

42

43

44 **Abstract**

45 *Phytophthora* species are oomycete plant pathogens that cause great economic and ecological impacts.

46 The *Phytophthora* genus includes over 180 known species, infecting a wide range of plant hosts including

47 crops, trees, and ornamentals. We sequenced 31 individual *Phytophthora* species genomes and 24

48 individual transcriptomes to study genetic relationships across the genus. *De novo* genome assemblies

49 revealed variation in genome sizes, numbers of predicted genes, and in repetitive element content across

50 the *Phytophthora* genus. A genus-wide comparison evaluated orthologous groups of genes. Predicted

51 effector gene counts varied across *Phytophthora* species by effector family, genome size, as well as plant

52 host range. Predicted numbers of apoplastic effectors increased as the host range of *Phytophthora* species

53 increased. Predicted numbers of cytoplasmic effectors also increased with host range but leveled off or
54 decreased in *Phytophthora* species that have enormous host ranges. With extensive sequencing across
55 the *Phytophthora* genus we now have the genomic resources to evaluate horizontal gene transfer events
56 across the oomycetes. Using a machine learning approach to identify horizontally transferred genes with
57 bacterial or fungal origin we identified 44 candidates over 36 *Phytophthora* species genomes. Phylogenetic
58 reconstruction indicates that the transfers of most of these 44 candidates happened in parallel to major
59 advances in the evolution of the oomycetes and *Phytophthoras*. We conclude that the 31 genomes
60 presented here are essential for investigating genus-wide genomic associations in *Phytophthora*.

61 **Introduction**

62 Members of the *Phytophthora* genus are oomycete plant pathogens that collectively infect a wide range of
63 plants (1, 2) and cause great economic, environmental, and societal impact (3). Oomycetes are
64 morphologically similar to filamentous fungi (4–7) but are classified as stramenopiles, a group that also
65 includes diatoms and brown algae (4, 8). Oomycetes include many plant pathogenic species besides
66 *Phytophthora* including numerous *Pythium* species that cause seed, seedling, root and fruit rots and a
67 broad diversity of obligate biotrophs that cause downy mildew.

68 *Phytophthora* species infect numerous plants including crops, trees, and ornamentals in managed and
69 natural ecosystems. The agent responsible for potato blight, *Phytophthora infestans* triggered the 1840s
70 potato famine (9, 10), and *Phytophthora ramorum* is responsible for sudden oak death in North America
71 and sudden larch death in the UK, which have destroyed millions of trees, in addition to infecting hundreds
72 of additional tree and ornamental species (11–14). Some *Phytophthora* species are relatively host-specific,
73 such as the soybean pathogen *Phytophthora sojae* (15), the strawberry pathogen *Phytophthora fragariae*
74 (16), and the lychee pathogen *Phytophthora litchi* (17). In contrast, others including *Phytophthora*
75 *cinnamomi* (18), *Phytophthora palmivora* (1), and *Phytophthora parasitica* (1), can infect a vast assortment
76 of plant hosts. The mechanistic basis of this large variation in apparent host specificity is currently unknown
77 (10, 19).

78 There are over 180 known *Phytophthora* species (20, 21) phylogenetically falling into 12 or more clades
79 (21–23) and further divided into numerous sub-clades (20). Previous genome sequencing studies have

80 examined species within the *Phytophthora* genus (9, 19, 20, 22, 24–28) with *P. sojae* and *P. ramorum* (29),
81 *P. infestans* (10, 30), and *Phytophthora capsici* (31) serving as key models for the genus. Overall, these
82 studies revealed highly dynamic genomes containing both rapidly evolving and conserved regions.

83 *Phytophthora* species infect plant hosts through the use of two broad classes of secreted effector proteins
84 (5, 32–35). Apoplastic effectors act outside the plant cells and include glycoside hydrolases, necrosis
85 inducing proteins (NLPs) (36), proteases, lipases, lipid-binding proteins, and protease inhibitors (37). Roles
86 of apoplastic effectors include weakening of plant physical and chemical defenses, and a source of nutrition
87 early in infection. In contrast, cytoplasmic effectors enter plant cells, often through the differentiation of
88 specialized structures called haustoria, and include RxLR effectors (29, 38, 39), crinkler effectors (CRN)
89 (40–44) and non-conventionally secreted effectors (45). In oomycetes, as well as other pathogens,
90 cytoplasmic effectors manipulate numerous aspects of host physiology and morphology to promote
91 susceptibility, including suppression of host immunity and programmed cell death (46, 47), and stimulating
92 and inhibiting the release of nutrients (5, 48–51). The genomes of oomycete pathogens sequenced to date
93 include large rapidly evolving gene families encoding these effectors (10, 29, 31). Many of these effector
94 genes, especially those encoding RxLR effectors, display evidence of accelerated evolution due to host-
95 pathogen co-evolutionary conflict (38, 52, 53).

96 Examination of previously sequenced genomes has identified two distinct partitions namely gene-dense,
97 repeat-poor regions and gene-sparse, repeat-rich regions (10, 29–31). Highly conserved housekeeping
98 genes are typically found in gene-dense regions, while rapidly evolving gene families associated with
99 infection are typically found in gene-sparse regions that are transposon-rich (10, 29–31, 54). This
100 arrangement has been labeled “the two-speed genome” (19, 24). It has been hypothesized that transposons
101 in the gene-sparse, transposon-rich regions may contribute to the genomic diversity and possibly to
102 epigenetic variability of expression of genes in those regions including infection-associated genes (55).

103 To investigate phylogenetic relationships, horizontal gene transfer (HGT), effector genomics, and possible
104 mechanisms underlying host ranges across members of the genus *Phytophthora*, we sequenced 31
105 genomes using Illumina short read technology. Our newly sequenced genomes include most species in
106 clade 7 as well as representative species from nine of the phylogenetic clades (56). Several genomes have

107 already been published individually as a result of this project: *P. litchii* (25), *Phytophthora megakarya* and
108 *Phytophthora palmivora* (26), *Phytophthora fragariae* and *Phytophthora rubi* (27), and *Phytophthora*
109 *cactorum* (28, 57). Here we present a combined analysis of the genome sequences of 37 *Phytophthora*
110 species, including the 31 newly sequenced species by our sequencing consortium, resulting in the first
111 large scale comparative genomic study including species from nine *Phytophthora* clades. This work
112 provides insights into genome architecture and evolution in the genus *Phytophthora* as well as novel
113 genomic resources of broad interest.

114 RESULTS

115 Sequencing and assembly of the 31 *Phytophthora* genomes

116 The 31 *Phytophthora* genomes sequenced by our consortium produced between 16.6M and 44.7M raw
117 reads per genome (Table 1 and Table S1). The sizes of the *Phytophthora* genome assemblies varied
118 greatly, ranging from 37.3 to 107.8 Mb (mean 61.3 ±17.6Mb). Due to variations in the numbers of reads
119 per genome and differences in genome sizes, the quality of assembled genomes varied as well. The
120 number of contigs per assembly ranged from 2,131 to 28,263 (mean 11380 ±7919.2). The more completely
121 assembled genomes benefited from deeper coverage. For example, the *Phytophthora boehmeriae*
122 assembly was composed of 2,866 contigs with an N₅₀ of 41,917 bp; this assembly benefitted from 87X
123 coverage as a result of receiving 34.7M reads to cover a 39.7 Mb assembly. In contrast, the *Phytophthora*
124 *lateralis* assembly had only 45X coverage (23.2M reads across a 50.5 Mb assembly size), resulting in
125 28,263 contigs and an N₅₀ of 2,396 bp (Table 1). Sequence read length did not seem to make a difference
126 in assembly quality. Two genomes (*P. cactorum* and *P. idaei*) with 250 bp reads (compared to most
127 assemblies with 50 bp reads) had an N₅₀ and number of contigs that were not better than the other genomes
128 when compared to genome size (*P. cactorum*: contigs 7,888, N₅₀ 15,053 size 56 Mb; *P. idaei*: contigs 7,163,
129 N₅₀ 14,461, size 53.5 Mb) (Table 1).

130 To aid with gene calling, and identify active genes, RNA sequencing was conducted for 25 *Phytophthora*
131 species on V8-grown mycelia and either germinated cysts or Plich-grown mycelia for those species that did
132 not readily yield zoospores (58). RNA sequencing produced 12.5M to 36.0M paired-end sequence reads
133 per sample, with resulting transcriptome assemblies averaging 36,189 contigs per assembly with an

134 average N_{50} of 1,822 bp. Most species' transcriptome assemblies had between 20K and 40K contigs, with
135 the exception of *Phytophthora parvispora* that produced more than 109K contigs. TransDecoder, which
136 reduces duplication in *de novo* transcriptome assemblies by identifying candidate coding regions and
137 removing duplicates, was run on the Trinity assemblies and lowered average transcriptome assembly to
138 33,200 contigs and raised average N_{50} to 2,753bp. Transcriptome size differences between species are
139 not correlated with genome size differences with the two largest genome assemblies (*P. megakarya* and
140 *P. palmivora*) both resulting in mid-range transcriptome assembly sizes (Table S1).

141 ***De novo* repeat identification and analysis**

142 Repeats were identified, classified, and masked to prepare genomes for gene prediction. *De novo* repeat
143 prediction identified between 27 and 295 different repeat sub-families per species. The percentage repeat
144 content of the assemblies varied greatly across the *Phytophthora* genomes sequenced. The genome
145 assemblies of *Phytophthora kernoviae*, *P. litchii*, and *Phytophthora agathidicida* contained very low repeat
146 content of 4.15%, 5.76%, and 5.98%, respectively (Fig. 1). On the other end, several genome assemblies
147 had high repeat content: *P. megakarya*, *Phytophthora hibernalis*, and *Phytophthora pinifolia* contained
148 32.94%, 32.46, and 33.00%, respectively.

149 Repeat annotations were classified into types (Class I Retrotransposons, Class II DNA transposons, and
150 other), families, and sub-families, (Fig. 1). Fifteen different DNA transposons were identified across all 31
151 species. Long terminal repeat (LTR) retrotransposons were more diverse across *Phytophthora* species.
152 As many as 57 Copia LTR retrotransposons and 144 Gypsy LTR retrotransposon types were found in each
153 genome assembly.

154 ***Phytophthora* gene prediction and annotation**

155 Gene predictions ranged from 12,391 to 37,283 (mean 19,943, $\pm 5,864$) across the newly sequenced
156 genomes. These gene counts per species are within the general range of previously published
157 *Phytophthora* genomes (*P. sojae*, *P. ramorum*, *P. infestans*, *P. capsici*, *P. cinnamomi*, and *P. parasitica*)
158 ranging from 16,066 to 26,584 genes per species, considering that we observed higher gene counts in
159 genomes with genome duplications (*P. palmivora* and *P. megakarya* (26)).

160 Some of the previously published *Phytophthora* genome sequences were annotated with the MAKER gene
161 prediction process outlined here to validate the methods. The *P. capsici* genome was reported to contain
162 19,805 predicted genes (31), while we obtained 18,917 predicted genes. The *P. sojae* genome v3.0 was
163 reported to contain 26,584 predicted genes (29), whereas we identified 21,447 MAKER-predicted genes.
164 Therefore, our MAKER pipeline may slightly undercount the gene content compared to other methods.

165 The completeness of the gene sets predicted from the genomes and transcriptomes was assessed by
166 identifying single-copy core orthologs using the BUSCO pipeline with the Alveolata_Stramenopiles
167 database (234 genes) as the reference. BUSCO analysis of the 31 genome assemblies identified 147-231
168 complete genes (mean 204 ± 27) of the 234 single copy genes in the database (Fig. 2A). Analysis of the
169 24 transcriptome assemblies identified 18 to 228 complete genes (mean 187 ± 54) (Fig. 2B). The *P.*
170 *kernoviae* and *P. lateralis* transcriptomes were outliers, with only 20 and 18 complete genes identified,
171 respectively. When *P. kernoviae* and *P. lateralis* were removed, transcriptome assemblies ranged from
172 142 to 228 complete (single and duplicated) genes (mean 203 ± 18). Results of BUSCO analyses run on
173 predicted proteins ranged from 139-222 complete (single and duplicated) genes (mean $192, \pm 25$) of the
174 234 conserved orthologous proteins in the database (Fig. 2C).

175 Predicted proteins from the MAKER gene prediction were functionally annotated by matching to published
176 *Phytophthora*, stramenopile, and fungal proteins. Across the 614,862 proteins predicted in the 31
177 *Phytophthora* species, when aligned to the NCBI and UniProt TrEMBL 294,146 *Phytophthora* proteins
178 produced alignments that passed the cutoff filter. Removing 'Uncharacterized Protein' or similarly
179 uninformative functional annotations yielded 196,652 proteins with functional classifications (mean $6,343.6$
180 $\pm 3,191.7$). When aligned to the *Phytophthora*, stramenopile, and fungal sequence databases, 445,458
181 proteins passed the alignment cutoffs, with 304,951 proteins (mean $9,837.1 \pm 2523.3$) that had informative
182 functional annotations.

183 InterProScan was used to identify domains and motifs in all predicted proteins. Of the 614,862 proteins,
184 173,727 had domains identified. GO terms were assigned from BLASTX alignments between the UniProt
185 BLASTX alignments and the InterProScan predictions, identifying 321,953 proteins with GO terms
186 assigned.

187 **Effector protein identification in *Phytophthora***

188 The cytoplasmic effector identification process predicted a total of 10,354 RxLR effector proteins and 4,415
189 CRN effector proteins from the genomes and transcriptomes of the species sequenced in this study (Fig.
190 3). The numbers of predicted RxLR effector genes differed greatly across genomes. *P. pinifolia* exhibited
191 the lowest number, with 46 predicted RxLR effectors, while *P. megakarya* exhibited the highest number,
192 with 1,183 predicted proteins. We also observed great variation in the number of predicted CRN effectors,
193 with *P. litchii* showing the lowest number of CRN effectors, 27, while *Phytophthora cajani* showed the
194 highest, 274.

195 Our search for apoplastic effectors identified 6,671 glycoside hydrolases, 1,191 NLPs, and 1,046 protease
196 inhibitors across the 31 *Phytophthora* genomes (Fig. 3). The predicted glycoside hydrolase genes range
197 from 139 (*Phytophthora brassicae*) to 386 (*P. palmivora*). The numbers of NLP genes range from 5 (*P.*
198 *pinifolia*) to 78 (*Phytophthora niederhauserii*). The counts of protease inhibitor genes range from 23
199 (*Phytophthora brassicae*) to 67 (*P. palmivora*).

200 **Orthology clustering of *Phytophthora* proteins**

201 The 715,980 predicted genes from the 31 genome assemblies along with those of *P. sojae*, *P. ramorum*,
202 *P. infestans*, *P. capsici*, *P. cinnamomi*, and *P. parasitica* were subjected to orthology analysis. In the first
203 step, the *Phytophthora* genes were matched against the pre-computed publicly available orthologous
204 groups. From this analysis, 560,201 genes were assigned to 7,829 unique clusters, leaving 155,779 genes
205 unassigned. In step two, these remaining genes were clustered using OrthoMCL yielding 13,474 additional
206 unique clusters. In total, the 715,980 genes were assigned to 21,303 orthologous clusters.

207 Orthologous groups were assigned functional annotations based on the proteins that composed the group.
208 Of the 21,303 orthologous clusters, 9,806 could be assigned informative functional annotations as defined
209 in the gene annotation section.

210 The numbers of genes present in orthologous groups encompassing all 37 *Phytophthora* species shows a
211 bimodal frequency distribution (Fig. 4), with peaks observed at 1 to 6 genes per group, and 34 to 41 genes
212 per group. We hypothesize this first peak represents rapidly evolving genes that are conserved in only a

213 few of the 37 *Phytophthora* species in this study. This first peak was much smaller when only genes with
214 meaningful annotations were considered, suggesting an enrichment for genes that have previously
215 uncharacterized functions. This peak included both small orthologous groups in which all genes were from
216 the same *Phytophthora* clade, as well as groups consisting of genes from multiple clades. The second
217 large peak was centered at 37 genes per ortholog group, thus representing ortholog groups that have one
218 gene per species. Additional groups include one or a few species missing the orthologous gene or one or
219 a few species with a second copy of an orthologous gene.

220 **Phylogenetic relationship across *Phytophthora* species**

221 We reconstructed the phylogenetic relationships of the sequenced species of the genus *Phytophthora* (Fig.
222 5) based on 61 single-copy core orthologous genes shared across 37 species. Predicted genes and amino
223 acid protein sequences used to build the phylogeny are found in Table S2. The RAxML phylogenetic tree
224 clustered these species into phylogenetic clades consistent with previous studies (20, 21, 56, 59, 60), with
225 the exception of *Phytophthora* taxon totara placed into clade 5. The separation of *P. taxon totara* from clade
226 3 containing *P. pluvialis* has been reported previously (59).

227 **Relationship of *Phytophthora* effector gene numbers to plant host range.**

228 To examine the assemblies for clues as to genomic basis for the diverse host ranges of the sequenced
229 species, *Phytophthora* species were categorized into plant host ranges as follows. Thirteen species were
230 defined as having 'Narrow', 12 as 'Multiple', six as 'Wide', and six as 'Huge' host range (Fig. 5). The
231 numbers of genes predicted to encode various families of effectors were plotted for each host range class.
232 Paralogous effectors with greater than 95% nucleotide identity over the full sequence length were counted
233 only once. Counts were plotted for each of two cytoplasmic effector categories (RxLR and CRN) and three
234 apoplastic effector categories (glycoside hydrolases, protease inhibitors, and NLPs) (Fig. 6). Subcategories
235 of the apoplastic effectors glycoside hydrolases and protease inhibitors were individually plotted (Fig. S1 A
236 and B). In each case, numbers of genes predicted to encode each effector sub-category for each species
237 were plotted against host range.

238 Apoplastic effectors show a distinct overall pattern; *Phytophthora* species with smaller host ranges had
 239 fewer predicted effector genes, with numbers of predicted effector genes increasing with increased host
 240 range (Fig. 6: A, B, C). Predicted cytoplasmic effector genes show a similar pattern, starting with low
 241 numbers of predicted genes in *Phytophthora* species with 'Narrow' host ranges and increasing in those with
 242 'Multiple' and 'Wide' host ranges. However, for both the RxLR and CRN effector categories, the numbers
 243 of predicted genes per species decreases from the 'Wide' to the 'Huge' host range species (Fig. 6: D and E).
 244 Two species were outliers with respect to the number of apoplastic NLP effector genes, *P. pistaciae* in the
 245 'Narrow' host category and *P. sojae* in the 'Multiple' host category had many more predicted apoplastic
 246 effector genes than the other species in each of their host range categories, respectively. Four species
 247 were outliers with respect to the numbers of predicted RxLR effector genes; *P. megakarya* and *P. pistaciae*
 248 in the 'Narrow' host category, *P. parvispora*, in the 'Multiple' host category, and *P. palmivora* in the 'Huge'
 249 host range category all had many more predicted RxLR genes than the other species in those categories.
 250 One outlier was observed in the CRN effector genes; *P. infestans* in the 'Wide' host range category had
 251 many more genes than the other species in that category.

252 **Horizontal Gene Transfer**

253 We evaluated all 31 genomes for evidence of HGT. We used machine learning to identify HGT candidates
 254 and phylogenetic approaches to validate candidate HGT genes.

255 **Support Vector Machine classifier predicted HGT candidates.** Analysis of the 722,232 transcripts with
 256 our support vector machine classifier (SVM) over the 31 genome assemblies and the six previously
 257 published *Phytophthora* genomes identified 35,246 HGT candidates. A total of 28,791 of these transcripts
 258 that could be regrouped in orthology groups encoding putative transposable elements were discarded,
 259 resulting in 6,455 non-TE HGT candidates. The number of candidates predicted ranged from 91 in *P.*
 260 *agathidicida* to 233 in *P. megakarya* and 262 in *P. palmivora* (mean 160.13 \pm 36.68). *P. agathidicida* has
 261 one of the lowest number of transcripts annotated (12,923 transcripts), while *P. palmivora* and *P.*
 262 *megakarya* have the highest gene content with 37,283 and 33,614 transcripts, respectively. Overall, we
 263 identified a significant linear correlation between gene space in each genome and the number of HGT
 264 candidates predicted with the SVM classifier ($r^2 = 0.45$; $p < 0.0001$).

265 **Phylogenetic filtering of HGT candidates.** The 6,455 non-TE HGT candidates predicted with the SVM
266 classifier were subject to a two-step filtering process to discard false positives. In the first step, we searched
267 for homologs among a database of sequences built from seven clades (including putative fungal and
268 bacterial donors), followed by phylogenetic tree reconstruction with bootstrap analysis. The phylogenetic
269 filter retained 2,214 candidates, among which 1,113 (50.3%) showed a strong phylogenetic discordance
270 and were seen nested within a distantly related clade (Fungi, Bacteria or Amoebozoa) in direct contradiction
271 to the expected phylogenetic relationships of the respective organisms. The 1,110 other candidates left
272 also branched within a clade of fungal or bacterial genes; however, in these cases, placement of the
273 *Phytophthora* transcript with Fungi or Bacteria was caused by the absence of homologs in the intermediate
274 clades Viridiplantae, Alveolata and/or Amoebozoa. Numbers of candidates that passed this filter ranged
275 from 36 in *Phytophthora europea* to 127 in *P. palmivora*; There was a significant correlation between the
276 total number of genes and the number of HGT candidates across the analyzed species ($r^2 = 0.49$; $p <$
277 0.0001) (Fig. S2).

278 **Sequence identity filtering of HGT candidates.** The 2,214 HGT candidates retained after the
279 phylogenetic filtering were submitted to a sequence identity discrepancy filter. A total of 1,688 candidates
280 were rejected after the first “identity test”, resulting in a “relaxed” set of 526 HGT candidates for which the
281 sequence identity between the candidate HGT sequence in *Phytophthora* and its closest homolog
282 sequences in the putative “donor” species was shorter than the average identity between the two species;
283 an average of 14.6 (± 6.2) candidates were retained per *Phytophthora* genome with a maximum of 33 for *P.*
284 *palmivora* and *P. niederhauserii* (Fig. S2). A gene enrichment analysis of this candidate set showed a
285 significant enrichment for GO terms related to oxidoreductase activity and hydrolysis and metabolism of
286 carbohydrates (cutinase activity, carbohydrate metabolic process) and proteins (Table S3).

287 Among the 526 candidates of the relaxed set, 44 passed the second “identity test”, constituting a “strict” set
288 of HGT candidates. For 28 of them (56.0%), BLAST search results indicated a strong homology with the
289 clade of the putative donor where the BLAST e-values with species of the putative donor clade were lower
290 than the e-values observed with species from non-donor clades. We then looked at their physical location
291 on their respective scaffold to eliminate potential contaminants; All the candidates were found on scaffolds

292 that had at least two gene models predicted on them. GO term enrichment analysis of this “strict” set
293 indicated significant enrichment for GO terms related to oxidoreductase activity (GO:0055114;
294 GO:0016491; GO: 0008670), and carbohydrates activity and cell wall modification (GO:0000272;
295 GO:0045490; GO: 0042545; GO:0045493; GO:0031176; GO:0030599) (Table 2).

296 **Phylogenetic reevaluation of the strict set of HGT candidates.** The 44 candidates of the “strict” set of
297 HGT candidates were subjected to reevaluation by sampling additional taxa within the oomycetes. Their
298 amino-acid sequences were first clustered into closely related groups of sequences by assigning them to
299 the 21,303 orthologous clusters previously defined (see *Orthology Clustering of Phytophthora Proteins*).
300 This process reduced the set of 44 candidates into 28 orthologous clusters, that were then searched against
301 the sequences of the 31 genome assemblies, five *Phytophthora* species sequenced in previous studies,
302 and 36 oomycete genomes (Table S4). Protein members of six of these clusters had homologs (BLASTp
303 e-values $\leq 1E-025$; Table S4) in the set of 21 strongly supported HGT candidates identified in the genome
304 of *P. ramorum*, *P. infestans* and *P. sojae* by Richards et al. (61). Following these searches, we
305 reconstructed maximum likelihood phylogenies for 19 of these candidates that had putative functions
306 related to the modification of compounds of the plant cell wall (e.g., pectin esterase, xylulose reductase,
307 tannase and endo-1,4-beta-xylanase), peptidases, oxidoreductases and putative elicitors such as a NPP1
308 protein and an ABC transporter (Fig. S3). In 15 cases, the HGT candidate was found nested within a group
309 of fungi or bacteria, as expected under the hypothesis of a transfer from one of these groups through a
310 horizontal transfer event; comparative topology analysis of alternative tree hypotheses (expected
311 phylogeny and transfer from an oomycete donor to a fungus or bacterium) using the Shimodaira-Hasegawa
312 test (SH-test) provided support for this observation in 14 cases (Table 3). In four other cases, the topology
313 test was significant for the opposite relationship where a transfer occurred from the oomycetes to fungi or
314 bacteria. For HGT9, taxon sampling was not sufficient to accurately infer with confidence the putative HGT
315 donor and enable tree topology testing (Table 3).

316 The distribution of sequence homologs of the “strict” set of HGT candidates among the oomycete phylogeny
317 was strongly variable (Fig. 7; Table S4). The majority of transfer events to oomycetes appear to have
318 occurred relatively recently; three candidates had strong statistical support for transfer from bacteria or

319 fungi to a common ancestor of the *Phytophthora* genus (HGT5, HGT7 and HGT10), two candidates to the
320 *Phytophthora* and Peronosporales with hemibiotrophic lifestyle (HGT2 and HGT15) and two to
321 Peronosporales with a hemibiotrophic or an obligate biotrophic lifestyle (HGT12 and HGT20) (Fig. 7A). Four
322 of these transfers reached close to gene fixation within the *Phytophthora* genus as they were found in more
323 than 80% of the species surveyed and in the nine *Phytophthora* phylogenetic clades considered (Fig. 7A).
324 However, fixation was not the general rule accompanying recent transfers. For instance, two HGT
325 candidates, with functions related to plant pathogenicity (NPP1 protein and peptidase S9) were unique to
326 clade 8 in *Phytophthora* and did not have a homolog in any other *Phytophthora* clade or oomycete species
327 (HGT5 and HGT7). Several HGT events with strong statistical support (Fig. 7A) appear to have occurred
328 following major lifestyle transitions within the oomycetes, i.e., necrotrophy in the Pythiales (HGT6, HGT13
329 and HGT14) to obligate biotrophy and hemibiotrophy in the Peronosporales (HGT2, HGT12, HGT15 and
330 HGT20) and transition to parasitism with three events trackable to a common ancestor of the
331 Saprolegniales, Pythiales and Peronosporales (HGT1, HGT4 and HGT8). Eight out of these ten genes had
332 homologs (BLASTp e-values from 1E-137 to 1E-012) with pathogenicity, virulence, and effector genes of
333 the Pathogen Host Interaction database (PHI-base; (62)). Transition to the necrotrophic lifestyle involved
334 transfers of genes encoding enzymes potentially involved in redox activity and toxin production (2,4-dienoyl-
335 CoA reductase and phenol acid decarboxylase) while two out of the four genes transfer at the transition to
336 hemibiotrophic lifestyle comprehended have putative functions related to the degradation of the cell wall
337 (xylulose reductase and endo-1,4-beta-xylanase).

338 Finally, the four significant transfers for the opposite relationship (oomycetes to bacteria or fungi) were all
339 for genes fixed in the *Phytophthora* genus and mapped within the Peronosporales (three candidates) or the
340 Peronosporales and Pythiales (one candidate), suggesting relatively recent transfer events (Fig. 7B).
341 Annotation of these genes indicates that they are potentially involved in the plant-pathogen interaction as
342 they encode proteins involved in protection against plant defensive molecules (tannase and ABC
343 transporter) and the oxidative stress occurring during the plant defense response (quinone oxidoreductase)
344 and remodeling of the plant cell wall (pectinesterase) (Table 3; Table S5).

345 **DISCUSSION**

346 In this comparative genome study of 37 *Phytophthora* spp., we sequenced and assembled 31 genomes *de*
347 *nov*o. We investigated these genomes for evidence of horizontal gene transfer, phylogenetic relationships
348 of genome structure and effectors, and association of host ranges. Horizontal gene transfer has been
349 identified as a significant source of variation in connection with the evolution of pathogenicity in
350 *Phytophthora*. So far, genome-wide analyses of HGT impact on oomycete and *Phytophthora* genome
351 evolution has identified putative transfers from fungi (61, 63) and bacteria (64), many of which involve
352 functions related to carbohydrate metabolism and pathogenicity. Our analysis supports these findings,
353 identifying a set of 44 HGT candidates in *Phytophthora* species, associated with enzymes putatively
354 involved in the deconstruction of plant cell wall components, evasion and protection against host defenses
355 (Table 3; Table S5). Our machine learning approach to identify HGT candidates aimed to identify genes
356 likely inherited from bacteria or fungi; validation of these candidates with classical methods based on the
357 identification of topological incongruence in phylogenies and the detection of discrepancies between gene
358 and species distances resulted in a more conservative list of candidates than those previously proposed
359 for *Phytophthora* species (61, 63, 64). Such a stringent approach had the power of rejecting the alternative
360 evolutionary scenario where the gene was present in the last common ancestor of the donor and recipient
361 and was lost in intermediate lineages. Despite such a conservative approach, 30% of HGT candidates
362 identified in a previous study (61) that included only three *Phytophthora* genomes were retrieved in our
363 analysis.

364 An underlying hypothesis related to laterally transferred genes is that they may have functional or ecological
365 roles, allowing the recipient to adapt to a novel lifestyle or to exploit a new ecological niche (65). Using the
366 comprehensive collection of *Phytophthora* genomes sequenced in this study and the oomycetes for which
367 genome assemblies were available, we have been able to assess the extent of distribution of homologs of
368 these candidates across the oomycete phylum. We confirmed that most of the HGTs into the oomycetes
369 have occurred coincident with the emergence of major lifestyle innovations, such as the acquisition of plant
370 parasitism, or biotrophy (obligate or hemibiotrophy). Many candidates were detected in a large majority of
371 the *Phytophthora* genomes sequenced, for example seven candidates (HGT6, HGT11, HGT17, HGT18,
372 HGT19, HGT21 and HGT22) were found in 94% or more of the 36 genomes surveyed. In some instances,
373 homologs have been retained in distinct genetic lineages among the oomycetes, suggesting that these

374 candidate genes may confer a function conserved across lineages with different lifestyles; for example, the
375 endonuclease encoding gene HGT1 was likely transferred before the radiation of the oomycetes and
376 retained in the five oomycete orders surveyed in this study. On the other hand, in some cases the acquisition
377 and/or retention of specific key pathogenicity genes appears to be restricted to some specific clades within
378 *Phytophthora* (e.g., HGT5 and 7, NPP1; Fig. 7), suggesting recent transfers following divergence of
379 *Phytophthora* clades. In cases where a putative HGT gene is present in a limited number of *Phytophthora*
380 species from diverse clades, e.g., HGT13, gene loss by drift in species where there was little benefit may
381 be an explanation. Rapid diversification of the HGT gene under positive selection might make the gene
382 undetectable to our algorithm in some species.

383 Oomycete-derived transfers to other kingdoms have been identified in a few rare instances, usually with
384 limited statistical support (61). With the comprehensive genome sampling of our study, we found strong
385 support for four transfers (out of 44) from oomycetes to either bacteria or fungi, indicating bi-directional
386 exchanges across kingdoms. By providing a source of novel genetic material that can increase the fitness
387 of micro-organisms to their environments or their hosts (66–68), genes transferred horizontally have the
388 potential to be traded back and forth across kingdoms. In the context of an ecological system in which a
389 host plant interacts with a multitude of micro-organisms (microbiota), we can hypothesize that some of the
390 evolutionary innovations that are generated during the co-evolutionary arms race between a pathogen and
391 the host could be shared within the microbiota. For host-associated micro-organisms sharing the same
392 ecological niche, the transfer of genetic material from those that are fit to the shared environment should
393 represent a straightforward mechanism that will drive rapid adaptation of others to this environment (69).

394 We investigated multiple aspects of *Phytophthora* genome structure and how this relates to the genus
395 phylogeny. Genome size, gene amounts, and counts of orthologous genes varied within phylogenetic
396 clades highlighting the great diversity within the *Phytophthora* genus and likely reflect the large observed
397 differences in repeat content, some of which resulted from genome duplication. While some variation in
398 repeat content may be due to differences in repeats collapsed in the genome assembly, repeat types and
399 lengths identified in this study and sequences used for assembly are generally consistent across the
400 sequenced genomes and therefore should collapse in assembly at similar rates. Interestingly, we noted

401 that none of the genomes sequenced in this study approaches the 73% repeat content reported in the
402 Sanger-assembled *P. infestans* genome (10) and is possibly due to the differences in sequencing
403 technologies including sequence longer sequence lengths. Greater repeat content was not necessarily an
404 indicator of large genome assembly size. While the five species with reported repeat content of greater
405 than 30% (*P. pinifolia*, *P. megakarya*, *P. palmivora*, *P. fragariae* and *P. hibernalis*) were within the nine
406 largest assembly sizes, other species with large assembly sizes had less repeat content. For example, *P.*
407 *niederhauserii* had an assembly size of 90Mb but only 20.9% repeat content which was considerably lower
408 than expected when compared to even moderately repetitive *Phytophthora* genomes such as *P. sojae* 40%
409 (29). Genome size estimation using K-mer analysis also shows assemblies are shorter than expected
410 (Table S1). These observations suggest that repeat content may be underestimated in short-read genome
411 assemblies and would expand with improved assembly and may also indicate missing repeat sequences
412 from the *de novo* repeat identification process.

413 The numbers of predicted genes per species, genes per orthologous groups, and effector genes per
414 species were consistent with those previously reported for *Phytophthora* species. Both the numbers of
415 genes and the average sizes of genes were well within the ranges of the six previously sequenced
416 *Phytophthora* species, for example *P. sojae* was shown to have 26K genes with an average size of 1,181
417 bp (29). This supports our observation that the smaller assembly sizes of the *Phytophthora* genomes
418 presented in this study were mainly associated with an overall reduction in repetitive regions while the gene-
419 containing sequences are relatively consistent in size. BUSCO analysis of the sequenced core ortholog
420 content also showed similar results to previous *Phytophthora* studies. Some genome assemblies, including
421 *P. palmivora* that underwent whole genome duplication, had lower single copy gene numbers due to
422 duplications. But overall, censuses of single-copy orthologs showed that both the genome assemblies and
423 gene predictions were quite complete and comprised the majority of genes in each individual species
424 sequenced. This suggests, that while genomes were small due to collapsed repeat regions, the majority
425 of core orthologs were captured in the assemblies and it can be extrapolated that the majority of gene
426 regions are assembled.

427 Effectors are proteins produced by pathogens that assist in host infection. Effectors are considered rapidly
428 evolving genes that are usually conserved among few closely related species and quickly diverge along the
429 phylogeny. Two types of ortholog groups were identified in our *Phytophthora* genus analysis supporting this
430 hypothesis: one group corresponds to well-conserved genes among all *Phytophthora* species responsible
431 for core cellular functions, while a second group includes rapidly evolving gene families likely responsible
432 for host infection and adaptation. We also investigated how the amounts of predicted apoplastic and
433 cytoplasmic effectors related to the host range of each *Phytophthora* species. There were large differences
434 in the numbers of effector genes identified per species. We did not observe a correlation between the
435 number of predicted effectors with phylogenetic relationships or genome size. However, a clear relationship
436 with host range was observed. Species with smaller host ranges had on average fewer predicted effectors
437 than those with larger host ranges. When the *Phytophthora* species in this study were separated into 4
438 host range categories, the distribution of apoplastic effectors increased as the range of infected hosts
439 increased, from narrow to multiple, multiple to wide, and wide to huge. Cytoplasmic effectors showed a
440 similar pattern, however, both the RxLR and CRN effector numbers dropped from wide to huge host ranges.
441 Our study does not include a detailed measurement of gene expression levels of these effector genes
442 during infection of numerous hosts, so there are limitations in how these correlations can be interpreted. In
443 the absence of that information, we speculate that a large diversity of apoplastic effectors may be important
444 for successfully overcoming the apoplastic defenses of a large diversity of host plants.

445 There may be a similar requirement for larger numbers of cytoplasmic effectors, but expression of very
446 large numbers of cytoplasmic effectors may limit host range due to plant immune surveillance mechanisms.
447 Detection of a single cytoplasmic effector by an NLR resistance protein may be sufficient to prevent
448 infection, therefore a limited number of cytoplasmic effectors may result in a greatly expanded host range.
449 Our observation of reduced cytoplasmic effector complements in huge host range species may also be
450 indicative of cryptic host-specialization within these *Phytophthora* species. Recent work in *P. cactorum*,
451 commonly considered a broad host-range pathogen, has shown genomic signatures of host specificity (57).
452 In this case, high resolution phylogenetics demonstrated that host adaptation was associated with effector
453 gene gain/loss between strawberry and apple infecting clades. Where such cryptic host-adaptation is

454 present, pangenomic analysis may be a useful tool to infer broad or narrow host range and provide insight
455 to associations of effector diversity across *Phytophthora*.

456 **METHODS**

457 **Collection and isolation of a genus-wide *Phytophthora* collection**

458 Mycelium samples were isolated for all *Phytophthora* species in this study, as well as germinated cyst
459 samples for RNA sequencing of a subset of the species. For mycelium tissue, plugs of mycelium grown on
460 standard V8 agar plates were added to a flask with 20% liquid V8 media clarified with calcium carbonate
461 and incubated with shaking at 45 rpm at 25°C for one week. Agar plugs were removed from the mycelium
462 mass and the tissue was ground to a powder with liquid nitrogen, followed by DNA extraction using the
463 methods in Moller et al. (1992) (70) except using 1% CTAB and phenol/chloroform treatment, or total RNA
464 extraction (71) using TRIzol (Invitrogen, Carlsbad, CA) following manufacture's instructions.

465 For *Phytophthora robiniae* and *Phytophthora vignae*, similar to the protocol for *P. sojae* (29) zoospores
466 were produced by repeated washing of 11 day-old V8-200 plates of mycelium with sterile double distilled
467 water followed by overnight incubation at 14°C. Germinated cysts were produced by exposing collected
468 zoospores to cleared V8 broth for 1 hour. For *P. parvispora*, mycelium mats were grown in liquid V8 for 5
469 days, then the liquid V8 was changed out for soil extract (soil collected with stream water, mixed, and filter-
470 sterilized) and zoospores were collected after three days, followed by germinated cyst induction as above.
471 For *P. cajani*, *P. europaea*, *Phytophthora foliorum*, *P. hibernalis*, *P. pistaciae*, and *Phytophthora uliginosa*
472 species, that did not readily yield zoospores, mycelium was grown in Plich medium (72) for RNA sequencing
473 to compare against V8 medium growth. Known ITS and CoxII sequences for each species were used to
474 confirm species identification before high-throughput sequencing. DNA and RNA quality were checked
475 with electrophoresis (DNA), Bioanalyzer (RNA), and NanoDrop.

476 Isolate P414 of the strawberry crown rot pathogen *P. cactorum* and isolate SCRP371 of the raspberry root
477 rot pathogen *P. idaei* were sequenced at the National Institute of Agricultural Botany at East Malling
478 Research (NIAB EMR). P414 and SCRP371 were isolated from symptomatic strawberry and raspberry
479 plants, respectively. DNA extraction was performed on freeze dried mycelium using a GenElute Plant

480 Genomic DNA Miniprep Kit (Sigma), following the manufacturers protocol with the following modifications:
481 the RNase A digestion step was not performed and samples were eluted using 2x 100 µL elution buffer for
482 P414 and 2x 75 µL for SCR371. Genomic libraries were prepared using a Nextera XT Library Preparation
483 Kit (Illumina) or TruSeq DNA LT Kit (Illumina) for *P. cactorum* and *P. idaei*, respectively.

484 *P. kernoviae*, *P. lateralis*, *P. cryptogea*, and *P. pinifolia* were collected and isolated as described (73). *P.*
485 *agathidicida*, *P. multivora*, *P. pluvialis*, and *P. taxon totara* were collected and isolated as described (74).

486 **Genome sequencing and assembly**

487 Thirty-one *Phytophthora* species were sequenced by our consortium. Genomes of 21 *Phytophthora*
488 species were sequenced by BGI Genomics (Shenzhen, China) (*P. boehmeriae*, *P. brassicae*, *P. cajani*, *P.*
489 *pini*, *P. europaea*, *P. foliorum*, *P. fragariae*, *P. hibernalis*, *P. litchii*, *P. megakarya*, *Phytophthora melonis*, *P.*
490 *niederhauserii*, *P. palmivora*, *P. parvispora*, *P. pisi*, *P. pistaciae*, *P. robiniae*, *P. rubi*, *P. syringae*, *P.*
491 *uliginosa*, and *P. vignae*) using 90-bp paired-end reads produced on the Illumina HiSeq2000 platform. Four
492 *Phytophthora* species were sequenced by the University of British Columbia (*P. kernoviae*, *P. lateralis*, *P.*
493 *pinifolia*, and *P. cryptogea*), using Illumina HiSeq 2000 100 bp paired-end reads (73). Genomes from four
494 *Phytophthora* species isolated from New Zealand (*P. agathidicida*, *P. multivora*, *P. pluvialis*, and
495 *Phytophthora taxon totara*) were sequenced by Scion (New Zealand Forest Research Institute, Ltd.), using
496 primarily Illumina HiSeq 100 bp paired-end reads (74). Two *Phytophthora* genomes were sequenced by
497 NIAB EMR (*P. idaei* and *P. cactorum*), using 250-bp paired-end reads produced on a MiSeq Benchtop
498 Analyser (Illumina, San Diego, CA, USA). BGI-sequenced genomes were adapter trimmed to remove
499 Illumina adapters and quality trimmed to remove Phred scores of less than Q20 from the ends of reads
500 (75). Genome sequences were assembled with SOAPdenovo2 (76). Several initial assemblies were done
501 to identify an optimal K-mer length for each genome. Gap filling and single base proofreading were
502 conducted with SOAPAligner (77). The University of British Columbia (UBC) genomes were quality trimmed
503 and assembled using ABySS (78) and a range of k-values from 32 to 96 (73). Scion genomes were
504 assembled using SPAdes (79) and contigs were extended using SSPACE (74, 80). Genomes sequenced
505 at NIAB EMR were trimmed and adapters removed using fastq-mcf (81) prior to *de novo* assembly of the
506 data using Velvet (82), at K-mer lengths of 61 and 41 bp for *P. cactorum* and *P. idaei*, respectively.

507 Genome size was estimated using K-mer counts of the raw Illumina sequence. K-mers were counted using
508 Jellyfish count (version 2.2.6, -m 32) (83) Histograms created using Jellyfish hist were plotted using R (84)
509 to identify the apex and boundaries of the single copy K-mer peak. Genome size was calculated by dividing
510 the total of unique K-mers by the mean coverage (peak K-mer frequency).

511 In order to separate mitochondrial genome contigs from the nuclear genome assembly, full length
512 mitochondrial genome sequences were collected from GenBank (85) for the following 9 *Phytophthora*
513 species; *P. andina*, *P. infestans*, *P. ipomoeae*, *P. mirabilis*, *P. parasitica*, *P. phaseoli*, *P. polonica*, *P.*
514 *ramorum*, and *P. sojae*. The consortium's 31 assembled *Phytophthora* genomes were aligned with Blat
515 (86) to identify mitochondrial contigs. Blat alignments were filtered to return alignments greater than 50%
516 of the aligned contig length, greater than 100 bp, and with gaps less than 50% of the contig length. Contigs
517 identified as mitochondrial were removed from the genome assembly and are a part of a different study.

518 **Transcriptome sequencing and assembly**

519 Twenty-four of the genome-sequenced *Phytophthora* species underwent RNA sequencing (*P. brassicae*,
520 *P. cactorum*, *P. cajani*, *P. pini*, *P. europaea*, *P. foliorum*, *P. fragariae*, *P. hibernalis*, *P. kernoviae*, *P. lateralis*,
521 *P. litchii*, *P. megakarya*, *P. melonis*, *P. niederhauserii*, *P. palmivora*, *P. parvispora*, *P. pinifolia*, *P. pisi*, *P.*
522 *pistaciae*, *P. robiniae*, *P. rubi*, *P. syringae*, *P. uliginosa*, and *P. vignae*). Two samples, V8-grown mycelia
523 and either Plich-grown mycelia or germinated cysts, were sequenced for each. Twenty-one species were
524 sequenced by the BGI using custom library construction protocol: random hexamer-primer were used to
525 synthesize the first-strand cDNA; second-strand cDNA was synthesized using buffer, dNTPs, RNase H and
526 DNA polymerase I; short fragments were purified with QiaQuick PCR extraction kit resolved with EB buffer
527 and connected with sequencing adaptors. Each *Phytophthora* transcriptome received 90 bp paired end
528 reads. Two of the above species were sequenced by UBC (*P. kernoviae*, and *P. lateralis*). RNA of *P.*
529 *cactorum* was sequenced by NIAB EMR.

530 To create a transcriptome reference for gene predictions, Trinity assemblies (87) were made for each
531 *Phytophthora* species using both RNA sequence samples (--seqType fq --min_contig_length 200). The *de*
532 *novo* transcriptome assemblies were cleaned using the 3-step TransDecoder process (88). A set of
533 predicted protein sequences was made by combining *Phytophthora* protein sequences from GenBank (85)

534 with protein sequences from the six previously sequenced and annotated *Phytophthora* species (*P. sojae*
535 (29), *P. ramorum* (29), *P. infestans* (10), *P. capsici* (31), *P. cinnanomi*
536 (<http://genome.jgi.doe.gov/Phyci1/Phyci1.home.html>), and *P. parasitica*
537 (https://www.ncbi.nlm.nih.gov/genome/11752?genome_assembly_id=49439)). Transdecoder.LongOrfs
538 (88) was used to identify the longest open reading frames in the Trinity assembly. BLASTP (89) was used
539 to align the longest ORFs to the set of constructed proteins identified from GenBank (parameters: -
540 max_target_seqs 1 -evaluate 1e-5). Finally, Transdecoder.Predict was used to predict the gene structure
541 from the transcriptome assembly. The resulting cleaned transcriptome assemblies were used in the
542 subsequent gene prediction methods.

543 ***De novo* repeat identification**

544 Each genome was repeat-masked to create a genome assembly ready for gene prediction as described
545 below. Repeat elements were *de novo* identified separately by species. *De novo* predictions were
546 combined along with previously identified *Phytophthora* repeats for species-specific repeat identification.

547 To identify *de novo* discover LTR retrotransposons, LTRharvest (90) and LTR_(91) finder were run on each
548 genome assembly. By species, LTR retrotransposon predictions from both LTRharvest and LTRfinder were
549 condensed by coordinates and reduced by Blat alignments. LTR retrotransposons, non-LTR
550 retrotransposons, DNA transposons, and other repeat elements were identified following the MAKER
551 'Repeat Library Construction-Advanced' (92) method
552 (http://weatherby.genetics.utah.edu/MAKER/wiki/index.php/Repeat_Library_Construction-Advanced).

553 This process utilizes the following programs: MITE-Hunter (with default parameters) (93); GenomeTools
554 suffixator, LTRharvest, LTRdigest (run with 99% and 85% identity) (94); RepeatModeler (95) which calls
555 RECON (96), RepeatScout (97), TRF (98), NSEG (99) and RMBlast
556 (<http://www.repeatmasker.org/RMBlast.html>); and sequence databases provided by the MAKER 'Repeat
557 Library Construction-Advanced' method.

558 *De novo* repeat identification was further supplemented by LTR_retriever (100) using results from
559 LTRharvest and LTRfinder. LTR_retriever retrotransposons were classified into sub-families by species.

560 For each assembled genome, predicted repetitive elements identified in the above methods were combined
561 with GIRM RepBase (volume 18, issue 9) (101) *Phytophthora* repeats. Genomes were repeat-masked using
562 RepeatMasker (v 4.0.6, run with the described combined custom *Phytophthora* library and default
563 parameters) (102) and the combined repeat database to create gene prediction-ready genome assemblies.

564 **Gene prediction and annotation in 31 *Phytophthora* species**

565 For each species sequenced, gene training models were made with both Augustus (103) and SNAP (104).
566 Augustus was trained using the genome assembly and the set of previously sequenced *Phytophthora*
567 proteins described in the transcriptome sequencing and assembly process in the text above. To train
568 SNAP, for each species BUSCO (105) was run using the Alveolata_Stramenopiles database in genome
569 mode on each genome assembly to identify core orthologs. BUSCO gff files were converted to zff using
570 maker2zff (92), SNAP tools fathom (-categorize 1000, -export 1000), forge, and hmm-assembler were used
571 to create a training HMM. Genes identified as single copy core orthologs were combined and used as the
572 SNAP training set.

573 Several supplementary files were created to run the MAKER gene prediction pipeline. For the 'EST
574 Evidence' section of MAKER the transcriptome result of the three-step TransDecoder process (88) was
575 used as the EST field. In the seven cases where RNA was not sequenced and therefore the TransDecoder
576 transcriptome was not created, the phylogenetically closest species with RNA sequences was used. A
577 concatenation of the gene sequences of previously sequenced *Phytophthora* species and TransDecoder
578 transcriptome assemblies was used for the alt-est field. For each genome assembly, *P. sojae*, *P. infestans*,
579 and *P. ramorum* gene predictions were combined with five representative TransDecoder-cleaned
580 transcriptome assemblies. To create species-specific alt-est sets the five representative species were
581 selected from within the *Phytophthora* phylogenetic clade (excluding the species of interest). If less than
582 five species received RNA sequencing, nearby clades were used until five transcriptome assemblies were
583 combined. This set of eight gene predictions and transcriptome assemblies was used in the alt-est field.
584 For the 'Protein Homology' section of MAKER all previously identified *Phytophthora* proteins were combined
585 from GenBank together with the six previously sequenced *Phytophthora* species.

586 To predict genes, MAKER was run on the 31 genomes. The repeat-masked genome for each assembly
587 was run using the Augustus and SNAP training models described above and the EST and protein evidence
588 sequence sets as described above.

589 For validation purposes, three sets of BUSCO analyses were run. BUSCO 3.02 was run on the 31 genomic
590 assemblies, on the 24 transcriptome assemblies, and on the 31 sets of predicted proteins. In all cases, the
591 Alveolata_Stramenopiles BUSCO database of 234 single copy orthologs was used.

592 Predicted genes were functionally annotated using BLASTX (89) to align against known proteins. First, all
593 predicted proteins were aligned against all *Phytophthora* species' proteins obtained from the RefSeq non-
594 redundant protein database in NCBI (85, 106) and the UniProt TrEMBL (107) database. Second, all
595 predicted proteins were aligned against all stramenopile proteins from NCBI RefSeq and UniProt. Third,
596 all predicted proteins were aligned against all Fungi proteins from NCBI RefSeq and UniProt. BLASTX
597 alignments were generated with the following parameter settings: -evalue 1e-5, -max_target-seqs 50 and
598 were further filtered to return only hits that were at least 50% identical for 50% of the length of the subject
599 protein. Protein functional annotation was made from the consensus of the top five protein alignments for
600 each taxonomic classification. All results per query protein were screened to return proteins with
601 informative functional annotations ranked by the two rounds of alignments.

602 Predicted proteins from MAKER were screened using InterProScan version 5.20-59.0 (108) to identify
603 functional domains. Gene Ontology (GO) (109, 110) terms were obtained from UniProt BLASTX alignments
604 and the InterProScan runs.

605 **Identification of Effector Proteins**

606 The prediction of cytoplasmic effectors of the RxLR and crinkler (CRN) families was performed on the six-
607 frame translations of the *Phytophthora* whole-genome assemblies using the application getorf (EMBOSS
608 suite) (111). We searched for evidence of the presence of the motifs of interest (RxLR+EER motif for RxLR
609 effectors (112), and LxLAK for CRN effectors (10, 42)) in each ORF translation by using a combination of
610 regular expressions using effectR (113).

611 To identify additional effector proteins that may not include one the canonical motifs, thus not recognized
612 by the RxLR or CRN regular expression, we searched against a profile-HMM (114). We built the HMM
613 profile using an intersect of each set of candidate effectors predicted using regular expressions for each
614 sequenced species in the consortium and the previously predicted effectors from the reference genomes
615 of *P. infestans*, *P. ramorum*, and *P. sojae* (10, 29). We searched for additional effectors in all ORF
616 translations against each of HMM profile using the hmmsearch program in HMMER (115) using default
617 threshold parameters. Predicted effectors from the motif method and the HMM method were examined for
618 signal peptides using SignalP 3.0 (116).

619 Putative apoplastic protease inhibitors were annotated by batch BLASTP (E-value < 1e-30) against
620 MEROPS database (117). The glycoside hydrolase proteins were annotated using the carbohydrate-active
621 enzyme database (cazy) annotation web server dbCAN (118). The hidden Markov model (HMM) profile of
622 NLP family (PF05630) was downloaded from Pfam database (119). The hmmsearch program (115) (with
623 default threshold parameters) was used to search for NLP proteins in each genome assembly.

624 **Classification into Orthologous Groups**

625 Predicted proteins from the 31 sequenced *Phytophthora* and from the six previously sequenced
626 *Phytophthora* species were combined into orthologous groups using OrthoMCL (120). Due to the large
627 data set of 37 full genomes, a two-stage process was used. In stage one, proteins were assigned to the
628 online pre-constructed OrthoMCL orthology groups (121). Predicted proteins from the MAKER process
629 were uploaded to the OrthoMCL web site (www.orthomcl.org). This returned a file of proteins assigned to
630 OrthoMCL groups. In stage two, all unassigned proteins were assigned to groups using the stand-alone
631 version of OrthoMCL. All unassigned proteins from all 37 species were combined into a single FASTA
632 sequence file. The protein FASTA file was aligned against itself using BLASTP. The BLASTP output was
633 converted for input into OrthoMCL which was run in 'Mode 4'.

634 **Phylogenetic analysis of single copy orthologs across *Phytophthora* species**

635 To estimate phylogenetic relationships across the 31 genomes and the six previously sequenced
636 *Phytophthora* species, we first identified the single-copy, core orthologous genes shared across all

637 sequenced species. We selected each of the orthology groups that contain exactly one gene from each of
638 the 37 genomes in the orthology construction.

639 We constructed a phylogenetic tree using 61 genes from each species. Each set of orthologous proteins
640 were multiply aligned using MAFFT ver. 7.271 (122, 123). The phylogenetic tree was reconstructed using
641 RAxML (124), using each gene as an independent partition with its own substitution model, bootstrapped
642 1,000 times. Only one tree was calculated using all partitions.

643 **Effector distribution across plant host ranges**

644 The USDA fungal database (<https://nt.ars-grin.gov/fungaldatabases>) was used to define the number of
645 known plant hosts infected by each *Phytophthora* species considered in this study. With this information,
646 host ranges were classified into four categories defined by the number of host genera containing known
647 hosts: 'Narrow', host species confined to 1 plant host genus (1-3 host species total); 'Multiple', host species
648 confined within 2 to 9 host genera (2 to 32 host species total); 'Wide', host species spanning 16-55 host
649 genera (22 to 119 host species total); and 'Huge', host species spanning 107-327 host genera (163-718
650 host species total).

651 Numbers of predicted cytoplasmic and apoplastic effector genes were plotted for each host range. In order
652 to reduce errors caused by genome assembly artifacts, and to limit counts of functionally identical effector
653 genes, near-identical paralogs were removed from the counts. To identify near-identical paralogs, effector
654 amino acid sequences were aligned to one another using the Smith-Waterman local aligner from the
655 EMBOSS package (111) to identify similarity. Effectors with greater than 95% amino acid identity over the
656 full sequence length were reduced to one representative effector sequence. The resulting reduced set of
657 effector predictions was used for analysis of the relationship of effector repertoires to host range. Host
658 ranges were plotted for each effector type using ggplot2 (125) in R (84).

659 **Horizontal Gene Transfer**

660 We used a two-step process to identify HGT gene candidates in *Phytophthora* genomes. In the first step,
661 we used a SVM classifier to predict HGT candidates. In the second step, we applied two filters to screen
662 out false positive candidates and assess the likelihood that the candidates were acquired through HGT.

663 **Support Vector Machine classifier for prediction of Horizontal Gene Transfer candidates**

664 We hypothesized that DNA sequence-composition features such as G + C content, codon bias and codon
665 usage frequency (126) can be used to identify genes of recent bacterial or fungal origin in *Phytophthora*
666 genomes. We constructed a multiclass SVM; (127) for composition-based analysis of *Phytophthora*
667 protein-coding genes and classification as either *Phytophthora*, bacterial or fungal origin. SVM is well suited
668 for sequence-composition classification because of the availability of SVM libraries that perform well with
669 large data sets with numerous variables and the ability of SVM to minimize unimportant features (128). The
670 SVM algorithm was implemented in a custom Python script using the SVC function, available from *Scikit-*
671 *learn* Python library (128).

672 Training sets consisted of 15,000 each of ascomycete, *Phytophthora* and bacterial transcripts, for a total of
673 45,000 transcripts. Ascomycete transcripts were selected by submitting a collection of complete transcript
674 sets predicted from the genomes of representative species of eight main ascomycete classes: *Tuber*
675 *melanosporum* (Pezizomycetes; GCA_000151645) (129), *Arthrobotrys oligosporus* (Orbiliomycetes;
676 GCA_000225545) (130), *Penicillium chrysogenum* (Eurotiomycetes; GCA_000226395) (131),
677 *Leptosphaeria maculans* (Dothideomycetes; GCA_000230375) (132), *Cladonia grayi* (Lecanoromycetes)
678 (133), *Sclerotinia sclerotiorum* (Leotiomycetes; GCA_000146945) (134), *Fusarium graminearum*
679 (Sordariomycetes; GCA_000240135.3) (135), and *Xylona heveae* (Xylonomycetes; GCA_001619985)
680 (136). Potential genes that underwent HGT were discarded from each transcript set by applying the
681 following protocol: 1, transcripts were translated into proteins and clustered using OrthoMCL (coverage and
682 identity of at least 50%, E-value cut-off of 1e-05, inflation parameter = 2.5) (120); 2, one protein from each
683 cluster was then queried against the NCBI nr database (max target sequences = 500); 3, clusters with at
684 least one hit in any other organisms than a fungal taxon were discarded; 4, for each remaining cluster, each
685 protein was queried against nr (max target sequences = 500) and step 3 was re-applied. *Phytophthora*
686 genes were selected by the same process, using transcripts from the following species: *P. syringae* (this
687 study), *P. sojae* (GCA_000149755) (29), *P. ramorum* (GCA_000149735) (29), *P. lateralis*
688 (GCA_000500205) (73), *P. pinifolia* (GCA_000500225) (73), *P. cryptogea* (GCA_000468175) (73), *P.*
689 *infestans* (GCA_000142945) (10), *P. brassicae* (this study), and *P. kernoviae* (GCA_000448265) (73) and

690 eliminating clusters with any protein match other than with an oomycete taxon. Bacterial transcripts were
691 selected following the same filtering approach on 21,096 transcripts retrieved from GenBank (representing
692 23 bacterial classes).

693 Sequence-composition features were used as input vectors to an SVM classifier and the curated training
694 sets (see above) were used as model data. Following a preliminary analysis, codon usage frequency and
695 GC content were selected as the sequence features as they resulted in a higher prediction accuracy than
696 codon bias (0.976 ± 0.002 vs. 0.973 ± 0.004 , $t = 10.4$, $p < 0.0001$; data not shown). This is consistent with
697 the point that codon use frequency is inherently the fusion of both codon usage bias and amino acid
698 composition signals (137). To choose the best kernel for the SVM, we first used principal component
699 analysis (PCA) to explore the relationships among the three different classes (Fig. S4). Radial basis function
700 (rbf) kernel parameters (C and γ) were systematically varied to optimize prediction accuracy using a
701 two-dimensional grid where both parameters were chosen from the set $\{10^{-3}, 10^{-2}, \dots, 10^6\}$. All these
702 optimizations were performed with fivefold cross-validation of the training set (randomly withholding one-
703 fifth of the training data as a testing data set; 100 random draws for each pair of parameters tested) (Fig.
704 S4). Accuracy as defined by $(TP + TN) / (TP + TN + FP + FN)$ was used as a measure of the quality of the
705 classification. Best classification accuracy (98.3%) was obtained with rbf kernel parameters of $C = 1000.0$
706 and $\gamma = 1.0$ (Fig. S4).

707 ***Phytophthora* transcript classification for Horizontal Gene Transfer**

708 The 618,240 transcripts predicted from the 31 genomes and 103,992 transcripts predicted from five
709 previously sequenced *Phytophthora* species (i.e. *P. sojae*, *P. ramorum*, *P. infestans*, *P. capsici* and *P.*
710 *cinnamomi* [see *Transcriptome sequencing and assembly*]) were submitted to the classifier and sorted into
711 *Phytophthora*-origin, bacterial-origin or fungal-origin classes depending on the probability returned by the
712 classifier for each of these classes. To generate a confidence score, we repeated the training of the
713 classifier 100 times before running the classification on each genome. To maximize the training process of
714 the classifier without increasing computing time and overloading memory we used a random subsample of
715 45,000 transcripts (15,000 genes in each of the three classes) as a training set each time. Preliminarily, we
716 determined the minimum threshold number of bootstrap replicates in which an HGT candidate was found

717 that would minimize the probability that this candidate was a false positive (e.g., misclassifying a
718 *Phytophthora* or a bacteria sequence as deriving from a fungal donor via HGT). This was done by submitting
719 a subsample of 1,500 sequences randomly picked in the training set (500 transcripts in each class) to the
720 classifier with the bootstrap procedure; then, false positive and true positive rates were calculated for
721 incremental values of bootstrap replicates. Based on this test, we determined that the chance of
722 misclassifying a fungal transcript as a *Phytophthora* or a bacterial sequence (i.e. a false positive) was <
723 0.2% (1/500) if it was classified as fungal in at least 89/100 bootstrap replicates; in such case the true
724 positive rate (recall; TP/(TP + FN)) would be 92.3% (Fig. S5A). For the bacterial sequences, this value was
725 $\geq 79/100$ bootstrap replicates; this corresponded to a true positive rate (recall) of 97.5% (Fig. S5B). These
726 two bootstrap replicate thresholds were then used for the identification of HGT candidates in *Phytophthora*
727 species.

728 **Horizontal Gene Transfer candidate false positive filtering**

729 HGT candidates predicted with the SVM classifier were submitted to a phylogenetic filtering step by
730 assessing the congruence of the gene phylogeny with the organism phylogeny. Each candidate transcript
731 was translated into a protein sequence and searched using DIAMOND BLASTp (minimum BLASTP E-value
732 of $1e-03$, sequence subject coverage of 50% and sequence query coverage of 50%) (138) for closest
733 homologs against protein-coding sequences downloaded from the NCBI Reference Sequence collection
734 (RefSeq) (106) for *Phytophthora* species. (72,639 sequences) and the following clades: heterokonts
735 (excluding *Phytophthora*; 164,619 sequences), Alveolata (1,527,928 sequences), Amoebozoa (113,408
736 sequences), Viridiplantae (5,556,940 sequences), Fungi (2,912,973 sequences), Archaea (1,830,006
737 sequences) and Bacteria (131,971,793 sequences) clades. Candidates with no hits in the Bacteria or Fungi
738 clades were directly rejected. Protein sequences for the top three DIAMOND BLASTp hits within each of
739 the above clade were retrieved and aligned with the query protein using MAFFT ver. 7.271 (123). Amino-
740 acid sites with a gap in more than one third of the sequences were removed. IQ-TREE was used to
741 determine the best-fitting substitution model and reconstruct a maximum-likelihood tree for each of the
742 alignments (139, 140) with node support assessed by using the ultrafast bootstrap approximation method
743 (141). Each phylogenetic tree was exported in Newick format, automatically rooted with sequences from

744 the Archaea or Bacteria clades and exported into a .png file using the BioPython package Phylo. For
745 facilitating visual examination of trees, png files were gathered into one single pdf catalog with the Python
746 library PyFPDF. Tree nodes were visually inspected to identify phylogenetic discordance (142). Two types
747 of discordance were examined: 1, “complete incongruence”, when the HGT candidate sequence clusters
748 with the fungi or bacteria clade with bootstrap support $\geq 50\%$, resulting in a phylogenetic tree completely
749 discordant with the expected organism phylogeny i.e. ((((((Phytophthora, Heterokonta), Alveolata),
750 Viridiplantae), (Fungi, Amoebozoa)), Archaea), Bacteria) (143, 144) 2, “missing clades”, when the HGT
751 candidate sequence clusters with the fungi or bacteria clade because other clades are missing (i.e. the
752 HGT candidate sequence didn’t have orthologs in intermediate clades such as Viriplantae, Amoebozoa and
753 Alveolata).

754 HGT candidates that passed phylogenetic filtering were submitted to a sequence identity discrepancy filter.
755 Assuming a molecular clock, the sequence identity between a pair of orthologous genes should be in the
756 same range as the average sequence identity between their respective species. However, for a pair of
757 sequences related through an HGT event between two species, the proportionality should be broken,
758 leading to an identity discrepancy when compared to the pairwise species identity (145). To identify such
759 discrepancies, we performed a first “identity test”: We calculated the nucleotide sequence identity between
760 the candidate HGT sequence in *Phytophthora* and its closest homolog sequences in the putative “donor”
761 species in Bacteria or Fungi. Then, the full transcriptome of the putative “donor” species was downloaded
762 and searched with BLASTN for 1,000 random transcripts from the *Phytophthora* species to identify one-to-
763 one orthologs and plot a distribution of expected nucleotide identity values. In a first “identity test”,
764 discrepancies were identified by comparing the observed nucleotide sequence identity found between the
765 HGT candidate in *Phytophthora* and its homolog sequence in the putative donor to the expected distribution
766 using a Wilcoxon sign-rank test; Candidates were rejected if the difference between the observed value
767 (sequence identity between the HGT candidate in *Phytophthora* and its homolog sequence in the putative
768 donor) and the average of the expected distribution was not significant and lower than an arbitrary
769 “discrepancy cutoff” of 8.56 (corresponding to the top quartile of the distribution of the difference between
770 the observed values and the expected values). Proteins retained at this step were included into a “relaxed”
771 list of candidates. To ascertain that the discrepancy was not caused by a high conservation of the gene

772 among the different clades, we validated this list with a second “identity test” that consisted of examining if
773 the nucleotide sequence identity between the HGT candidate and the closest species in the non-donor
774 clades was not significantly higher than the average identity expected between the two species. Only
775 candidates for which the difference in nucleotide sequence identity between the HGT candidate in
776 *Phytophthora* and its homolog sequence in the putative donor was lower than 52% (corresponding to the
777 uppermost quartile of the distribution of the difference between the observed values and the expected
778 values of nucleotide sequence identity between pairs of homologs from the two species) were retained after
779 this stage. When the second “identity test” could not be performed due to the absence of sequence
780 homologs in non-donor clades (i.e. Viriplantae, Amoebozoa and Alveolata), the “discrepancy cutoff” i.e. the
781 difference between the nucleotide sequence identity for the HGT candidate in *Phytophthora* and its homolog
782 sequence in the putative donor and the average of the expected distribution was raised to 80.83% identity
783 corresponding to the 5% upper quantile of the of the distribution of the difference between the observed
784 values and the expected values. Proteins that passed this second filter were kept in a “strict” list of
785 candidates.

786 We assessed if the HGT candidate could have been a bacterial or fungal contaminant mistakenly
787 sequenced and assembled with a genome assembly generated in this study. HGT candidates were
788 considered as a putative “contaminant” candidates if they were the only coding sequences to map to a
789 given scaffold.

790 **Data Availability**

791 Genome assemblies and genome and transcriptome sequences that were created in this study have been
792 deposited in NCBI under BioProjects PRJNA746351, PRJNA714689, and PRJNA702516. *P. cactorum* and
793 *P. idaei* data are available under BioProjects PRJNA383548 and PRJNA391273. Other genomic resources
794 including assembly files, gene/protein predictions and annotations, differential expression analysis, and
795 orthology analysis can be accessed at <https://phyto-seq.cqls.oregonstate.edu>.

796 **Acknowledgments**

797 NJG was supported by USDA Agricultural Research Service project 2072-22000-041-000-D, National
798 Institute of Food and Agriculture grant 2018- 67013-27823, and the J Frank Schmidt Foundation.

799 Genome sequencing of *P. pini* was supported by the California Walnut Board and the United States
800 Department of Agriculture Agriculture Research Service, CRIS Project # 5306-22000-014-00D to TK. We
801 thank Gregory Browne and Daniel Kluepfel for *P. pini* isolate and valuable inputs.

802 This work was supported in part by grants to YW from China National Funds for Distinguished Young
803 Scientists (31225022).

804 RJH, ADA and CFN were supported by grants from the UK Biotechnology and Biological Sciences
805 Research Council (BBSRC; BB/K017071/1, BB/K017071/2 and BB/N006682/1).

806 RM, PP and NW were funded by the New Zealand Ministry of Business, Innovation and Employment
807 (grant number CO4X1305), the Forest Growers Levy Trust (administered by the New Zealand Forest
808 Owners Association) and the Radiata Pine Breeding Company under the “Healthy trees, Healthy future”
809 research programme at Scion (NZFRI, Ltd).

810

811 **References**

- 812 1. Erwin DC, Ribeiro OK. 1996. *Phytophthora* diseases worldwide. American Phytopathological
813 Society (APS Press), St. Paul, Minnesota.
- 814 2. Judelson HS, Blanco FA. 2005. The spores of *Phytophthora*: weapons of the plant destroyer. *Nat*
815 *Rev Microbiol* 3:47–58.
- 816 3. Drake B, Jones G. 2017. Public value at risk from *Phytophthora ramorum* and *Phytophthora*
817 *kernoviae* spread in England and Wales. *J Environ Manage* 191.
- 818 4. Gunderson JH, Elwood H, Ingold A, Kindle K, Sogin ML. 1987. Phylogenetic relationships between
819 chlorophytes, chrysophytes, and oomycetes. *Proceedings of the National Academy of Sciences*
820 84:5823–5827.
- 821 5. Jiang RHY, Tyler BM. 2012. Mechanisms and Evolution of Virulence in Oomycetes. *Annu Rev*
822 *Phytopathol* 50:295–318.
- 823 6. Thines M, Kamoun S. 2010. Oomycete–plant coevolution: recent advances and future prospects.
824 *Curr Opin Plant Biol* 13:427–433.
- 825 7. Thines M. 2014. Phylogeny and evolution of plant pathogenic oomycetes—a global overview. *Eur*
826 *J Plant Pathol* 138:431–447.

- 827 8. Dick MW. 2001. The Peronosporomycetes, p. 39–72. *In* Systematics and Evolution.
- 828 9. TURNER RS. 2005. After the famine: Plant pathology, *Phytophthora infestans*, and the late blight
829 of potatoes, 1845—1960. *Historical Studies in the Physical and Biological Sciences* 35:341–370.
- 830 10. Haas BJ, Kamoun S, Zody MC, Jiang RHY, Handsaker RE, Cano LM, Grabherr M, Kodira CD,
831 Raffaele S, Torto-Alalibo T, Bozkurt TO, Ah-Fong AM v., Alvarado L, Anderson VL, Armstrong MR,
832 Avrova A, Baxter L, Beynon J, Boevink PC, Bollmann SR, Bos JIB, Bulone V, Cai G, Cakir C,
833 Carrington JC, Chawner M, Conti L, Costanzo S, Ewan R, Fahlgren N, Fischbach MA, Fugelstad J,
834 Gilroy EM, Gnerre S, Green PJ, Grenville-Briggs LJ, Griffith J, Grünwald NJ, Horn K, Horner NR, Hu
835 C-H, Huitema E, Jeong D-H, Jones AME, Jones JDG, Jones RW, Karlsson EK, Kunjeti SG, Lamour K,
836 Liu Z, Ma L, MacLean D, Chibucos MC, McDonald H, McWalters J, Meijer HJG, Morgan W, Morris
837 PF, Munro CA, O'Neill K, Ospina-Giraldo M, Pinzón A, Pritchard L, Ramsahoye B, Ren Q, Restrepo
838 S, Roy S, Sadanandom A, Savidor A, Schornack S, Schwartz DC, Schumann UD, Schwessinger B,
839 Seyer L, Sharpe T, Silvar C, Song J, Studholme DJ, Sykes S, Thines M, van de Vondervoort PJI,
840 Phuntumart V, Wawra S, Weide R, Win J, Young C, Zhou S, Fry W, Meyers BC, van West P,
841 Ristaino J, Govers F, Birch PRJ, Whisson SC, Judelson HS, Nusbaum C. 2009. Genome sequence
842 and analysis of the Irish potato famine pathogen *Phytophthora infestans*. *Nature* 461:393–398.
- 843 11. Goheen EM, Hansen EM, Kanaskie A, McWilliams MG, Osterbauer N, Sutton W. 2002. Sudden
844 Oak Death Caused by *Phytophthora ramorum* in Oregon. *Plant Dis* 86:441–441.
- 845 12. Rizzo DM, Garbelotto M, Hansen EM. 2005. *Phytophthora ramorum*: Integrative Research and
846 Management of an Emerging Pathogen in California and Oregon Forests. *Annu Rev Phytopathol*
847 43:309–335.
- 848 13. Rizzo DM, Garbelotto M, Davidson JM, Slaughter GW, Koike ST. 2002. *Phytophthora ramorum* as
849 the Cause of Extensive Mortality of *Quercus* spp. and *Lithocarpus densiflorus* in California. *Plant*
850 *Dis* 86:205–214.
- 851 14. GRÜNWARD NJ, GOSS EM, PRESS CM. 2008. *Phytophthora ramorum* : a pathogen with a
852 remarkably wide host range causing sudden oak death on oaks and ramorum blight on woody
853 ornamentals. *Mol Plant Pathol* 9.
- 854 15. TYLER BM. 2007. *Phytophthora sojae*: root rot pathogen of soybean and model oomycete. *Mol*
855 *Plant Pathol* 8:1–8.
- 856 16. KENNEDY DM, DUNCAN JM, DUGARD PI, TOPHAM PH. 1986. Virulence and aggressiveness of
857 single-zoospore isolates of *Phytophthora fragariae*. *Plant Pathol* 35:344–354.
- 858 17. Kao CW, Leu LS. 1980. Sporangium Germination of *Peronophythora Litchii* , The Causal Organism
859 of Litchi Downy Blight. *Mycologia* 72:737–748.
- 860 18. HARDHAM AR. 2005. *Phytophthora cinnamomi*. *Mol Plant Pathol* 6:589–604.
- 861 19. Raffaele S, Kamoun S. 2012. Genome evolution in filamentous plant pathogens: why bigger can
862 be better. *Nat Rev Microbiol* 10:417–430.
- 863 20. Yang X, Tyler BM, Hong C. 2017. An expanded phylogeny for the genus *Phytophthora*. *IMA*
864 *Fungus* 8:355–384.

- 865 21. Kroon LPNM, Brouwer H, de Cock AWAM, Govers F. 2012. The Genus *Phytophthora* Anno 2012.
866 *Phytopathology* 102:348–364.
- 867 22. Jung T, Jung MH, Cacciola SO, Cech T, Bakonyi J, Seress D, Mosca S, Schena L, Seddaiu S, Pane A,
868 di San Lio GM, Maia C, Cravador A, Franceschini A, Scanu B. 2017. Multiple new cryptic
869 pathogenic *Phytophthora* species from Fagaceae forests in Austria, Italy and Portugal. *IMA*
870 *Fungus* 8.
- 871 23. Brasier C, Scanu B, Cooke D, Jung T. 2022. *Phytophthora*: an ancient, historic, biologically and
872 structurally cohesive and evolutionarily successful generic concept in need of preservation. *IMA*
873 *Fungus* 13:12.
- 874 24. Dong S, Raffaele S, Kamoun S. 2015. The two-speed genomes of filamentous pathogens: waltz
875 with plants. *Curr Opin Genet Dev* 35:57–65.
- 876 25. Ye W, Wang Y, Shen D, Li D, Pu T, Jiang Z, Zhang Z, Zheng X, Tyler BM, Wang Y. 2016. Sequencing
877 of the Litchi Downy Blight Pathogen Reveals It Is a *Phytophthora* Species With Downy Mildew-
878 Like Characteristics. *Molecular Plant-Microbe Interactions*® 29:573–583.
- 879 26. Ali SS, Shao J, Lary DJ, Kronmiller BA, Shen D, Strem MD, Amoako-Attah I, Akrofi AY, Begoude
880 BAD, ten Hoopen GM, Coulibaly K, Kebe BI, Melnick RL, Guiltinan MJ, Tyler BM, Meinhardt LW,
881 Bailey BA. 2017. *Phytophthora megakarya* and *Phytophthora palmivora*, Closely Related Causal
882 Agents of Cacao Black Pod Rot, Underwent Increases in Genome Sizes and Gene Numbers by
883 Different Mechanisms. *Genome Biol Evol* 9:536–557.
- 884 27. Tabima JF, Kronmiller BA, Press CM, Tyler BM, Zasada IA, Grünwald NJ. 2017. Whole Genome
885 Sequences of the Raspberry and Strawberry Pathogens *Phytophthora rubi* and *P. fragariae*.
886 *Molecular Plant-Microbe Interactions*® 30:767–769.
- 887 28. Armitage AD, Lysøe E, Nellist CF, Lewis LA, Cano LM, Harrison RJ, Brurberg MB. 2018.
888 Bioinformatic characterisation of the effector repertoire of the strawberry pathogen
889 *Phytophthora cactorum*. *PLoS One* 13:e0202305.
- 890 29. Tyler BM. 2006. *Phytophthora* Genome Sequences Uncover Evolutionary Origins and
891 Mechanisms of Pathogenesis. *Science* (1979) 313:1261–1266.
- 892 30. Knaus BJ, Tabima JF, Shakya SK, Judelson HS, Grünwald NJ. 2020. Genome-Wide Increased Copy
893 Number is Associated with Emergence of Dominant Clones of the Irish Potato Famine Pathogen
894 *Phytophthora infestans*. *mBio* 11.
- 895 31. Lamour KH, Mudge J, Gobena D, Hurtado-Gonzales OP, Schmutz J, Kuo A, Miller NA, Rice BJ,
896 Raffaele S, Cano LM, Bharti AK, Donahoo RS, Finley S, Huitema E, Hulvey J, Platt D, Salamov A,
897 Savidor A, Sharma R, Stam R, Storey D, Thines M, Win J, Haas BJ, Dinwiddie DL, Jenkins J, Knight
898 JR, Affourtit JP, Han CS, Chertkov O, Lindquist EA, Detter C, Grigoriev I v., Kamoun S, Kingsmore
899 SF. 2012. Genome Sequencing and Mapping Reveal Loss of Heterozygosity as a Mechanism for
900 Rapid Adaptation in the Vegetable Pathogen *Phytophthora capsici*. *Molecular Plant-Microbe*
901 *Interactions*® 25:1350–1360.

- 902 32. McGowan J, Fitzpatrick DA. 2017. Genomic, Network, and Phylogenetic Analysis of the Oomycete
903 Effector Arsenal. *mSphere* 2.
- 904 33. Asai S, Shirasu K. 2015. Plant cells under siege: plant immune system versus pathogen effectors.
905 *Curr Opin Plant Biol* 28:1–8.
- 906 34. Wang W, Jiao F. 2019. Effectors of *Phytophthora* pathogens are powerful weapons for
907 manipulating host immunity. *Planta* 250:413–425.
- 908 35. Wang S, Boevink PC, Welsh L, Zhang R, Whisson SC, Birch PRJ. 2017. Delivery of cytoplasmic and
909 apoplastic effectors from *Phytophthora infestans* haustoria by distinct secretion pathways. *New*
910 *Phytologist* 216:205–215.
- 911 36. Dong S, Kong G, Qutob D, Yu X, Tang J, Kang J, Dai T, Wang H, Gijzen M, Wang Y. 2012. The NLP
912 Toxin Family in *Phytophthora sojae* Includes Rapidly Evolving Groups That Lack Necrosis-Inducing
913 Activity. *Molecular Plant-Microbe Interactions*® 25:896–909.
- 914 37. Tian M, Win J, Song J, van der Hoorn R, van der Knaap E, Kamoun S. 2007. A *Phytophthora*
915 *infestans* Cystatin-Like Protein Targets a Novel Tomato Papain-Like Apoplastic Protease. *Plant*
916 *Physiol* 143:364–377.
- 917 38. Jiang RHY, Tripathy S, Govers F, Tyler BM. 2008. RXLR effector reservoir in two *Phytophthora*
918 species is dominated by a single rapidly evolving superfamily with more than 700 members.
919 *Proceedings of the National Academy of Sciences* 105.
- 920 39. Morgan W, Kamoun S. 2007. RXLR effectors of plant pathogenic oomycetes. *Curr Opin Microbiol*
921 10:332–338.
- 922 40. Zhang M, Li Q, Liu T, Liu L, Shen D, Zhu Y, Liu P, Zhou J-M, Dou D. 2014. Two Cytoplasmic Effectors
923 of *Phytophthora sojae* Regulate Plant Cell Death via Interactions with Plant Catalases. *Plant*
924 *Physiol* 167.
- 925 41. Schornack S, van Damme M, Bozkurt TO, Cano LM, Smoker M, Thines M, Gaulin E, Kamoun S,
926 Huitema E. 2010. Ancient class of translocated oomycete effectors targets the host nucleus.
927 *Proceedings of the National Academy of Sciences* 107.
- 928 42. Stam R, Jupe J, Howden AJM, Morris JA, Boevink PC, Hedley PE, Huitema E. 2013. Identification
929 and Characterisation CRN Effectors in *Phytophthora capsici* Shows Modularity and Functional
930 Diversity. *PLoS One* 8.
- 931 43. Win J, Kanneganti T-D, Torto-Alalibo T, Kamoun S. 2006. Computational and comparative
932 analyses of 150 full-length cDNA sequences from the oomycete plant pathogen *Phytophthora*
933 *infestans*. *Fungal Genetics and Biology* 43:20–33.
- 934 44. Torto TA. 2003. EST Mining and Functional Expression Assays Identify Extracellular Effector
935 Proteins From the Plant Pathogen *Phytophthora*. *Genome Res* 13:1675–1685.
- 936 45. Liu T, Song T, Zhang X, Yuan H, Su L, Li W, Xu J, Liu S, Chen L, Chen T, Zhang M, Gu L, Zhang B, Dou
937 D. 2014. Unconventionally secreted effectors of two filamentous pathogens target plant
938 salicylate biosynthesis. *Nat Commun* 5.

- 939 46. Oh S-K, Young C, Lee M, Oliva R, Bozkurt TO, Cano LM, Win J, Bos JIB, Liu H-Y, van Damme M,
940 Morgan W, Choi D, van der Vossen EAG, Vleeshouwers VGAA, Kamoun S. 2009. In Planta
941 Expression Screens of *Phytophthora infestans* RXLR Effectors Reveal Diverse Phenotypes,
942 Including Activation of the *Solanum bulbocastanum* Disease Resistance Protein Rpi-blb2. *Plant*
943 *Cell* 21:2928–2947.
- 944 47. Wang Q, Han C, Ferreira AO, Yu X, Ye W, Tripathy S, Kale SD, Gu B, Sheng Y, Sui Y, Wang X, Zhang
945 Z, Cheng B, Dong S, Shan W, Zheng X, Dou D, Tyler BM, Wang Y. 2011. Transcriptional
946 Programming and Functional Interactions within the *Phytophthora sojae* RXLR Effector
947 Repertoire . *Plant Cell* 23:2064–2086.
- 948 48. Torto-Alalibo T, Collmer CW, Gwinn-Giglio M, Lindeberg M, Meng S, Chibucos MC, Tseng T-T,
949 Lomax J, Biehl B, Ireland A, Bird D, Dean RA, Glasner JD, Perna N, Setubal JC, Collmer A, Tyler BM.
950 2010. Unifying Themes in Microbial Associations with Animal and Plant Hosts Described Using the
951 Gene Ontology. *Microbiology and Molecular Biology Reviews* 74.
- 952 49. Wang Y, Tyler BM, Wang Y. 2019. Defense and Counterdefense During Plant-Pathogenic
953 Oomycete Infection. *Annu Rev Microbiol* 73.
- 954 50. Bozkurt TO, Schornack S, Win J, Shindo T, Ilyas M, Oliva R, Cano LM, Jones AME, Huitema E, van
955 der Hoorn RAL, Kamoun S. 2011. *Phytophthora infestans* effector AVRblb2 prevents secretion of
956 a plant immune protease at the haustorial interface. *Proceedings of the National Academy of*
957 *Sciences* 108:20832–20837.
- 958 51. Caillaud M, Piquerez SJM, Fabro G, Steinbrenner J, Ishaque N, Beynon J, Jones JDG. 2012.
959 Subcellular localization of the *Hpa* RxLR effector repertoire identifies a tonoplast-associated
960 protein HaRxL17 that confers enhanced plant susceptibility. *The Plant Journal* 69:252–265.
- 961 52. Shen D, Liu T, Ye W, Liu L, Liu P, Wu Y, Wang Y, Dou D. 2013. Gene Duplication and Fragment
962 Recombination Drive Functional Diversification of a Superfamily of Cytoplasmic Effectors in
963 *Phytophthora sojae*. *PLoS One* 8.
- 964 53. Ye W, Wang Y, Tyler BM, Wang Y. 2016. Comparative Genomic Analysis among Four
965 Representative Isolates of *Phytophthora sojae* Reveals Genes under Evolutionary Selection. *Front*
966 *Microbiol* 7.
- 967 54. Gijzen M. 2009. Runaway repeats force expansion of the *Phytophthora infestans* genome.
968 *Genome Biol* 10:241.
- 969 55. Wang L, Chen H, Li J, Shu H, Zhang X, Wang Y, Tyler BM, Dong S. 2020. Effector gene silencing
970 mediated by histone methylation underpins host adaptation in an oomycete plant pathogen.
971 *Nucleic Acids Res* 48.
- 972 56. Blair JE, Coffey MD, Park S-Y, Geiser DM, Kang S. 2008. A multi-locus phylogeny for *Phytophthora*
973 utilizing markers derived from complete genome sequences. *Fungal Genetics and Biology*
974 45:266–277.

- 975 57. Nellist CF, Armitage AD, Bates HJ, Sobczyk MK, Luberti M, Lewis LA, Harrison RJ. 2021.
976 Comparative Analysis of Host-Associated Variation in *Phytophthora cactorum*. *Front Microbiol*
977 12.
- 978 58. van der Lee T, de Witte I, Drenth A, Alfonso C, Govers F. 1997. AFLP Linkage Map of the
979 Oomycete *Phytophthora infestans*. *Fungal Genetics and Biology* 21:278–291.
- 980 59. McCarthy CGP, Fitzpatrick DA. 2017. Phylogenomic Reconstruction of the Oomycete Phylogeny
981 Derived from 37 Genomes. *mSphere* 2.
- 982 60. Martin FN, Blair JE, Coffey MD. 2014. A combined mitochondrial and nuclear multilocus
983 phylogeny of the genus *Phytophthora*. *Fungal Genetics and Biology* 66.
- 984 61. Richards TA, Soanes DM, Jones MDM, Vasieva O, Leonard G, Paszkiewicz K, Foster PG, Hall N,
985 Talbot NJ. 2011. Horizontal gene transfer facilitated the evolution of plant parasitic mechanisms
986 in the oomycetes. *Proceedings of the National Academy of Sciences* 108.
- 987 62. Urban M, Cuzick A, Seager J, Wood V, Rutherford K, Venkatesh SY, De Silva N, Martinez MC,
988 Pedro H, Yates AD, Hassani-Pak K, Hammond-Kosack KE. 2019. PHI-base: the pathogen–host
989 interactions database. *Nucleic Acids Res* <https://doi.org/10.1093/nar/gkz904>.
- 990 63. Richards TA, Dacks JB, Jenkinson JM, Thornton CR, Talbot NJ. 2006. Evolution of Filamentous
991 Plant Pathogens: Gene Exchange across Eukaryotic Kingdoms. *Current Biology* 16.
- 992 64. McCarthy CGP, Fitzpatrick DA. 2016. Systematic Search for Evidence of Interdomain Horizontal
993 Gene Transfer from Prokaryotes to Oomycete Lineages. *mSphere* 1.
- 994 65. Keeling PJ, Palmer JD. 2008. Horizontal gene transfer in eukaryotic evolution. *Nat Rev Genet* 9.
- 995 66. Husnik F, McCutcheon JP. 2018. Functional horizontal gene transfer from bacteria to eukaryotes.
996 *Nat Rev Microbiol* 16.
- 997 67. Feurtey A, Stukenbrock EH. 2018. Interspecific Gene Exchange as a Driver of Adaptive Evolution
998 in Fungi. *Annu Rev Microbiol* 72.
- 999 68. van Etten J, Bhattacharya D. 2020. Horizontal Gene Transfer in Eukaryotes: Not if, but How
1000 Much? *Trends in Genetics* 36.
- 1001 69. Soucy SM, Huang J, Gogarten JP. 2015. Horizontal gene transfer: building the web of life. *Nat Rev*
1002 *Genet* 16.
- 1003 70. Möller EM, Bahnweg G, Sandermann H, Geiger HH. 1992. A simple and efficient protocol for
1004 isolation of high molecular weight DNA from filamentous fungi, fruit bodies, and infected plant
1005 tissues. *Nucleic Acids Res* 20:6115–6116.
- 1006 71. Johansen LK, Carrington JC. 2001. Silencing on the Spot. Induction and Suppression of RNA
1007 Silencing in the *Agrobacterium* -Mediated Transient Expression System. *Plant Physiol* 126:930–
1008 938.
- 1009 72. Kamoun S. 1993. Extracellular Protein Elicitors from *Phytophthora* : Host-Specificity and Induction
1010 of Resistance to Bacterial and Fungal Phytopathogens. *Molecular Plant-Microbe Interactions* 6.

- 1011 73. Feau N, Taylor G, Dale AL, Dhillon B, Bilodeau GJ, Birol I, Jones SJM, Hamelin RC. 2016. Genome
1012 sequences of six *Phytophthora* species threatening forest ecosystems. *Genom Data* 10:85–88.
- 1013 74. Studholme DJ, McDougal RL, Sambles C, Hansen E, Hardy G, Grant M, Ganley RJ, Williams NM.
1014 2016. Genome sequences of six *Phytophthora* species associated with forests in New Zealand.
1015 *Genom Data* 7:54–56.
- 1016 75. Martin M. 2011. Cutadapt removes adapter sequences from high-throughput sequencing reads.
1017 *EMBnet J* 17:10.
- 1018 76. Luo R, Liu B, Xie Y, Li Z, Huang W, Yuan J, He G, Chen Y, Pan Q, Liu Y, Tang J, Wu G, Zhang H, Shi Y,
1019 Liu Y, Yu C, Wang B, Lu Y, Han C, Cheung DW, Yiu S-M, Peng S, Xiaoqian Z, Liu G, Liao X, Li Y, Yang
1020 H, Wang J, Lam T-W, Wang J. 2012. SOAPdenovo2: an empirically improved memory-efficient
1021 short-read de novo assembler. *Gigascience* 1:18.
- 1022 77. Gu S, Fang L, Xu X. 2013. Using SOAPaligner for Short Reads Alignment. *Curr Protoc*
1023 *Bioinformatics* 44.
- 1024 78. Simpson JT, Wong K, Jackman SD, Schein JE, Jones SJM, Birol I. 2009. ABySS: A parallel assembler
1025 for short read sequence data. *Genome Res* 19:1117–1123.
- 1026 79. Bankevich A, Nurk S, Antipov D, Gurevich AA, Dvorkin M, Kulikov AS, Lesin VM, Nikolenko SI,
1027 Pham S, Prjibelski AD, Pyshkin A v., Sirotkin A v., Vyahhi N, Tesler G, Alekseyev MA, Pevzner PA.
1028 2012. SPAdes: A New Genome Assembly Algorithm and Its Applications to Single-Cell Sequencing.
1029 *Journal of Computational Biology* 19:455–477.
- 1030 80. Boetzer M, Henkel C v., Jansen HJ, Butler D, Pirovano W. 2011. Scaffolding pre-assembled contigs
1031 using SSPACE. *Bioinformatics* 27:578–579.
- 1032 81. Aronesty E. 2013. Comparison of Sequencing Utility Programs. *Open Bioinforma J* 7:1–8.
- 1033 82. Zerbino DR, Birney E. 2008. Velvet: Algorithms for de novo short read assembly using de Bruijn
1034 graphs. *Genome Res* 18:821–829.
- 1035 83. Marçais G, Kingsford C. 2011. A fast, lock-free approach for efficient parallel counting of
1036 occurrences of k-mers. *Bioinformatics* 27.
- 1037 84. R Core Team. 2019. R: A language and environment for statistical computing. R Foundation for
1038 Statistical Computing, Vienna, Austria. <https://www.R-project.org/>.
- 1039 85. Clark K, Karsch-Mizrachi I, Lipman DJ, Ostell J, Sayers EW. 2016. GenBank. *Nucleic Acids Res*
1040 44:D67–D72.
- 1041 86. Kent WJ. 2002. BLAT---The BLAST-Like Alignment Tool. *Genome Res* 12:656–664.
- 1042 87. Grabherr MG, Haas BJ, Yassour M, Levin JZ, Thompson DA, Amit I, Adiconis X, Fan L,
1043 Raychowdhury R, Zeng Q, Chen Z, Mauceli E, Hacohen N, Gnirke A, Rhind N, di Palma F, Birren
1044 BW, Nusbaum C, Lindblad-Toh K, Friedman N, Regev A. 2011. Full-length transcriptome assembly
1045 from RNA-Seq data without a reference genome. *Nat Biotechnol* 29:644–652.

- 1046 88. Haas BJ, Papanicolaou A, Yassour M, Grabherr M, Blood PD, Bowden J, Couger MB, Eccles D, Li B,
1047 Lieber M, MacManes MD, Ott M, Orvis J, Pochet N, Strozzi F, Weeks N, Westerman R, William T,
1048 Dewey CN, Henschel R, LeDuc RD, Friedman N, Regev A. 2013. De novo transcript sequence
1049 reconstruction from RNA-seq using the Trinity platform for reference generation and analysis.
1050 *Nat Protoc* 8:1494–1512.
- 1051 89. Altschul SF, Gish W, Miller W, Myers EW, Lipman DJ. 1990. Basic local alignment search tool. *J*
1052 *Mol Biol* 215:403–410.
- 1053 90. Ellinghaus D, Kurtz S, Willhoeft U. 2008. LTRharvest, an efficient and flexible software for de novo
1054 detection of LTR retrotransposons. *BMC Bioinformatics* 9:18.
- 1055 91. Xu Z, Wang H. 2007. LTR_FINDER: an efficient tool for the prediction of full-length LTR
1056 retrotransposons. *Nucleic Acids Res* 35:W265–W268.
- 1057 92. Cantarel BL, Korf I, Robb SMC, Parra G, Ross E, Moore B, Holt C, Sanchez Alvarado A, Yandell M.
1058 2007. MAKER: An easy-to-use annotation pipeline designed for emerging model organism
1059 genomes. *Genome Res* 18:188–196.
- 1060 93. Han Y, Wessler SR. 2010. MITE-Hunter: a program for discovering miniature inverted-repeat
1061 transposable elements from genomic sequences. *Nucleic Acids Res* 38:e199–e199.
- 1062 94. Gremme G, Steinbiss S, Kurtz S. 2013. GenomeTools: A Comprehensive Software Library for
1063 Efficient Processing of Structured Genome Annotations. *IEEE/ACM Trans Comput Biol Bioinform*
1064 10:645–656.
- 1065 95. Smit A, Hubley R. RepeatModeler Open-1.0. 2008-2015 <<http://www.repeatmasker.org>>.
- 1066 96. Bao Z. 2002. Automated De Novo Identification of Repeat Sequence Families in Sequenced
1067 Genomes. *Genome Res* 12:1269–1276.
- 1068 97. Price AL, Jones NC, Pevzner PA. 2005. De novo identification of repeat families in large genomes.
1069 *Bioinformatics* 21:i351–i358.
- 1070 98. Benson G. 1999. Tandem repeats finder: a program to analyze DNA sequences. *Nucleic Acids Res*
1071 27:573–580.
- 1072 99. Wootton JC, Federhen S. 1996. Methods in Enzymology; Analysis of compositionally biased
1073 regions in sequence databases, p. 554–571. *In* .
- 1074 100. Ou S, Jiang N. 2018. LTR_retriever: A Highly Accurate and Sensitive Program for Identification of
1075 Long Terminal Repeat Retrotransposons. *Plant Physiol* 176:1410–1422.
- 1076 101. Bao W, Kojima KK, Kohany O. 2015. Repbase Update, a database of repetitive elements in
1077 eukaryotic genomes. *Mob DNA* 6:11.
- 1078 102. Smit A, Hubley R, Green P. RepeatMasker Open-4.0. 2013-2015 <<http://www.repeatmasker.org>>.
- 1079 103. Stanke M, Morgenstern B. 2005. AUGUSTUS: a web server for gene prediction in eukaryotes that
1080 allows user-defined constraints. *Nucleic Acids Res* 33:W465–W467.

- 1081 104. Korf I. 2004. Gene finding in novel genomes. *BMC Bioinformatics* 5:59.
- 1082 105. Seppey M, Manni M, Zdobnov EM. 2019. BUSCO: Assessing Genome Assembly and Annotation
1083 Completeness, p. 227–245. *In* .
- 1084 106. O’Leary NA, Wright MW, Brister JR, Ciufo S, Haddad D, McVeigh R, Rajput B, Robbertse B, Smith-
1085 White B, Ako-Adjei D, Astashyn A, Badretdin A, Bao Y, Blinkova O, Brover V, Chetvernin V, Choi J,
1086 Cox E, Ermolaeva O, Farrell CM, Goldfarb T, Gupta T, Haft D, Hatcher E, Hlavina W, Joardar VS,
1087 Kodali VK, Li W, Maglott D, Masterson P, McGarvey KM, Murphy MR, O’Neill K, Pujar S, Rangwala
1088 SH, Rausch D, Riddick LD, Schoch C, Shkeda A, Storz SS, Sun H, Thibaud-Nissen F, Tolstoy I, Tully
1089 RE, Vatsan AR, Wallin C, Webb D, Wu W, Landrum MJ, Kimchi A, Tatusova T, DiCuccio M, Kitts P,
1090 Murphy TD, Pruitt KD. 2016. Reference sequence (RefSeq) database at NCBI: current status,
1091 taxonomic expansion, and functional annotation. *Nucleic Acids Res* 44.
- 1092 107. 2019. UniProt: a worldwide hub of protein knowledge. *Nucleic Acids Res* 47:D506–D515.
- 1093 108. Jones P, Binns D, Chang H-Y, Fraser M, Li W, McAnulla C, McWilliam H, Maslen J, Mitchell A, Nuka
1094 G, Pesseat S, Quinn AF, Sangrador-Vegas A, Scheremetjew M, Yong S-Y, Lopez R, Hunter S. 2014.
1095 InterProScan 5: genome-scale protein function classification. *Bioinformatics* 30:1236–1240.
- 1096 109. 2019. The Gene Ontology Resource: 20 years and still GOing strong. *Nucleic Acids Res* 47:D330–
1097 D338.
- 1098 110. Ashburner M, Ball CA, Blake JA, Botstein D, Butler H, Cherry JM, Davis AP, Dolinski K, Dwight SS,
1099 Eppig JT, Harris MA, Hill DP, Issel-Tarver L, Kasarskis A, Lewis S, Matese JC, Richardson JE,
1100 Ringwald M, Rubin GM, Sherlock G. 2000. Gene Ontology: tool for the unification of biology. *Nat*
1101 *Genet* 25:25–29.
- 1102 111. Rice P, Longden I, Bleasby A. 2000. EMBOSS: The European Molecular Biology Open Software
1103 Suite. *Trends in Genetics* 16:276–277.
- 1104 112. Win J, Morgan W, Bos J, Krasileva K v., Cano LM, Chaparro-Garcia A, Ammar R, Staskawicz BJ,
1105 Kamoun S. 2007. Adaptive Evolution Has Targeted the C-Terminal Domain of the RXLR Effectors
1106 of Plant Pathogenic Oomycetes. *Plant Cell* 19:2349–2369.
- 1107 113. Tabima JF, Grünwald NJ. 2019. *effectR* : An Expandable R Package to Predict Candidate RxLR and
1108 CRN Effectors in Oomycetes Using Motif Searches. *Molecular Plant-Microbe Interactions*® 32.
- 1109 114. Eddy SR. 1998. Profile hidden Markov models. *Bioinformatics* 14:755–763.
- 1110 115. Eddy SR. HMMER www.hmmerr.org.
- 1111 116. Dyrlov Bendtsen J, Nielsen H, von Heijne G, Brunak S. 2004. Improved Prediction of Signal
1112 Peptides: SignalP 3.0. *J Mol Biol* 340.
- 1113 117. Rawlings ND, Barrett AJ, Bateman A. 2012. MEROPS: the database of proteolytic enzymes, their
1114 substrates and inhibitors. *Nucleic Acids Res* 40:D343–D350.
- 1115 118. Yin Y, Mao X, Yang J, Chen X, Mao F, Xu Y. 2012. dbCAN: a web resource for automated
1116 carbohydrate-active enzyme annotation. *Nucleic Acids Res* 40:W445–W451.

- 1117 119. El-Gebali S, Mistry J, Bateman A, Eddy SR, Luciani A, Potter SC, Qureshi M, Richardson LJ, Salazar
1118 GA, Smart A, Sonnhammer ELL, Hirsh L, Paladin L, Piovesan D, Tosatto SCE, Finn RD. 2019. The
1119 Pfam protein families database in 2019. *Nucleic Acids Res* 47:D427–D432.
- 1120 120. Li L. 2003. OrthoMCL: Identification of Ortholog Groups for Eukaryotic Genomes. *Genome Res*
1121 13:2178–2189.
- 1122 121. Chen F. 2006. OrthoMCL-DB: querying a comprehensive multi-species collection of ortholog
1123 groups. *Nucleic Acids Res* 34:D363–D368.
- 1124 122. Nakamura T, Yamada KD, Tomii K, Katoh K. 2018. Parallelization of MAFFT for large-scale multiple
1125 sequence alignments. *Bioinformatics* 34:2490–2492.
- 1126 123. Katoh K, Standley DM. 2013. MAFFT Multiple Sequence Alignment Software Version 7:
1127 Improvements in Performance and Usability. *Mol Biol Evol* 30:772–780.
- 1128 124. Stamatakis A. 2014. RAxML version 8: a tool for phylogenetic analysis and post-analysis of large
1129 phylogenies. *Bioinformatics* 30:1312–1313.
- 1130 125. H. Wickham. 2016. *ggplot2: Elegant Graphics for Data Analysis*. Springer-Verlag.
- 1131 126. Sharp PM, Matassi G. 1994. Codon usage and genome evolution. *Curr Opin Genet Dev* 4:851–
1132 860.
- 1133 127. Boser BE, Guyon IM, Vapnik VN. 1992. A training algorithm for optimal margin classifiers, p. 144–
1134 152. *In Proceedings of the fifth annual workshop on Computational learning theory - COLT '92*.
- 1135 128. Pedregosa F, Varoquaux G, Gramfort A, Michel V, Thirion B, Grisel O, Blondel M, Prettenhofer P,
1136 Weiss R, Dubourg V, Vanderplas J, Passos A, Cournapeau D, Brucher M, Perrot M, Duchesnay É.
1137 2011. Scikit-Learn: Machine Learning in Python. *J Mach Learn Res* 12:2825–2830.
- 1138 129. Martin F, Kohler A, Murat C, Balestrini R, Coutinho PM, Jaillon O, Montanini B, Morin E, Noel B,
1139 Percudani R, Porcel B, Rubini A, Amicucci A, Amselem J, Anthouard V, Arcioni S, Artiguenave F,
1140 Aury J-M, Ballario P, Bolchi A, Brenna A, Brun A, Buée M, Cantarel B, Chevalier G, Couloux A, da
1141 Silva C, Denoeud F, Duplessis S, Ghignone S, Hilselberger B, Iotti M, Marçais B, Mello A, Miranda
1142 M, Pacioni G, Quesneville H, Riccioni C, Ruotolo R, Splivallo R, Stocchi V, Tisserant E, Viscomi AR,
1143 Zambonelli A, Zampieri E, Henrissat B, Lebrun M-H, Paolocci F, Bonfante P, Ottonello S, Wincker
1144 P. 2010. Périgord black truffle genome uncovers evolutionary origins and mechanisms of
1145 symbiosis. *Nature* 464.
- 1146 130. Yang J, Wang L, Ji X, Feng Y, Li X, Zou C, Xu J, Ren Y, Mi Q, Wu J, Liu S, Liu Y, Huang X, Wang H, Niu
1147 X, Li J, Liang L, Luo Y, Ji K, Zhou W, Yu Z, Li G, Liu Y, Li L, Qiao M, Feng L, Zhang K-Q. 2011. Genomic
1148 and Proteomic Analyses of the Fungus *Arthrobotrys oligospora* Provide Insights into Nematode-
1149 Trap Formation. *PLoS Pathog* 7.
- 1150 131. van den Berg MA, Albang R, Albermann K, Badger JH, Daran J-M, M Driessen AJ, Garcia-Estrada C,
1151 Fedorova ND, Harris DM, Heijne WHM, Joardar V, W Kiel JAK, Kovalchuk A, Martín JF, Nierman
1152 WC, Nijland JG, Pronk JT, Roubos JA, van der Klei IJ, van Peij NNME, Veenhuis M, von Döhren H,
1153 Wagner C, Wortman J, Bovenberg RAL. 2008. Genome sequencing and analysis of the
1154 filamentous fungus *Penicillium chrysogenum*. *Nat Biotechnol* 26.

- 1155 132. Rouxel T, Grandaubert J, Hane JK, Hoede C, van de Wouw AP, Couloux A, Dominguez V,
1156 Anthouard V, Bally P, Bourras S, Cozijnsen AJ, Ciuffetti LM, Degrave A, Dilmaghani A, Duret L,
1157 Fudal I, Goodwin SB, Gout L, Glaser N, Linglin J, Kema GHJ, Lapalu N, Lawrence CB, May K, Meyer
1158 M, Ollivier B, Poulain J, Schoch CL, Simon A, Spatafora JW, Stachowiak A, Turgeon BG, Tyler BM,
1159 Vincent D, Weissenbach J, Amselem J, Quesneville H, Oliver RP, Wincker P, Balesdent M-H,
1160 Howlett BJ. 2011. Effector diversification within compartments of the *Leptosphaeria maculans*
1161 genome affected by Repeat-Induced Point mutations. *Nat Commun* 2.
- 1162 133. Yang J, Wang L, Ji X, Feng Y, Li X, Zou C, Xu J, Ren Y, Mi Q, Wu J, Liu S, Liu Y, Huang X, Wang H, Niu
1163 X, Li J, Liang L, Luo Y, Ji K, Zhou W, Yu Z, Li G, Liu Y, Li L, Qiao M, Feng L, Zhang K-Q. 2011. Genomic
1164 and Proteomic Analyses of the Fungus *Arthrobotrys oligospora* Provide Insights into Nematode-
1165 Trap Formation. *PLoS Pathog* 7.
- 1166 134. Amselem J, Cuomo CA, van Kan JAL, Viaud M, Benito EP, Couloux A, Coutinho PM, de Vries RP,
1167 Dyer PS, Fillinger S, Fournier E, Gout L, Hahn M, Kohn L, Lapalu N, Plummer KM, Pradier J-M,
1168 Quévillon E, Sharon A, Simon A, ten Have A, Tudzynski B, Tudzynski P, Wincker P, Andrew M,
1169 Anthouard V, Beever RE, Beffa R, Benoit I, Bouzid O, Brault B, Chen Z, Choquer M, Collémare J,
1170 Cotton P, Danchin EG, da Silva C, Gautier A, Giraud C, Giraud T, Gonzalez C, Grossetete S,
1171 Guldener U, Henrissat B, Howlett BJ, Kodira C, Kretschmer M, Lappartient A, Leroch M, Levis C,
1172 Mauceli E, Neuvéglise C, Oeser B, Pearson M, Poulain J, Poussereau N, Quesneville H, Rasclé C,
1173 Schumacher J, Ségurens B, Sexton A, Silva E, Sirven C, Soanes DM, Talbot NJ, Templeton M,
1174 Yandava C, Yarden O, Zeng Q, Rollins JA, Lebrun M-H, Dickman M. 2011. Genomic Analysis of the
1175 Necrotrophic Fungal Pathogens *Sclerotinia sclerotiorum* and *Botrytis cinerea*. *PLoS Genet* 7.
- 1176 135. Cuomo CA, Guldener U, Xu J-R, Trail F, Turgeon BG, di Pietro A, Walton JD, Ma L-J, Baker SE, Rep
1177 M, Adam G, Antoniw J, Baldwin T, Calvo S, Chang Y-L, DeCaprio D, Gale LR, Gnerre S, Goswami RS,
1178 Hammond-Kosack K, Harris LJ, Hilburn K, Kennell JC, Kroken S, Magnuson JK, Mannhaupt G,
1179 Mauceli E, Mewes H-W, Mitterbauer R, Muehlbauer G, Munsterkotter M, Nelson D, O'Donnell K,
1180 Ouellet T, Qi W, Quesneville H, Roncero MIG, Seong K-Y, Tetko I v., Urban M, Waalwijk C, Ward
1181 TJ, Yao J, Birren BW, Kistler HC. 2007. The *Fusarium graminearum* Genome Reveals a Link
1182 Between Localized Polymorphism and Pathogen Specialization. *Science* (1979) 317.
- 1183 136. Gazis R, Kuo A, Riley R, LaButti K, Lipzen A, Lin J, Amirebrahimi M, Hesse CN, Spatafora JW,
1184 Henrissat B, Hainaut M, Grigoriev I v., Hibbett DS. 2016. The genome of *Xylona heveae* provides a
1185 window into fungal endophytism. *Fungal Biol* 120.
- 1186 137. WU X-M. 2007. The analysis method and progress in the study of codon bias. *Hereditas* 29:420.
- 1187 138. Buchfink B, Xie C, Huson DH. 2015. Fast and sensitive protein alignment using DIAMOND. *Nat*
1188 *Methods* 12:59–60.
- 1189 139. Kalyaanamoorthy S, Minh BQ, Wong TKF, von Haeseler A, Jermini LS. 2017. ModelFinder: fast
1190 model selection for accurate phylogenetic estimates. *Nat Methods* 14:587–589.
- 1191 140. Nguyen L-T, Schmidt HA, von Haeseler A, Minh BQ. 2015. IQ-TREE: A Fast and Effective Stochastic
1192 Algorithm for Estimating Maximum-Likelihood Phylogenies. *Mol Biol Evol* 32:268–274.

- 1193 141. Hoang DT, Chernomor O, von Haeseler A, Minh BQ, Vinh LS. 2018. UFBoot2: Improving the
1194 Ultrafast Bootstrap Approximation. *Mol Biol Evol* 35:518–522.
- 1195 142. Stöver BC, Müller KF. 2010. TreeGraph 2: Combining and visualizing evidence from different
1196 phylogenetic analyses. *BMC Bioinformatics* 11:7.
- 1197 143. Burki F, Roger AJ, Brown MW, Simpson AGB. 2020. The New Tree of Eukaryotes. *Trends Ecol Evol*
1198 35.
- 1199 144. Keeling PJ, Burki F. 2019. Progress towards the Tree of Eukaryotes. *Current Biology* 29.
- 1200 145. Novichkov PS, Omelchenko M v., Gelfand MS, Mironov AA, Wolf YI, Koonin E v. 2004. Genome-
1201 Wide Molecular Clock and Horizontal Gene Transfer in Bacterial Evolution. *J Bacteriol* 186:6575–
1202 6585.
- 1203
- 1204

Table 1. Sequencing and assembly statistics for 31 *Phytophthora* species grouped by clade.

Species	Clade	Genome			Annotations	
		Contigs	N ₅₀	Assembly Length	Repeat Percent	Predicted Genes
<i>P. cactorum</i>	1	7888	15053	56443298	19.96	18027
<i>P. idaei</i>	1	7163	14461	53468943	16.19	18038
<i>P. pini</i>	2	2131	42987	38730000	7.31	14019
<i>P. multivora</i>	2	2844	46133	40059192	10.86	13682
<i>P. pluvialis</i>	3	4340	30816	53616150	16.04	16285
<i>P. litchii</i>	4	2543	34546	38200938	5.98	12391
<i>P. palmivora</i>	4	24815	6694	107798747	29.62	37283
<i>P. megakarya</i>	4	24073	7093	101609312	31.94	33614
<i>P. agathidicida</i>	5	3754	19544	37337699	5.76	12923
<i>P. taxon totara</i>	5	4425	30809	55576372	16.56	17619
<i>P. parvispora</i>	7	9906	6820	46825958	8.75	15642
<i>P. pisi</i>	7	7667	15253	58856683	16.80	18953
<i>P. robiniae</i>	7	14865	8754	69938814	25.58	23128
<i>P. niederhauseri</i>	7	26463	4805	90270009	20.96	29587
<i>P. cajani</i>	7	18255	5113	64854085	20.65	19840
<i>P. vignae</i>	7	10330	8363	56137732	17.45	18535
<i>P. melonis</i>	7	11353	15342	73416743	25.93	21276
<i>P. pistaciae</i>	7	10414	10302	63209321	18.56	19423
<i>P. uliginosa</i>	7	8955	10095	57072031	24.16	17226
<i>P. europaea</i>	7	8301	11551	58787065	23.33	17117
<i>P. fragariae</i>	7	8544	20362	76969737	30.81	20448
<i>P. rubi</i>	7	9434	17808	74863594	29.48	23476
<i>P. pinifolia</i>	6	22610	6021	74478861	33.00	23717
<i>P. lateralis</i>	8	28263	2396	50496828	23.39	19503
<i>P. hibernalis</i>	8	6587	21408	71256216	32.46	23578
<i>P. foliorum</i>	8	5320	15800	48973082	19.26	16083
<i>P. brassicae</i>	8	12447	12337	72849437	28.39	26010
<i>P. syringae</i>	8	6572	15987	57045526	21.71	18234
<i>P. cryptogea</i>	8	25944	4730	69446343	17.65	24936
<i>P. boehmeriae</i>	10	2866	41917	39747814	7.83	13325
<i>P. kernoviae</i>	10	13710	5225	42698878	4.15	14322

Table 2. Over-represented GO terms for a set of 44 candidate HGT transcripts found in 36 *Phytophthora* genomes.

GO	Term	# terms in full set ^a	# terms in HGT set ^b	Pr(X=k) ^c
Biological process				
GO:0055114	obsolete oxidation-reduction process	1543	5	<0.001
GO:0034079	butanediol biosynthetic process	28	5	<0.001
GO:0045493	xylan catabolic process	151	1	<0.01
GO:0008152	Metabolism	3663	3	<0.01
GO:0042545	cell wall modification	493	1	<0.02
GO:0000272	polysaccharide catabolism	635	1	<0.02
GO:0002084	protein depalmitoylation	374	1	<0.02
GO:0006118	electron transport	1389	1	<0.05
GO:0045490	pectin catabolic process	865	1	<0.05
Molecular function				
GO:0016491	oxidoreductase activity	10881	11	<0.001
GO:0000721	(R,R)-butanediol dehydrogenase activity	28	5	<0.001
GO:0003939	L-iditol 2-dehydrogenase activity	11	1	<0.001
GO:0016831	carboxy-lyase activity	201	6	<0.001
GO:0008080	N-acetyltransferase activity	1082	3	<0.001
GO:0008270	zinc ion binding	26982	8	<0.001
GO:0005488	Binding	2200	2	<0.01
GO:0031176	endo-1,4-beta-xylanase activity	111	1	<0.01
GO:0008670	2,4-dienoyl-CoA reductase (NADPH) activity	15	1	<0.01
GO:0004022	alcohol dehydrogenase activity	102	1	<0.01
GO:0030599	pectinesterase activity	498	1	<0.02
GO:0008474	palmitoyl-(protein) hydrolase activity	457	1	<0.02
GO:0051213	dioxygenase activity	460	1	<0.02
GO:0045330	aspartyl esterase activity	423	1	<0.02
GO:0030570	pectate lyase activity	657	1	<0.02
GO:0015267	channel activity	742	1	<0.05
Cellular component				
GO:0005576	extracellular region	4624	2	<0.02

^aTranscriptome of 35 *Phytophthora* genomes.

^b44 HGT candidates.

^cProbability (q-value) of obtaining the same number of transcripts (k) or more by chance as given by a hypergeometric probability distribution.

Table 3. Summary of 19 HGT candidates with strong phylogenetic support identified among *Phytophthora* spp.

	Putative function	Best hit on PHI-base (e-value) ^a	HGT identification ²	# of Phyto. species	# of Phyto. clades	Closest clade ³
Transfer from other groups to oomycetes						
HGT_1	Endonuclease	PHI:5754, endonuclease, <i>Fusarium graminearum</i> (3.0e-024)	SVM, IP, D, T	29	8	Fungi
HGT_2	Xylulose reductase	PHI:2256, xylitol dehydrogenase, <i>Parastagonospora nodorum</i> (1.0e-128)	SVM, IP, D, T	12	5	Fungi
HGT_15	Zinc-binding dehydrogenase, Polyketide synthase, enoylreductase domain	PHI:8321, gluconate 5-dehydrogenase, <i>Salmonella enterica</i> (1.0e-016)	SVM, IP, D, T	21	8	Bacteria
HGT_4	Aquaporin	PHI:7047, water channel protein aquaporin, <i>Cryptococcus neoformans</i> (4.0e-012)	SVM, IP, D, T	30	8	Bacteria
HGT_5	NPP1	-	SVM, IP, D, T	4	1	Bacteria
HGT_6	Phenol acid carboxylase	-	SVM, MC, D, T	35	9	Fungi
HGT_7	Peptidase S9	-	SVM, IP, D, T	8	1	Fungi
HGT_8	UDP-N-acetylglucosamine-peptide N-acetylglucosaminyl-transferase	PHI:4921, flagellin glycosyltransferase, <i>Burkholderia cenocepacia</i> (1.0e-021)	SVM, IP, D, T	2	2	Bacteria
HGT_9	Alternative oxidase	-	SVM, IP, D	10	4	Fungi
HGT_10	Dioxygenase	-	SVM, MC, D, T	33	9	Fungi
HGT_11	Thioesterase	PHI:4988, sfp-type 4'-phosphopantetheinyl transferase, <i>Bipolaris maydis</i> (3.0e-005)	SVM, IP, D, T	35	8	Amoebozoa
HGT_12	Endo-1,4-beta-xylanase GH10	PHI:7912, endo-beta-1,4-xylanase <i>Phytophthora parasitica</i> (1.0e-137)	SVM, IP, D, T	33	9	Fungi
HGT_13	4-coumarate CoA ligase	PHI:10606, long-chain-fatty-acid-Co Aligase, <i>Pseudomonas aeruginosa</i> (1.0e-032)	SVM, IP, D, T	4	4	Fungi/ Bacteria
HGT_14	2,4-dienoyl-CoA reductase	PHI:8134, 3-Oxoacyl-[acyl-carrier-protein] reductase, <i>Salmonella enterica</i> (1.0e-014)	SVM, IP, D	28	7	Bacteria/ Archaea
HGT_20	Ribosomal-protein-alanine acetyltransferase	-	SVM, IP, D	29	9	Bacteria

Transfer from oomycetes to other groups						
HGT_3	Quinone oxidoreductase	-	SVM, IP, D, T	23	9	Fungi
HGT_16	Putative tannase	PHI:10222, feruloyl esterase, <i>Valsa mali</i> (4.0e-030)	SVM, IP, D, T	33	8	Bacteria
HGT_17	Putative pectinesterase CE8	PHI:278, pectin methylesterase, <i>Botrytis cinerea</i> (4.0e-077)	SVM, IP, D, T	34	9	Fungi
HGT_18	ATP-binding Cassette (ABC)	-	SVM, IP, D,	34	9	Fungi

^a Best BLASTp hit on the Pathogen Host Interaction database PHI-base (Urban et al. 2019); ²SVM, support vector machine; IP, incongruent phylogeny; MC, missing clades; D, distance; T, Alternate topology test (Shimodaira-Hasegawa-test) significant; ³as reported in BLASTp analysis; ³HB, only hemibiotrophic Peronosporales i.e. *Phytophthora*, *Phytophthium* and *Nothophytophthora*.

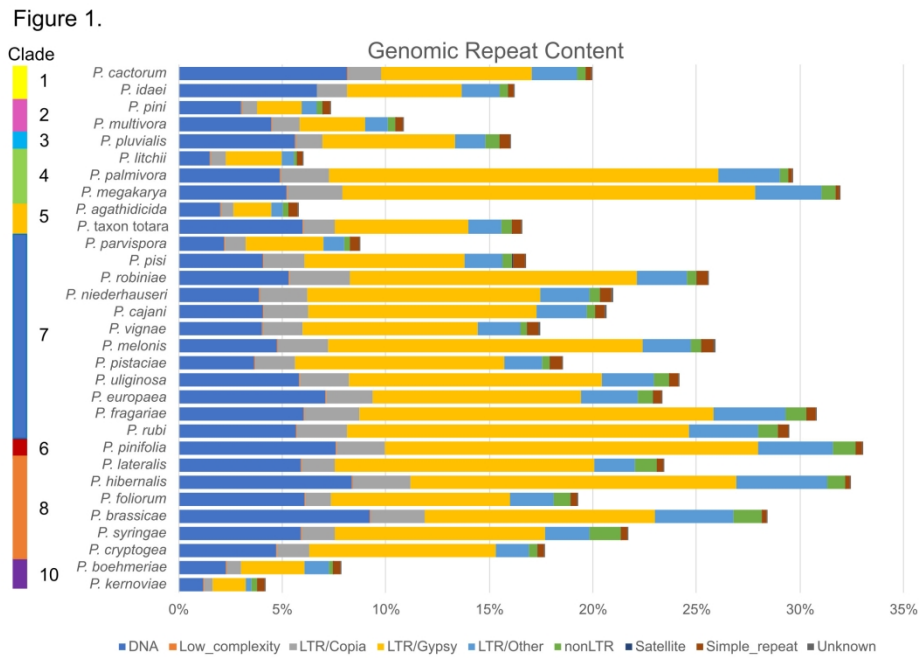


Figure 1. Analysis of 31 *Phytophthora* species shows an abundance of repetitive elements. Species are shown in phylogenetic clade order; clade designations are shown on the left. Repeat content is displayed as percentage of the total genome content. Repeat classifications are shown as colored bar segments.

705x481mm (90 x 90 DPI)

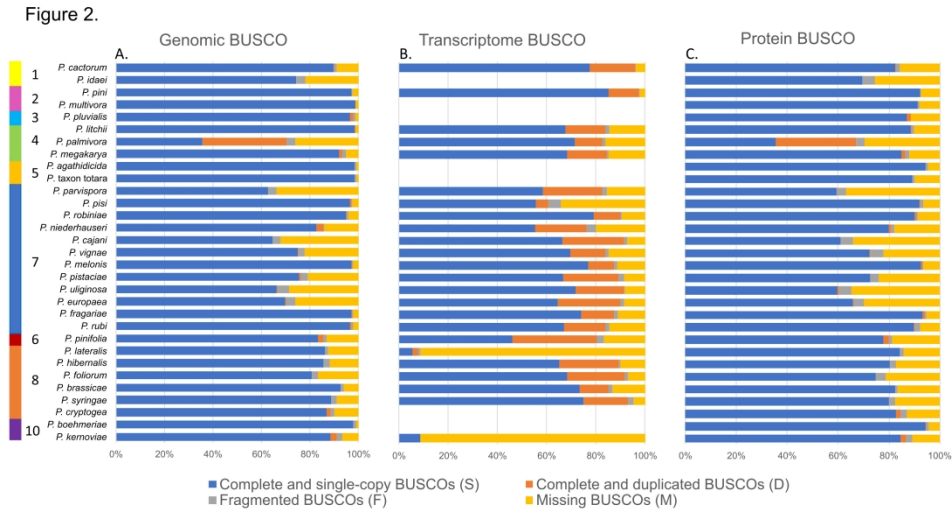


Figure 2. BUSCO analysis demonstrates completeness of the 31 *Phytophthora* species in this study. A) genomic assembly, B) transcriptome assembly, and C) predicted proteins. Species are shown in phylogenetic clade order and clade designations are shown on the left. For each BUSCO analysis, results from searching 234 single copy orthologs in the Alveolata_Stamenopiles dataset are shown.

987x518mm (90 x 90 DPI)

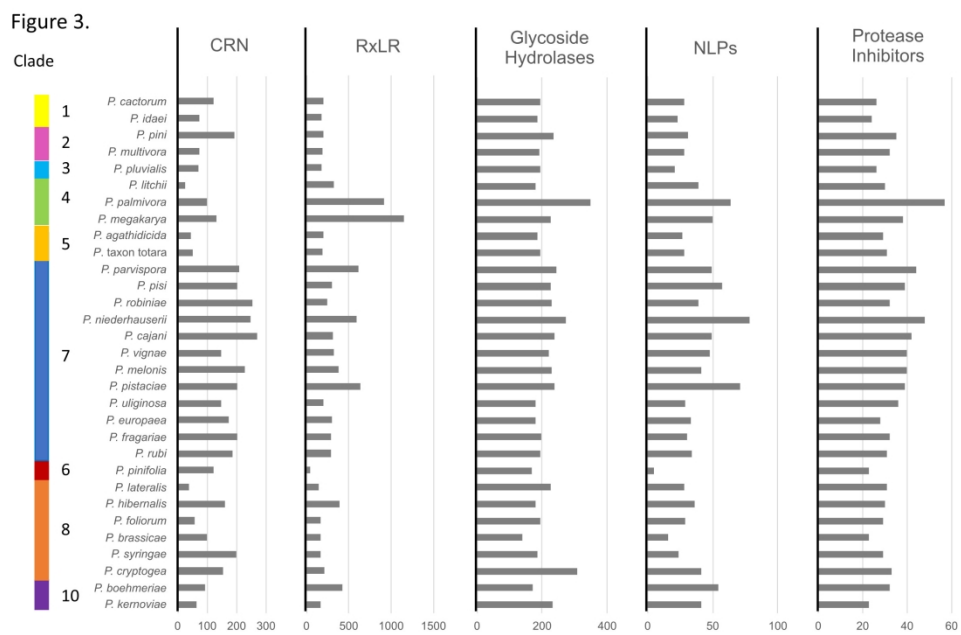


Figure 3. The number of predicted effectors varied across the *Phytophthora* genomes. Bar chart representing amounts of effector genes found in 31 *Phytophthora* species for crinkler (CRN), RxLR, glycoside hydrolases, necrosis inducing proteins (NLPs), and protease inhibitors. Species are shown in phylogenetic clade order, clade designations are shown on the left.

705x481mm (90 x 90 DPI)

Figure 4.

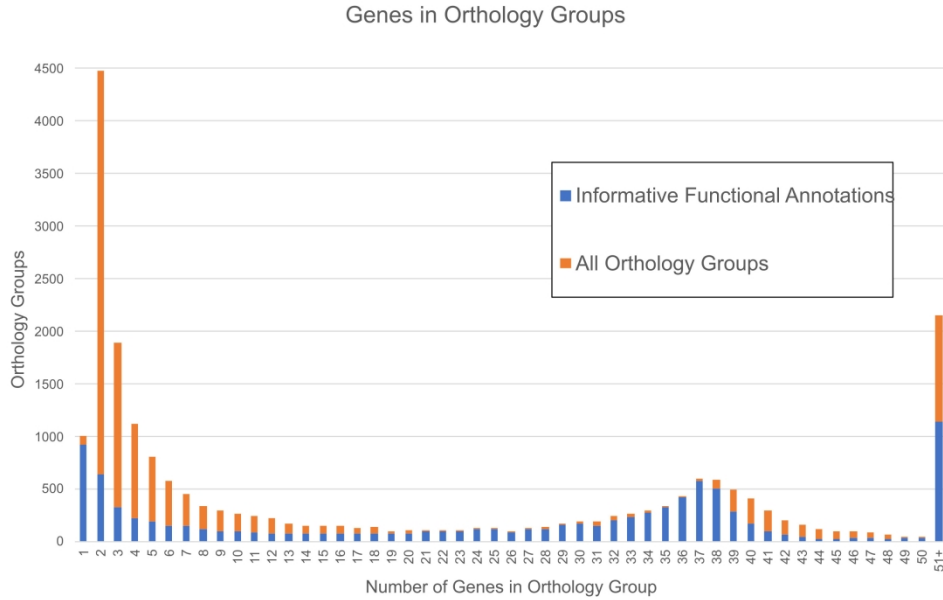


Figure 4. Distribution of genes in *Phytophthora* orthology shows a bimodal frequency distribution, highlighting genes that are conserved in only a few genomes and orthology groups that have one gene per species. Amounts of genes assigned to orthology cluster with OrthoMCL (118) are shown. The 31 sequenced *Phytophthora* and six additional previously sequenced *Phytophthora* genomes (*P. capsici*, *P. cinnanomi*, *P. infestans*, *P. parasitica*, *P. ramorum*, *P. sojae*) are included. 'All Orthology Groups' (orange) show all genes assigned into orthology groups. 'Informative Functional Annotations' show genes assigned into orthology groups that have useful functional definitions and exclude genes labeled as 'uncharacterized', 'hypothetical', or similar.

846x623mm (90 x 90 DPI)

Figure 5.

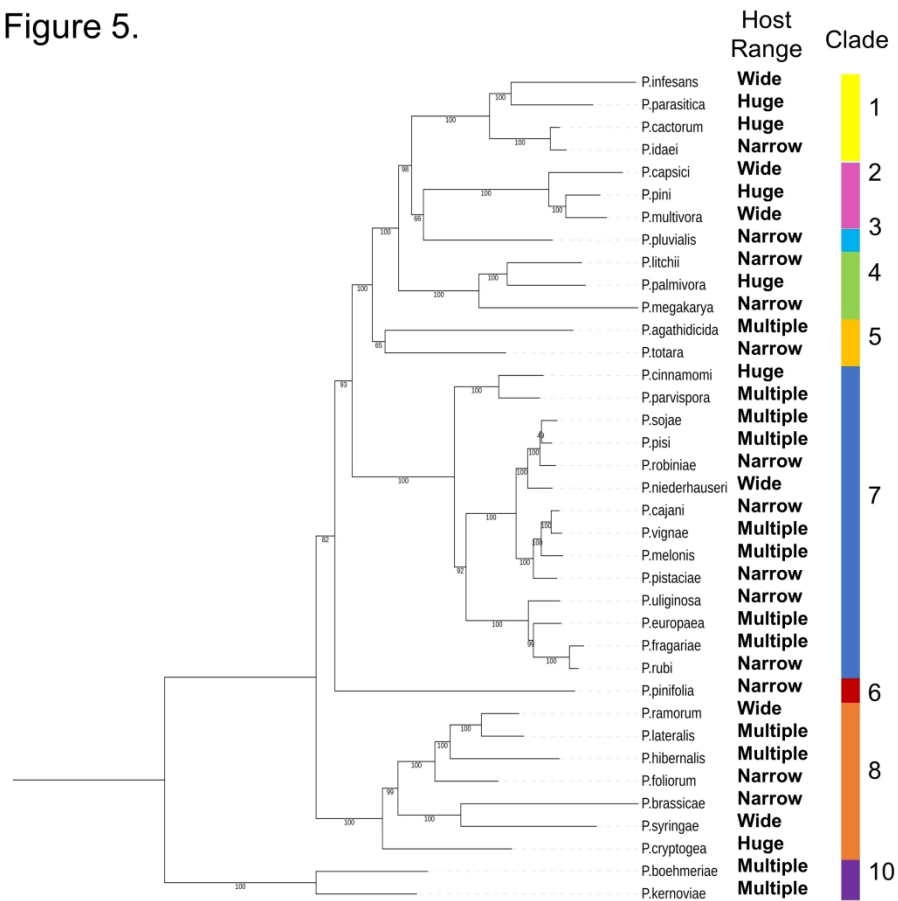


Figure 5. Phylogenetic relationships of the 31 sequenced *Phytophthora* spp. and six additional previously sequenced *Phytophthora* spp. Sixty-one single-copy core orthologous proteins shared across 37 species were used to create a RAxML (122) phylogenetic tree using each gene as an independent partition with its own substitution model and bootstrapped 1,000 times. Ranges of infected hosts are shown next to the phylogenetic tree species defined as 'Narrow', host species confined to 1 plant host genus; 'Multiple', host species confined within 2 to 9 host genera; 'Wide', host species spanning 16-55 host genera; and 'Huge', host species spanning 107-327 host genera. Clade assignments are shown on the right.

812x762mm (96 x 96 DPI)

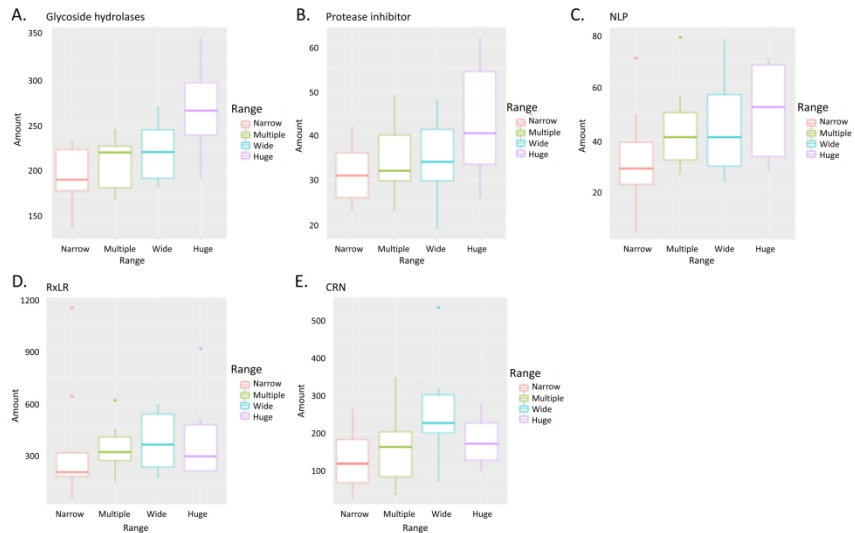


Figure 6. Generally, *Phytophthora* with larger host range showed a greater predicted number of effector genes. Box plots showing amounts of effectors found per *Phytophthora* species, categorized into 'Narrow' (1 plant genera), 'Multiple' (2-9 plant genus), 'Wide' (16-55 host genera), and 'Huge' (107-327 host genera) host ranges. Effectors glycoside hydrolases (A), protease inhibitors (B), NLPs (C), RxLRs (D), and CRNs (E) are shown. Near identical paralogs were removed; proteins with greater than 95% amino acid identity over the full sequence length were reduced to one representative effector sequence. Statistically significant classifications were seen between the Narrow-Wide and Narrow-Huge comparisons in glycoside hydrolases (A).

1016x571mm (90 x 90 DPI)

Figure 7.

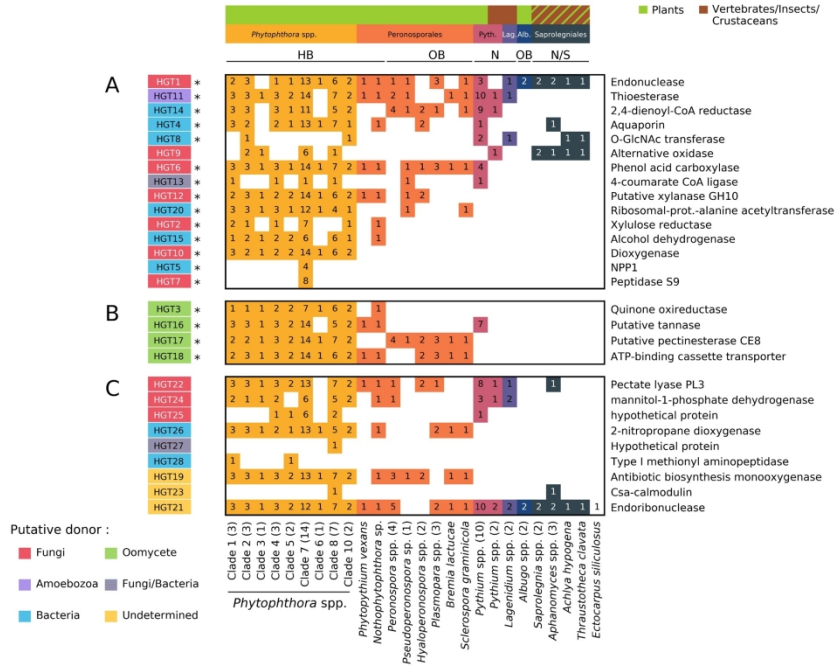


Figure 7. Conservation level of the 44 *Phytophthora* HGT candidates in oomycetes. A and B, set of 19 HGT candidates for which a maximum likelihood phylogeny was reconstructed and alternate tree topologies were tested with the Shimodaira-Hasegawa test (an asterisk indicate significant topological difference [P < 0.05] between the constrained alternate topology and the observed topology; A, HGT to oomycetes; B, HGT for the opposite relationships i.e. transfers from oomycetes to fungi or bacteria; C, HGT candidates with no maximum likelihood phylogeny support. For each HGT candidate the number of sequence homologs identified among 37 *Phytophthora* and 30 oomycetes transcriptomes (identified by reciprocal DIAMOND BLASTp, minimum E-value of 1e-03, sequence subject coverage of 50% and sequence query coverage of 50%; a dash indicates the absence of a one-to-one ortholog) is reported. The filamentous brown alga *Ectocarpus siliculosus* (Ectocarpales, Ectocarpaceae) was used as an outgroup. Putative functions are indicated on the right. Top rows: Pyth., Pythiales; Lag., Lagenidiales; Alb., Albuginales; HB, hemibiotrophic lifestyle; OB, obligate biotrophic; S, saprotrophic; N, necrotrophic. Species names, *Phytophthora* clade names and group of species names are indicated on the bottom; numbers between brackets indicate the number of species considered in a group.

Figure S1.

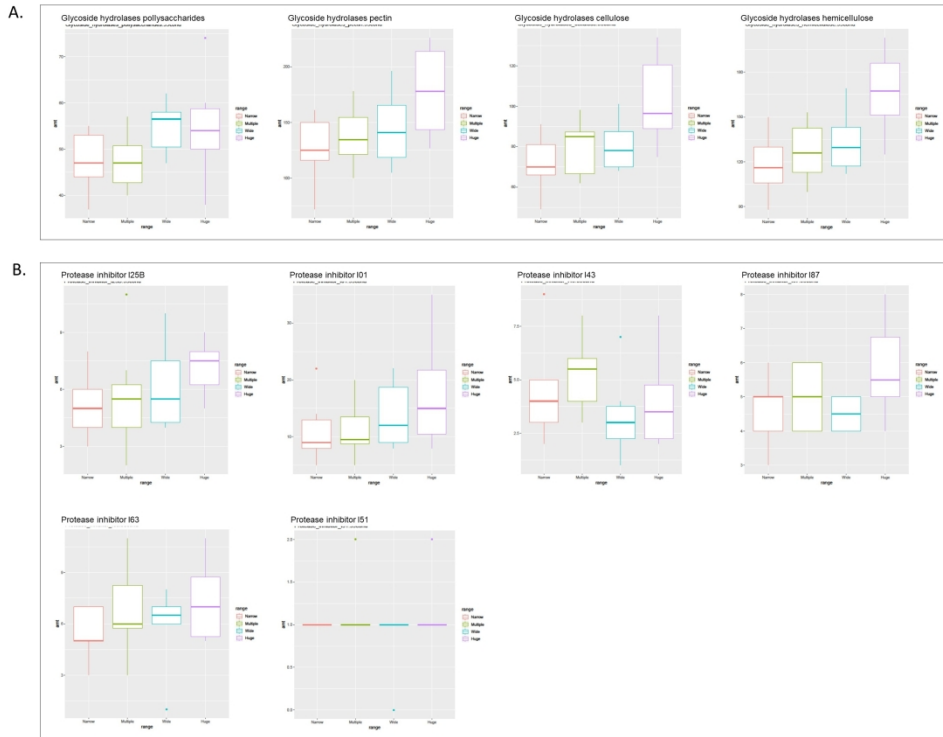


Figure S1. Box plots showing amounts of glycoside hydrolases, sorted by substrate, in *Phytophthora* species and categorized into host ranges 'Narrow' (1 plant genera), 'Multiple' (2-9 plant genus), 'Wide' (16-55 host genera), and 'Huge' (107-327 host genera). Glycoside hydrolases polysaccharides, pectins, cellulose, and hemicellulose are shown (A). For protease inhibitors, I01, I25B, I43, I51, I63, and I87 are shown (B). Near identical paralogs were removed; proteins with greater than 95% amino acid identity over the full sequence length were reduced to one representative effector sequence.

762x609mm (96 x 96 DPI)

Figure S2.

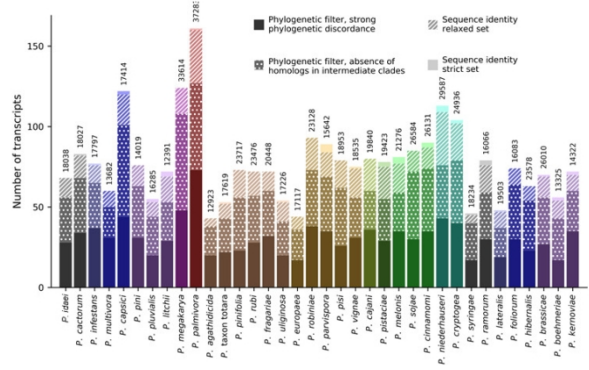


Figure S2. Number of HGT candidates (transcripts) retained for 37 *Phytophthora* genomes after false positive filtering of candidates initially identified with a Support Vector Machine classifier with two “phylogenetic” and “identity” tests. The total number of transcripts predicted for each *Phytophthora* genome is indicated above bars.

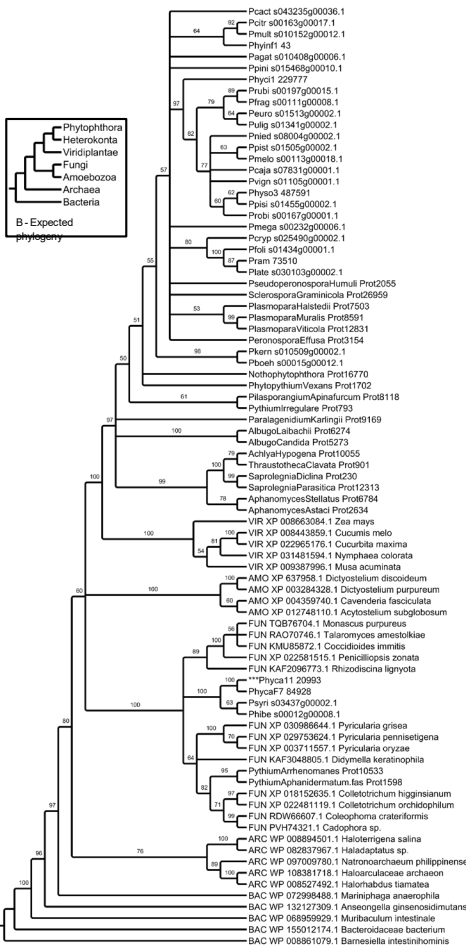
855x481mm (38 x 38 DPI)

Figure S3. Horizontal gene transfer for 19 candidate genes in *Phytophthora* spp. A, Maximum likelihood phylogeny showing relationships between candidate HGT gene(s) (indicated by three asterisks) and closest relative sequences found within seven clades (Heterokonta, Alveolata, Viridiplantae, Fungi, Amoebozoa, Archaea and Bacteria); B. expected phylogeny according to Burki et al. (2020) and Keeling et al. (2019). C and D, sequence identity between the candidate HGT sequence in *Phytophthora* and its closest homolog sequences in the putative “donor” species; the distribution represent the expected nucleotide identity values for the two same species calculated from a random sample of 1000 sequences; D, the arrow indicates the sequence identity between the candidate HGT sequence and the closest species in the non-donor clades; the distribution represents the expected nucleotide identity values for the two same from a random sample of 1000 sequences. Bottom table, Shimodaira-Hasegawa test (SH-test) between the observed ML tree and alternative tree topologies.

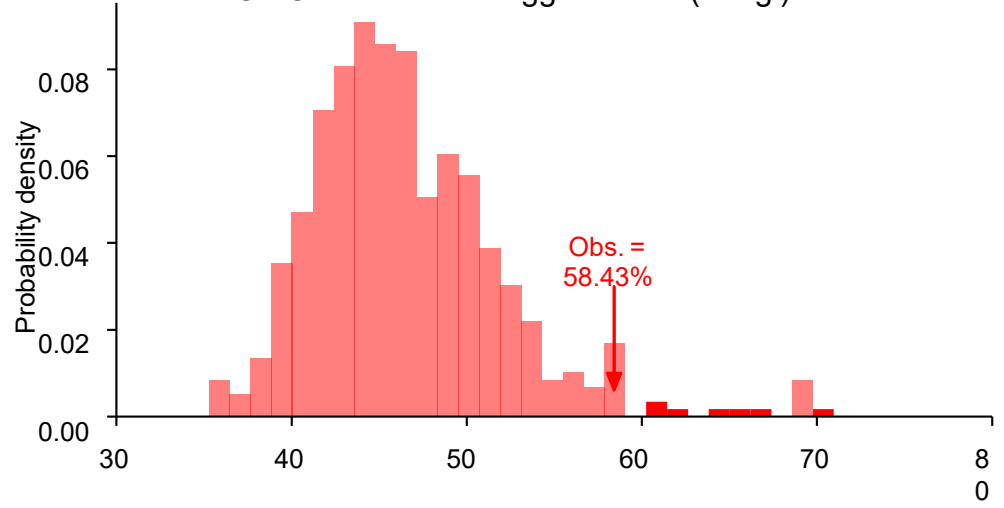
Burki, Fabien et al. 2020. The New Tree of Eukaryotes. Trends in Ecology & Evolution, 35: 43 – 55.

Keeling, Patrick J. et al. 2019 Progress towards the Tree of Eukaryotes. Current Biology, 29: R808 - R817.

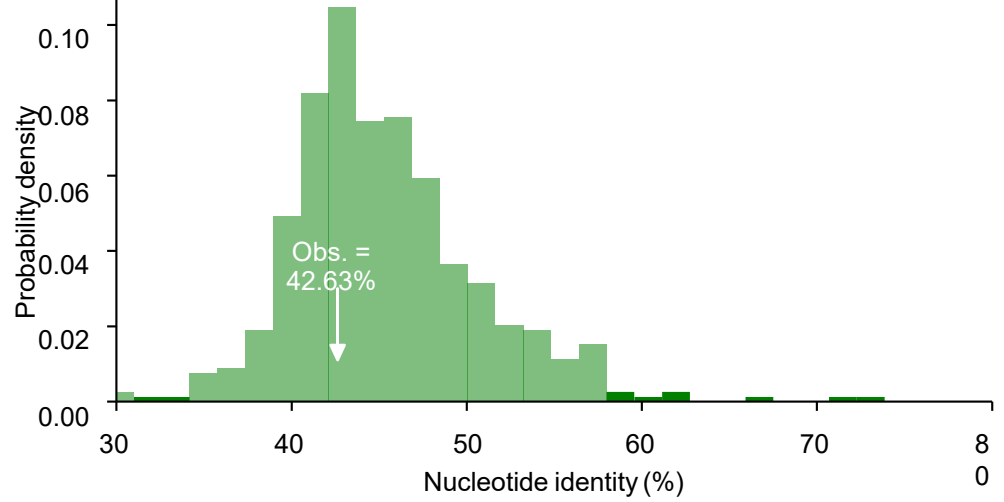
A - Observed phylogeny



C - Colletotrichum higginsianum (Fungi)



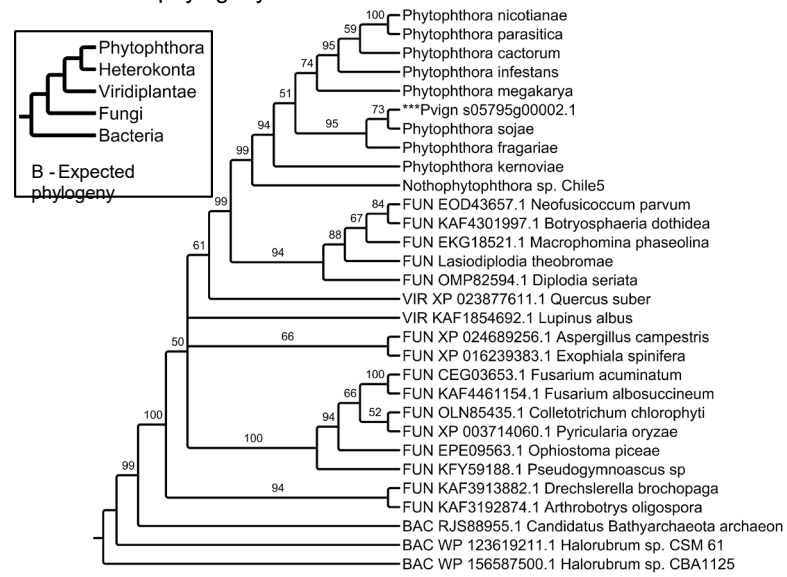
D - Cucumis melo (Viridiplantae)



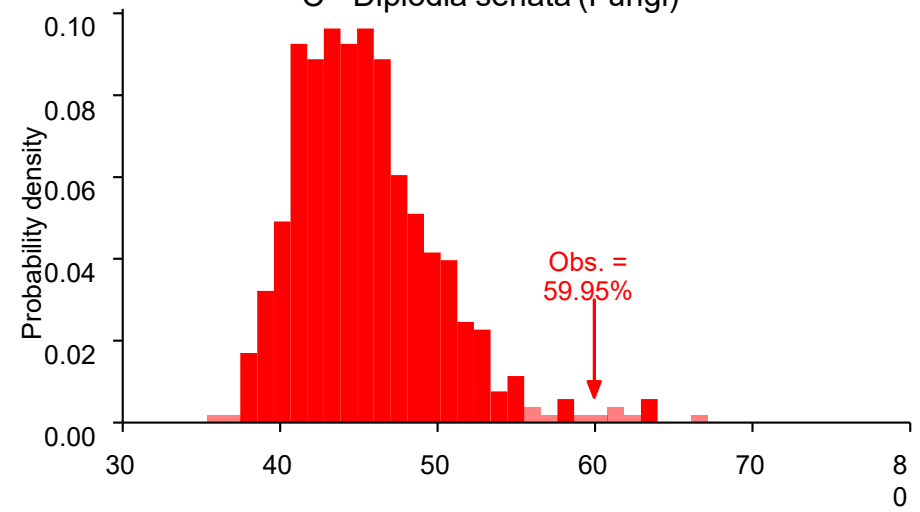
Taxonomy	-Ln	D(-Ln)	PadjLee
Clade: eukaryotes	245668889	0	ns
Eukaryotes	252088888	55477488	<<000011
Fungi	249088886	6877722	<<000011

Fig. S3_1 - HGT_1 (Endonuclease)

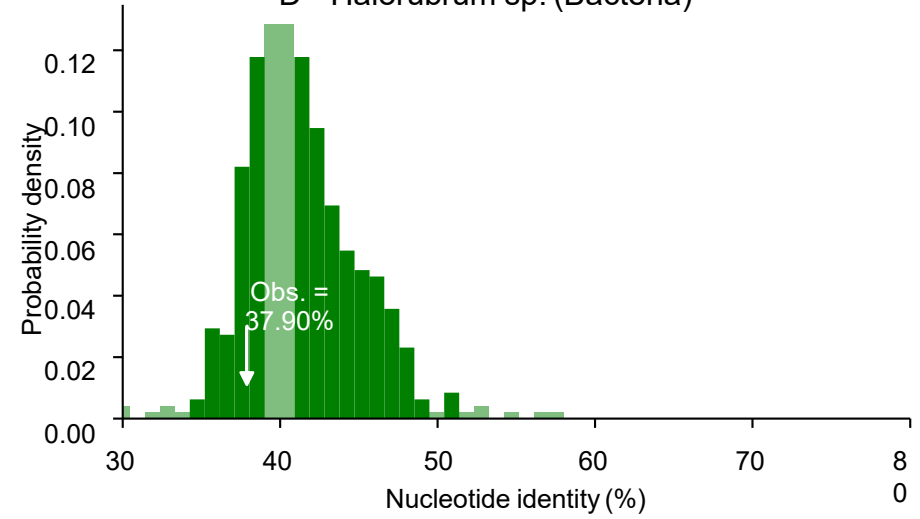
A - Observed phylogeny



C - Diplodia seriata (Fungi)

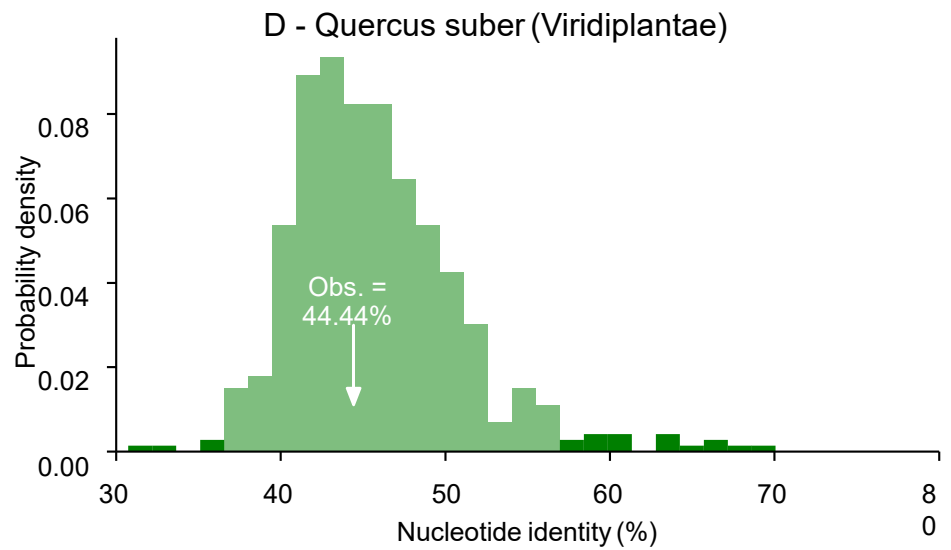
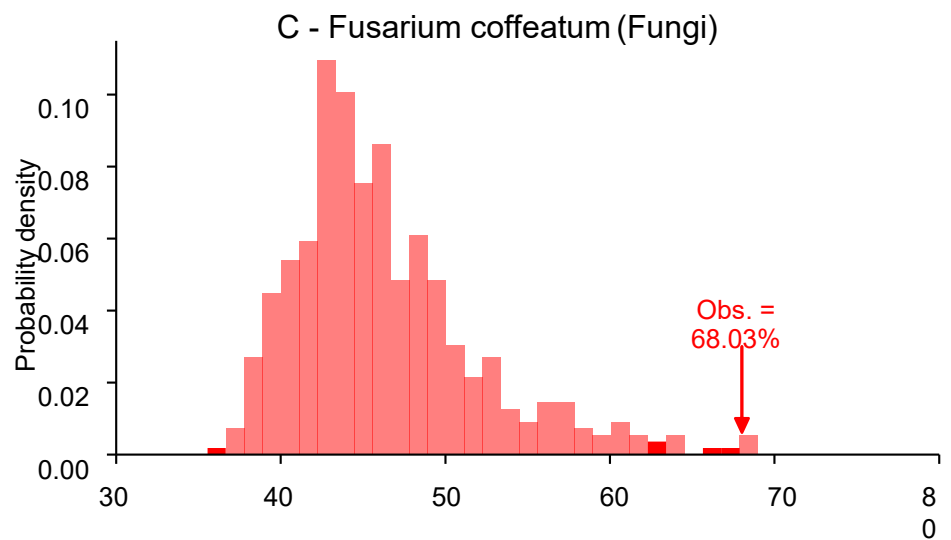
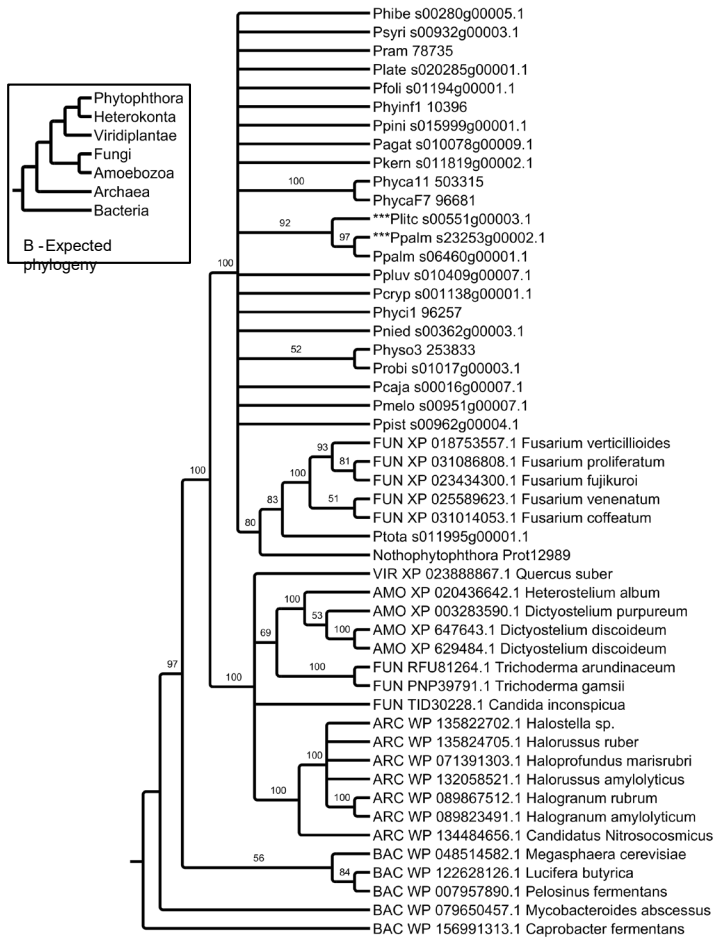


D - Halorubrum sp. (Bacteria)



Topology	-Ln	D(-Ln)	P-value
Observed topology	88033886	0	ns
Expected topology	8890444	1400257	<<0.001
Fungi (Fungi + Bacteria + Archaea + Viridiplantae + Heterokonta + Phytophthora)	88788800	744894	<<0.001
Bacteria (Bacteria + Archaea + Viridiplantae + Fungi + Fungi + Fungi + Fungi)	88188133	144227	ns

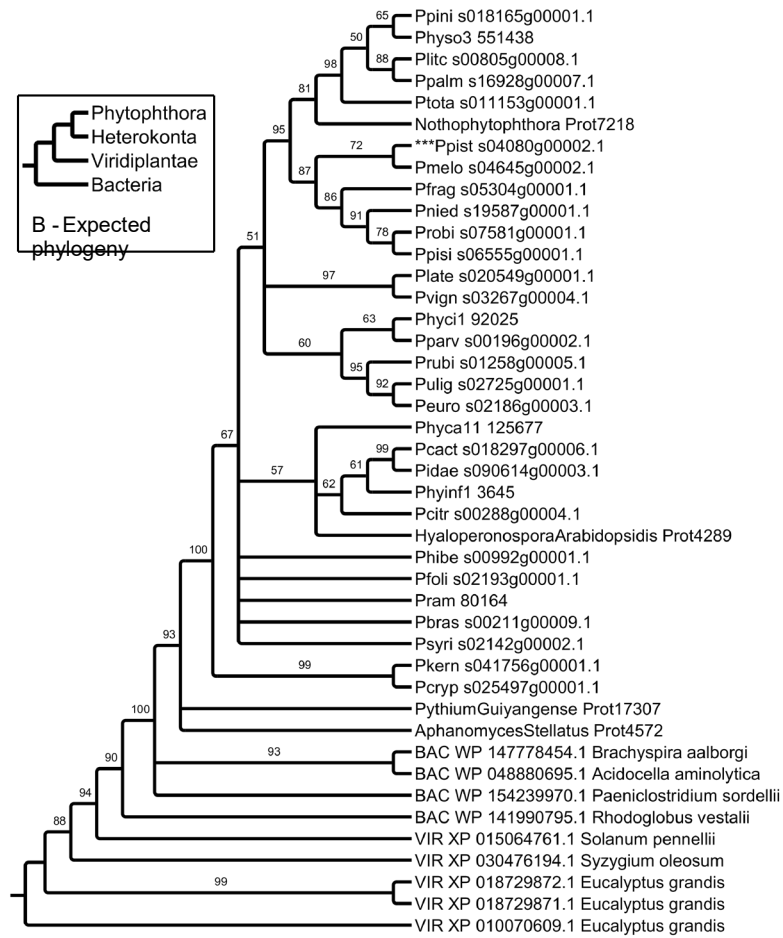
Fig. S3_2 - HGT_2 (Xylulose reductase)



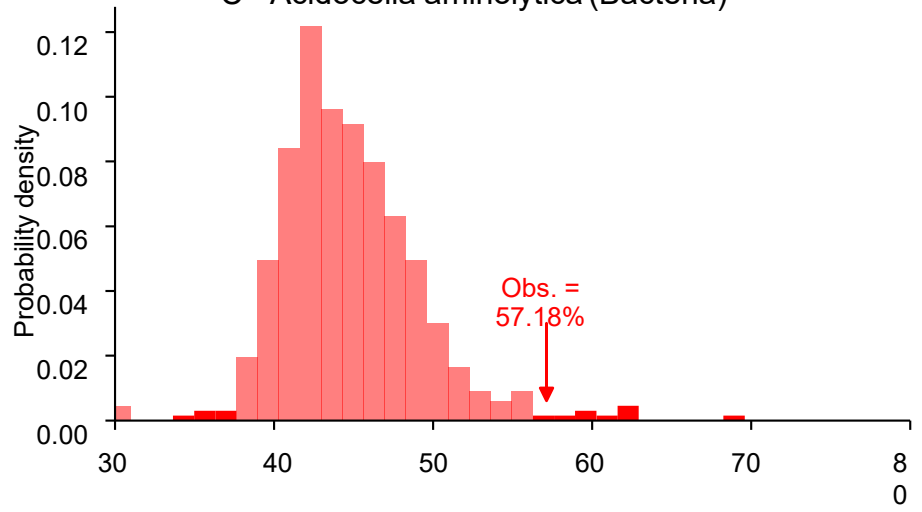
Taxonomy	-Ln	D(-Ln)	PadjLee
Clade: Ascomycota	13123265474	0	ns
Clade: Basidiomycota	13143878722	222214477	<<000011
Clade: Basidiomycota (Fungi) (Fungal donor)	13133767322	14022177	<<000011

Fig. S3_3 - HGT_3 (Quinone oxidoreductase)

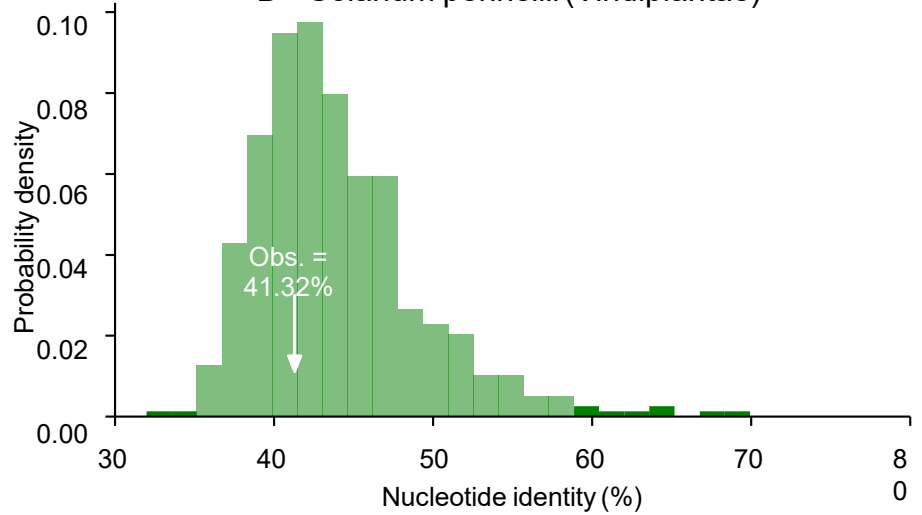
A - Observed phylogeny



C - Acidocella aminolytica (Bacteria)



D - Solanum pennellii (Viridiplantae)



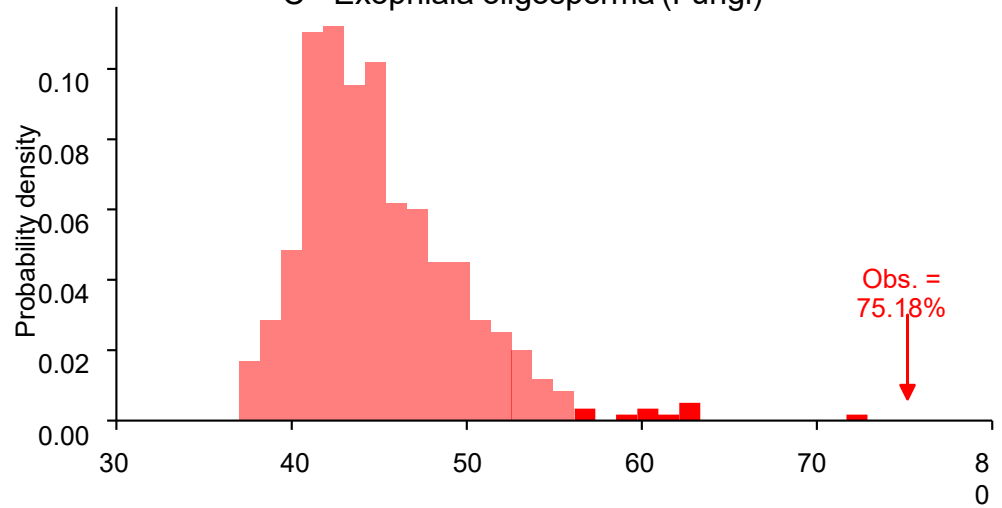
Topology	-Ln	D(-Ln)	P _{adj} LB
Observed topology	71123395	0	ns
Expected topology	7221003	98807	<0.0001
Base-Biased randomization (Heterokonta (Heterokonta) donor)	71192774	68878	<0.0001
Base-Biased randomization (Viridiplantae (Viridiplantae) donor)	71124229	-0.33	ns

Fig. S3_4 - HGT_4 (Aquaporin)

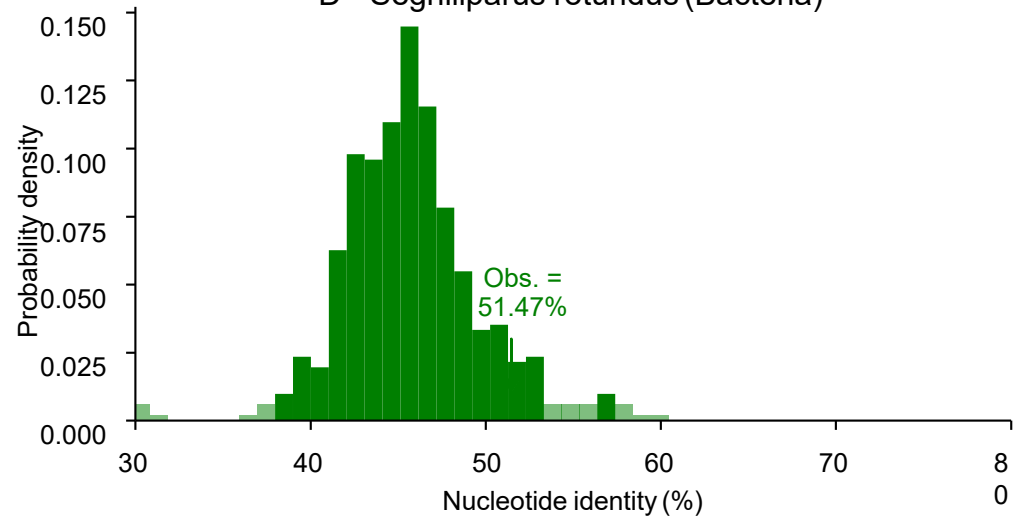
A - Observed phylogeny



C - Exophiala oligosperma (Fungi)

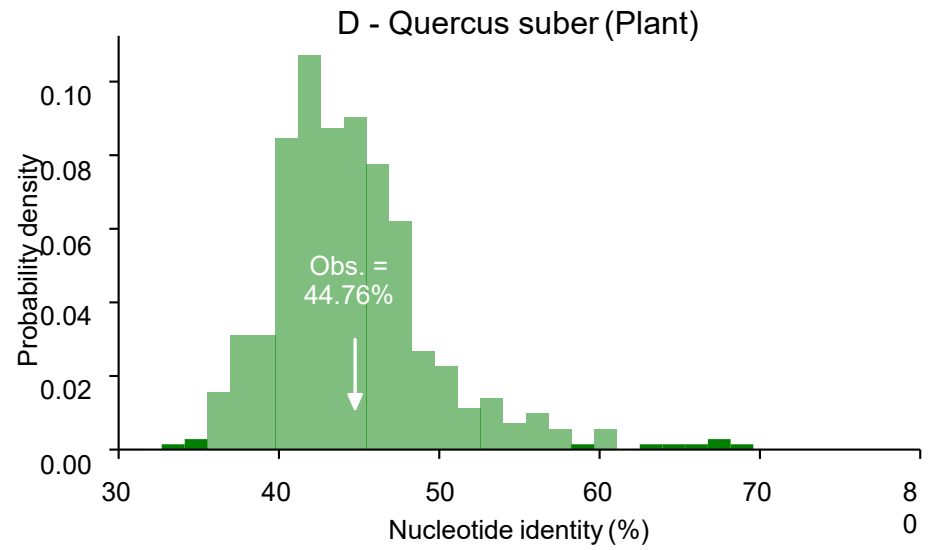
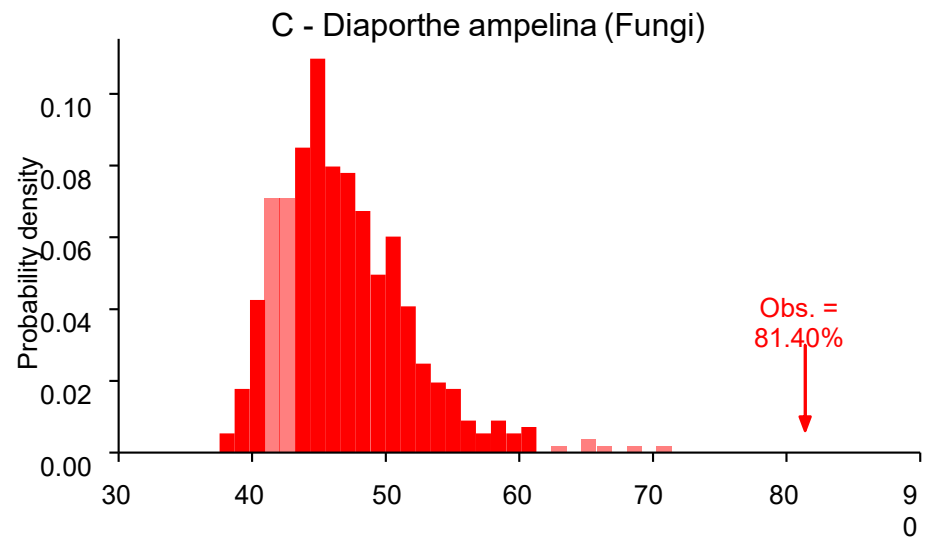
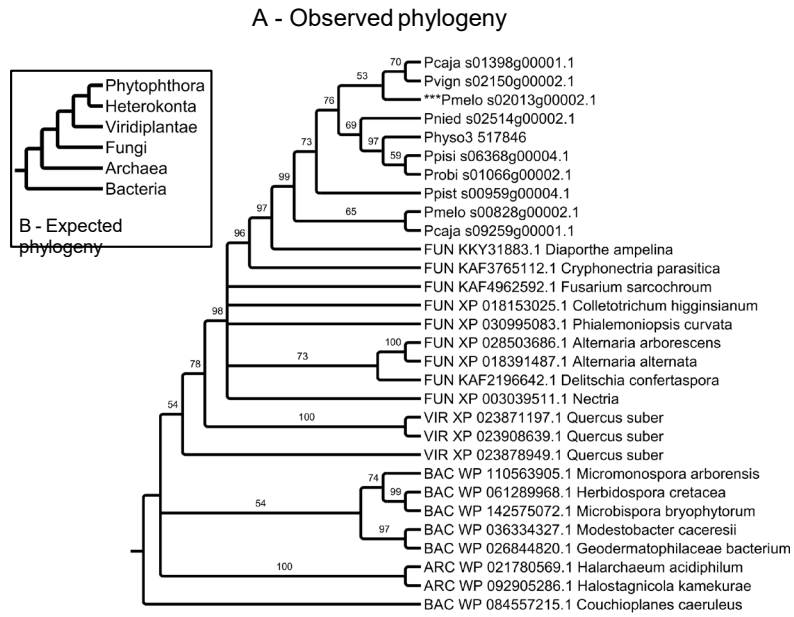


D - Segniliparus rotundus (Bacteria)



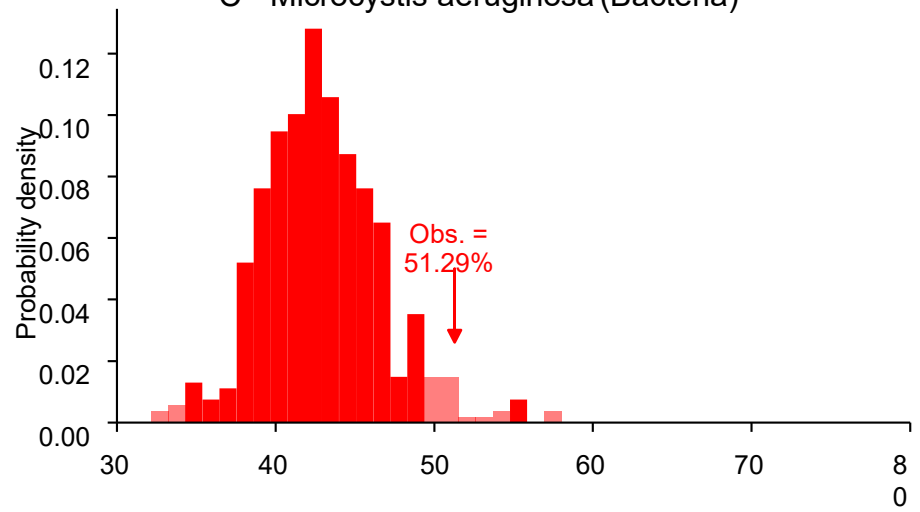
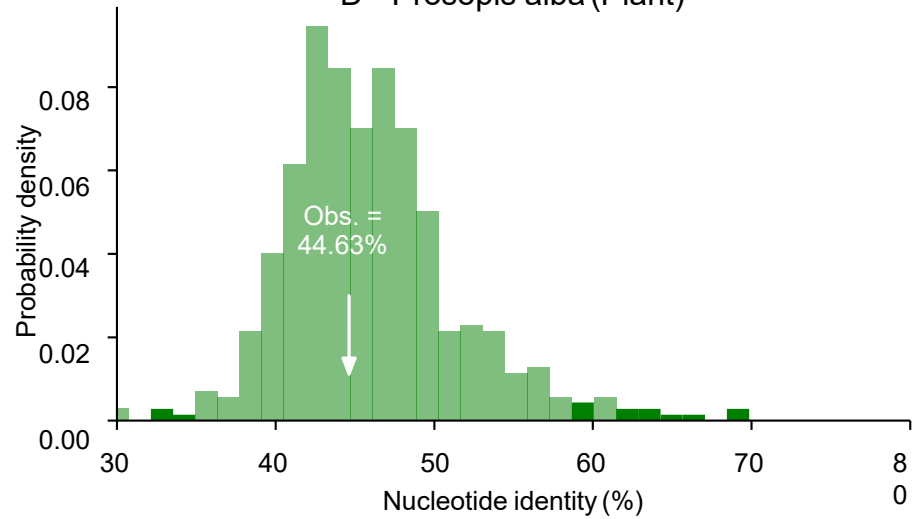
Topology	-Ln	D(-Ln)	PvalLee
Clade seed (phylogeny)	8822521133	0	ns
Bacterial clade (phylogeny)	886009966	44088888	<<0.0001
Fungal clade (phylogeny)	8833911165	14380002	<<0.0001
Clade bacterial clade (phylogeny)	882267228	1451692	ns

Fig. S3_6 - HGT_6 (Phenol acid carboxylase)

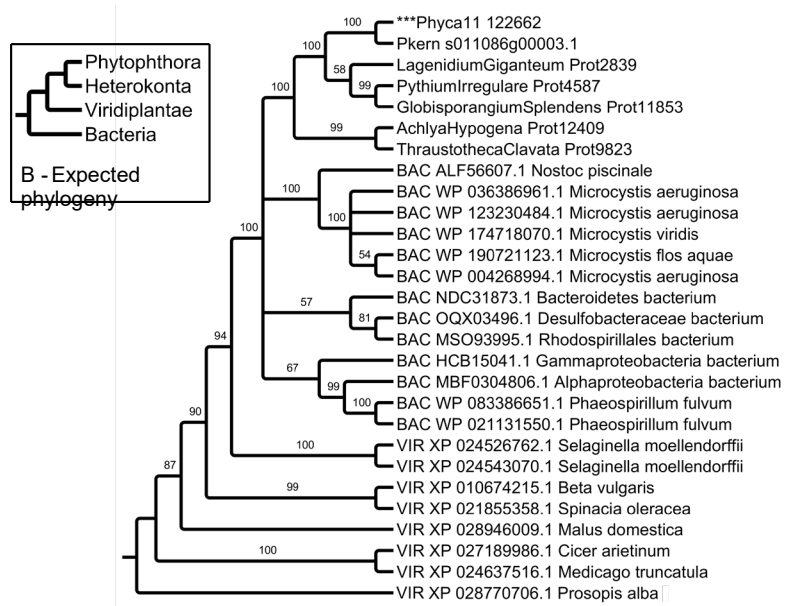


Topology	-Ln	D(-Ln)	P-value
Clade: Archaea, Bacteria, Fungi, Viridiplantae, Phytosphthora	881822889	0	ns
Clade: Bacteria, Archaea, Fungi, Viridiplantae, Phytosphthora	882261229	778410	<<0.001
Clade: Fungi, Bacteria, Archaea, Viridiplantae, Phytosphthora	882368886	555886	<<0.001
Clade: Bacteria, Archaea, Fungi, Viridiplantae, Phytosphthora	882558883	442388	<<0.001

Fig. S3_7 - HGT_7 (Peptidase S9)

C - *Microcystis aeruginosa* (Bacteria)D - *Prosopis alba* (Plant)

A - Observed phylogeny



Topology

-Ln

D(-Ln)

P-value

Observed topology

1818173088

0

ns

Expected topology

1818173033

4439665

<0.0001

Bacteria to plant (with donor)

1818173035

1889986

<0.0001

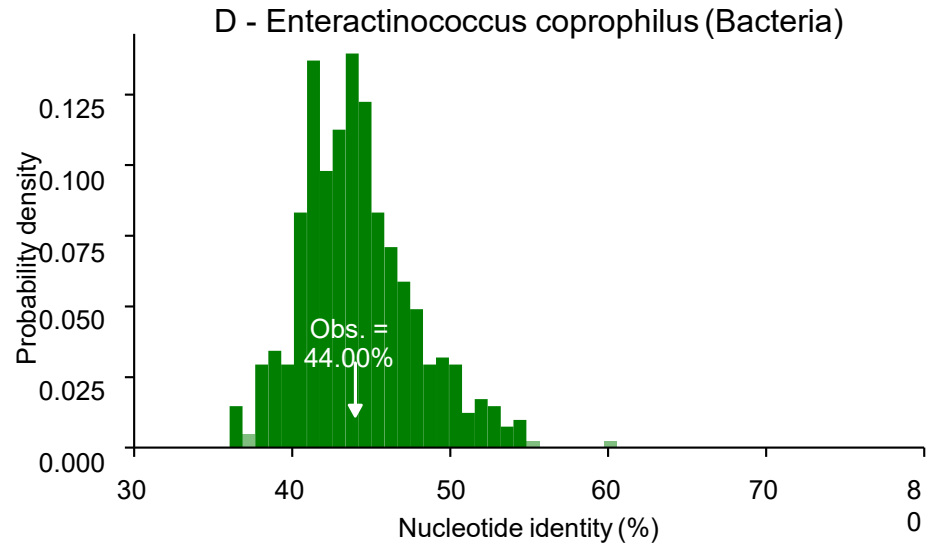
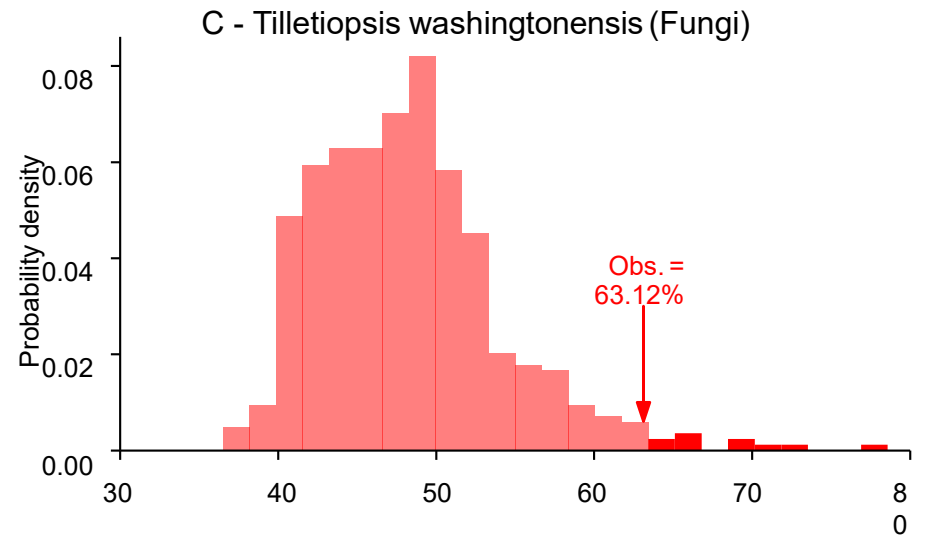
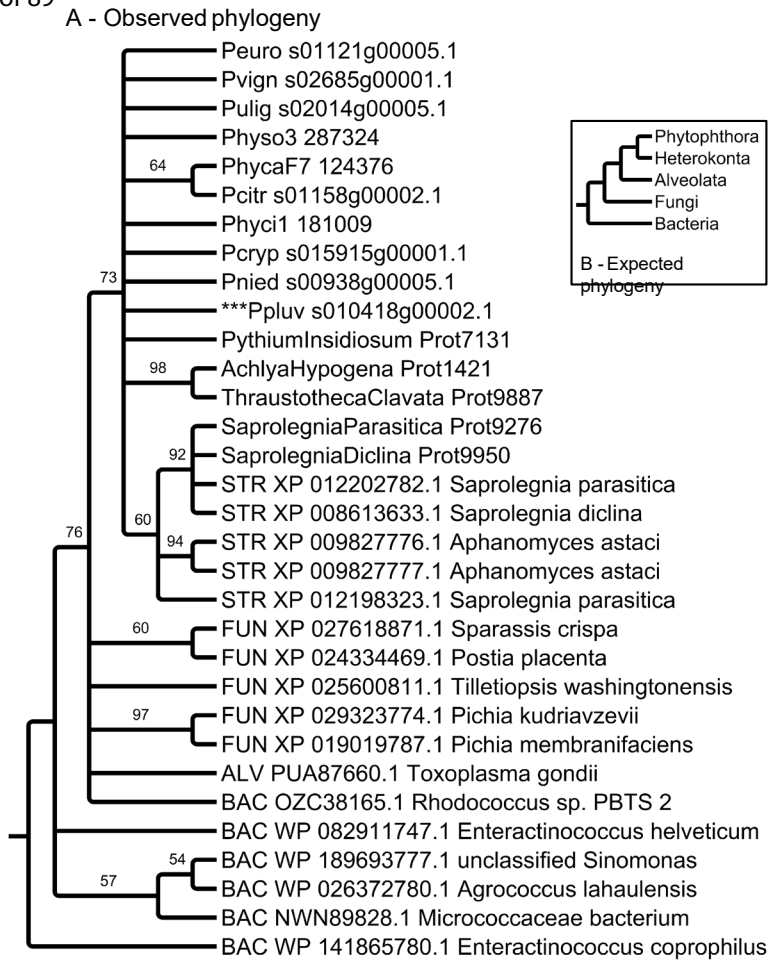
Heterokonta to plant (with donor)

1818173038

-3.30

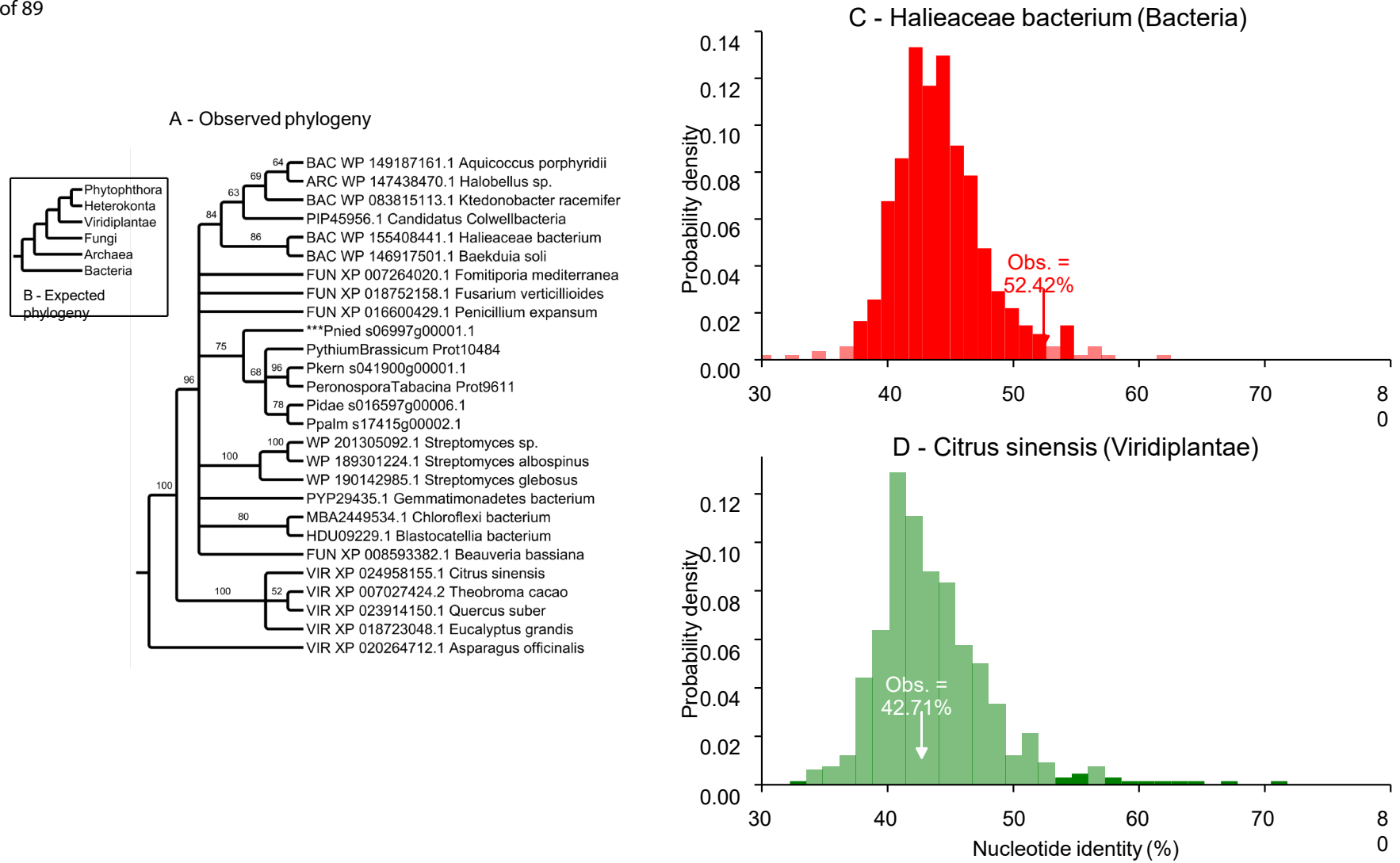
ns

Fig. S3_8 - HGT_8 (UDP-N-acetylglucosamine-peptide N-acetylglucosaminyltransferase)



Topology	-Ln	D(-Ln)	P-value
Observed topology	14380888	0	ns
Expected topology	14384077	143224	ns
Fungi (Fungi+Alveolata+Heterokonta+Phytosphthora)	1438622	14339	ns
Heterokonta+Alveolata+Phytosphthora (Fungi+donor)	1438606	-5.23	ns

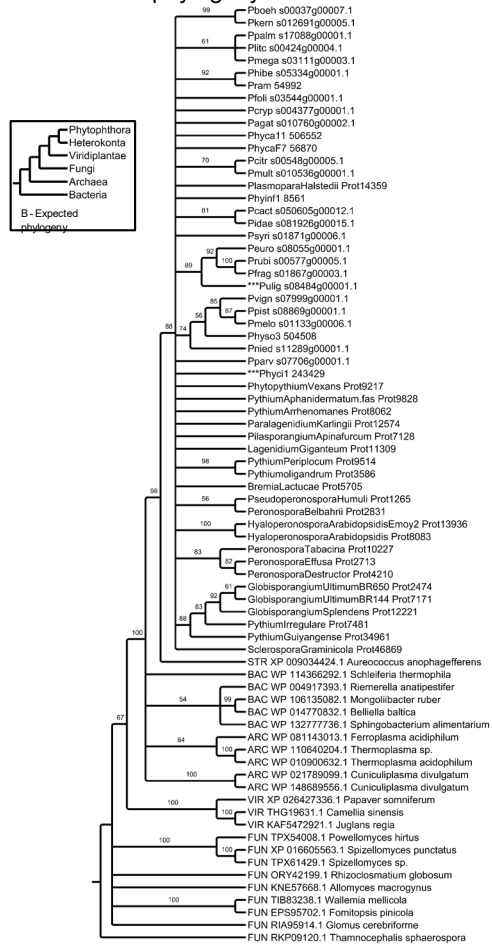
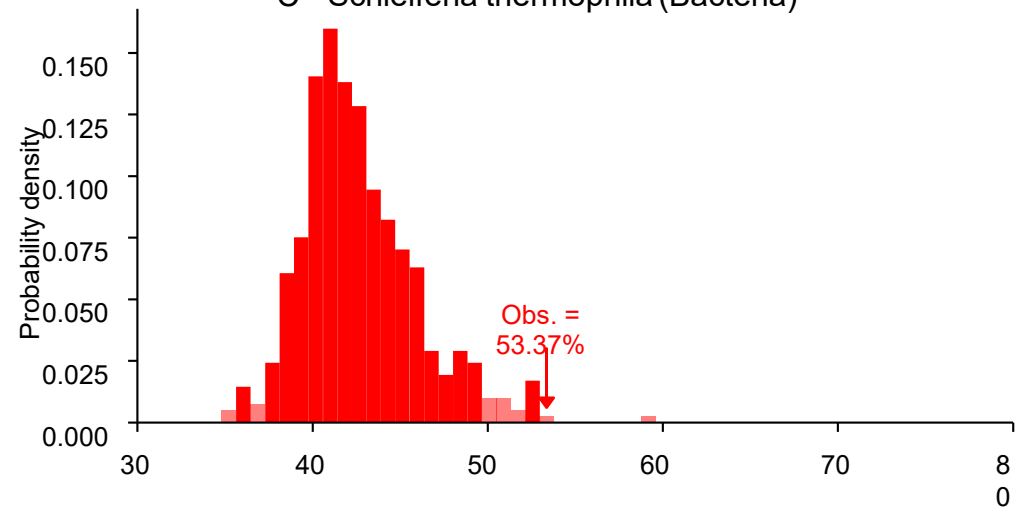
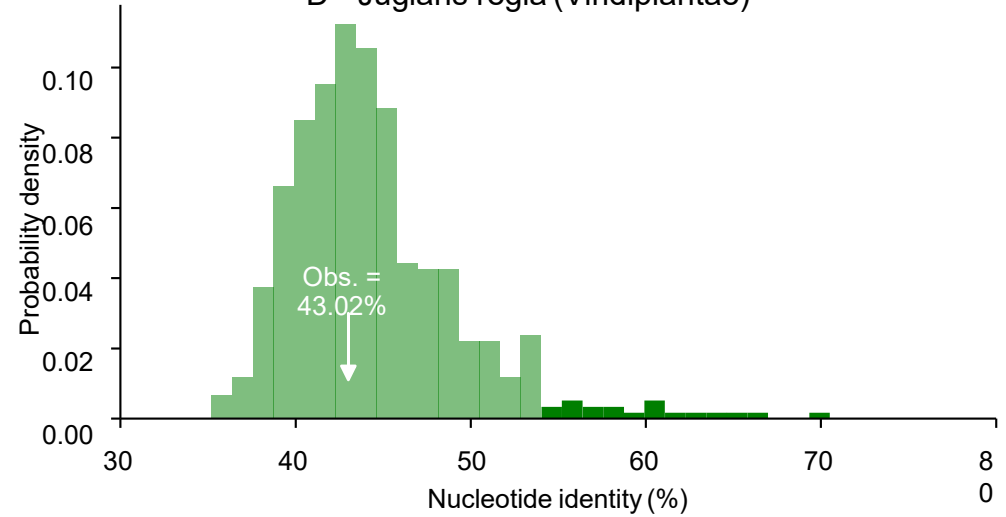
Fig. S3_9 - HGT_9 (Alternative oxidase)



Topology	-Ln	D(-Ln)	Pval
O:Ostreococcus	7228334	0	ns
E:Escherichia	78818886	90262	<0.001
O:Oryza	78812238	88224	<0.001
O:Oryza	7382221	938371	<0.001
F:Faust	7773380	48336	<0.001
H:Halobacterium	72281139	-2.84	ns

Fig. S3_13 - HGT_13 (4-coumarate CoA ligase)

A - Observed phylogeny

C - *Schleiferia thermophila* (Bacteria)D - *Juglans regia* (Viridiplantae)

Topology

-Ln

D(-Ln)

P-value

Observed topology

141166964

0

ns

Expected topology

142820322

1444108

<0.0001

Bacterial taxa (Archaea, Bacteria) vs. Fungal taxa (Fungi) donor

141866444

384855

<0.0001

Hudud-Hudud (Hudud-Hudud) vs. Fungal taxa (Fungi) donor

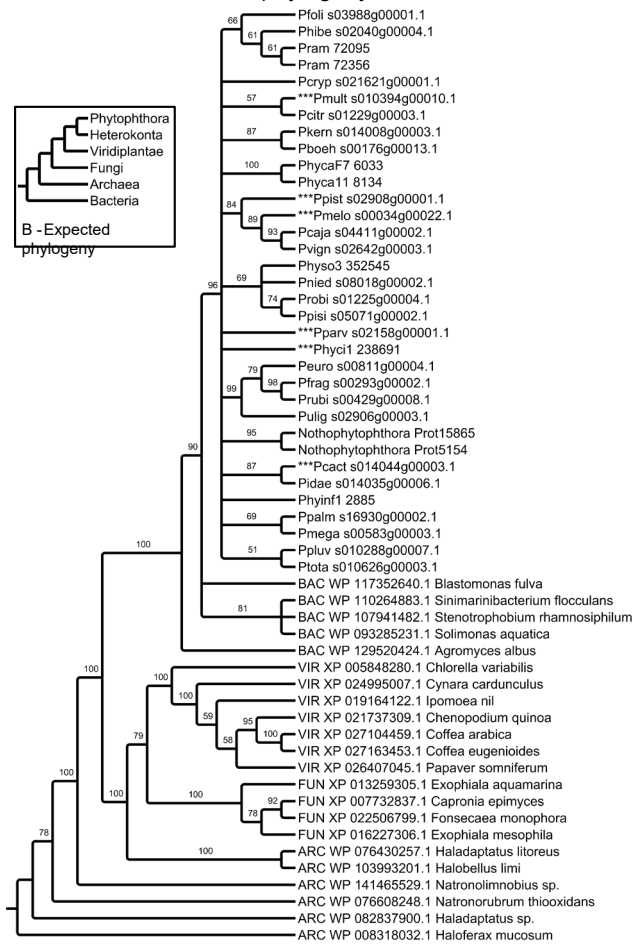
141813227

144838

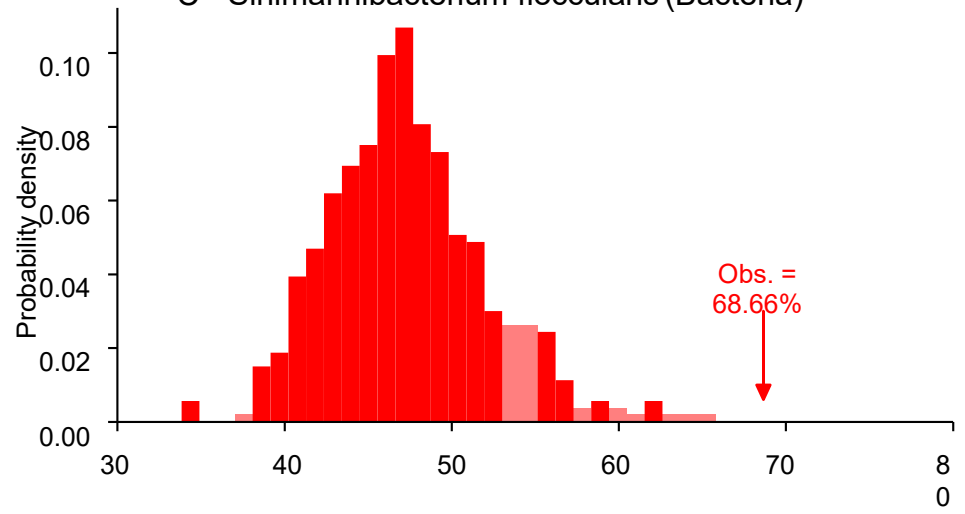
ns

Fig. S3_14 - HGT_14 (2,4-dienoyl-CoA reductase)

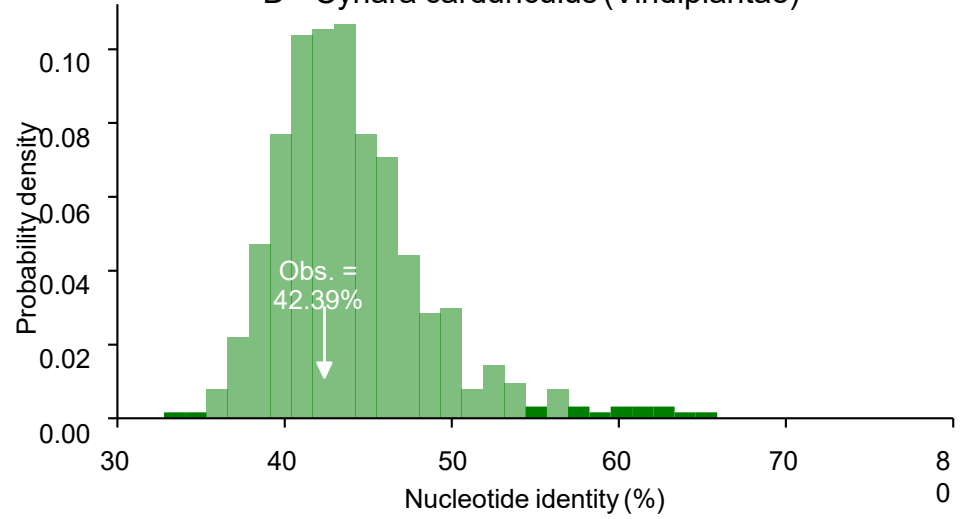
A - Observed phylogeny



C - Sinimaribacterium flocculans (Bacteria)



D - Cynara cardunculus (Viridiplantae)



Topology

-Ln

D(-Ln)

P-value

Observed topology

12.02388004

0

ns

Expected topology

12.72339122

444.1088

<<0.001

Base-Blastomastixidae (Heterokonta) (donor)

12.02388004

337.488

<<0.001

Base-Blastomastixidae (Viridiplantae) (donor)

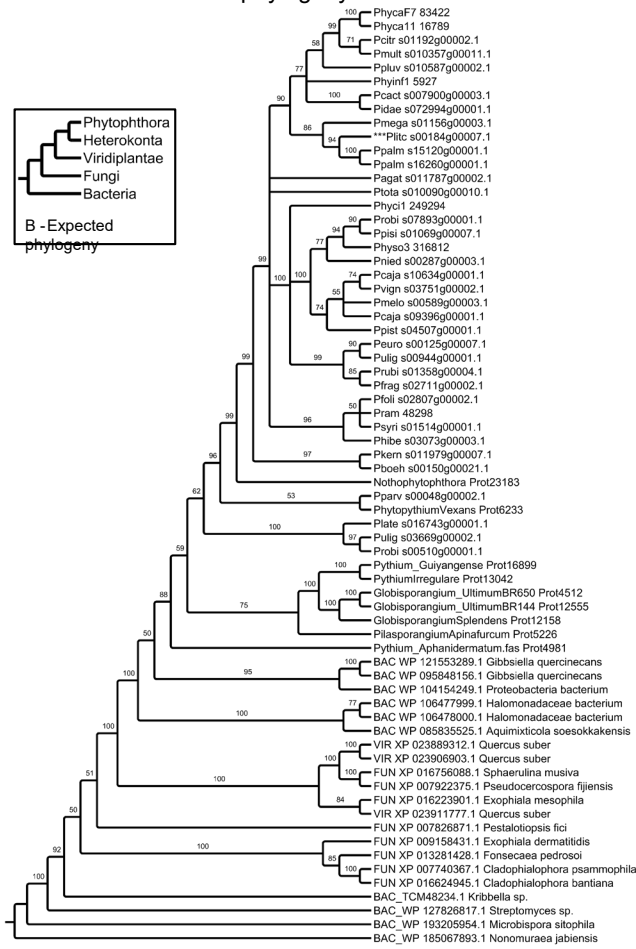
12.02388004

-1.55

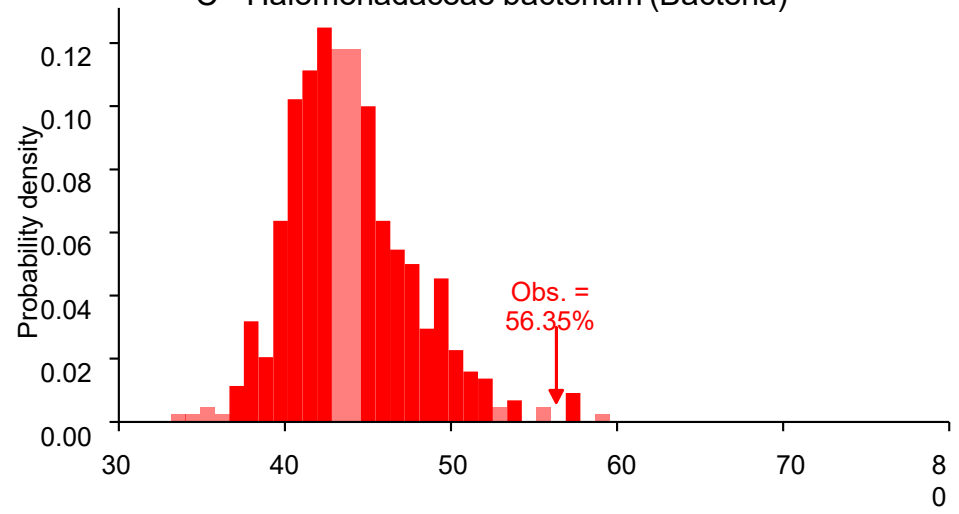
ns

Fig. S3_15 - HGT_15 (Alcohol dehydrogenase)

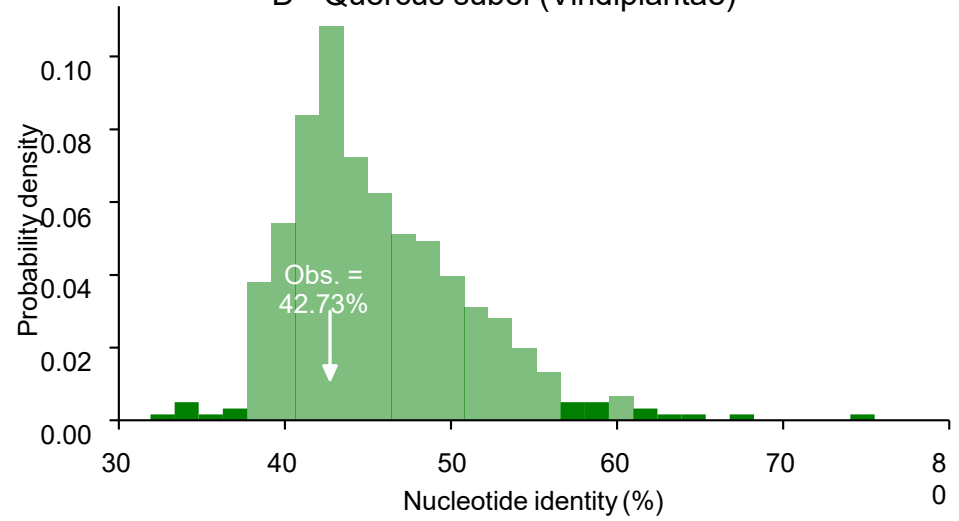
A - Observed phylogeny



C - Halomonadaceae bacterium (Bacteria)



D - Quercus suber (Viridiplantae)



T_{topology}

-Ln

D(-Ln)

P_{adj}Leis

Observed topology

331891511

0

ns

Expected topology

323208923

1228105

<<0.001

Observed topology with Heterokonta (Heterokonta) donor

3232041474

90857

<<0.001

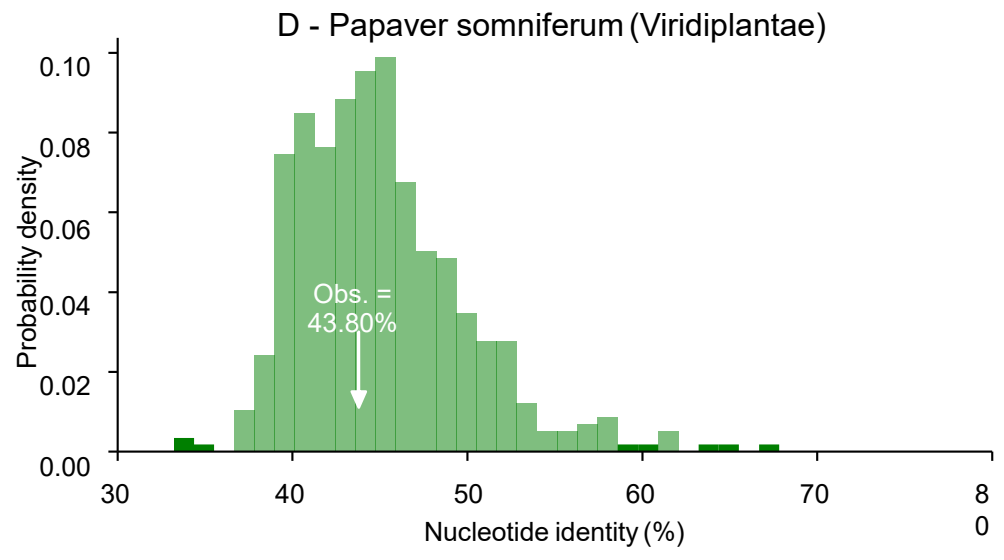
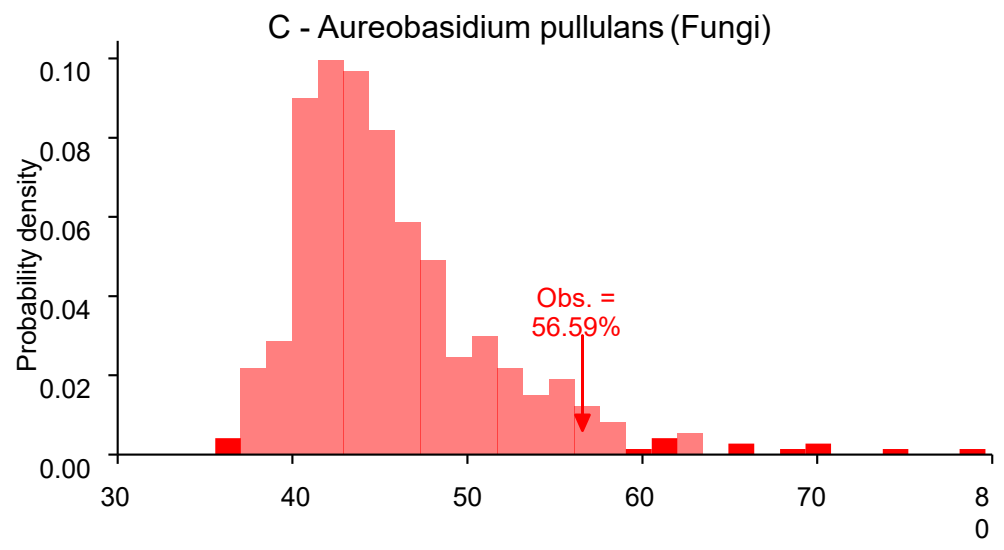
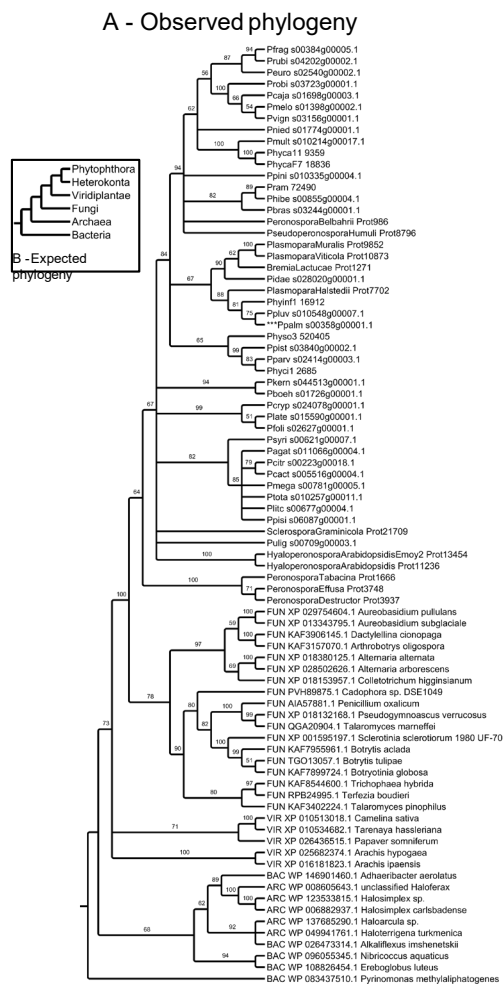
Observed topology with Bacteria (Bacteria) donor

323204766

394888

<<0.001

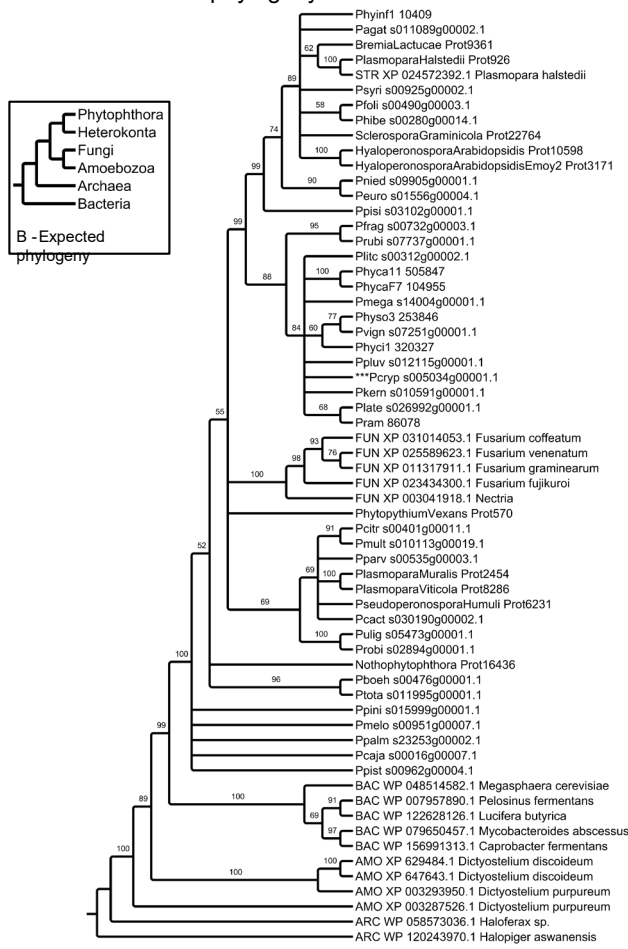
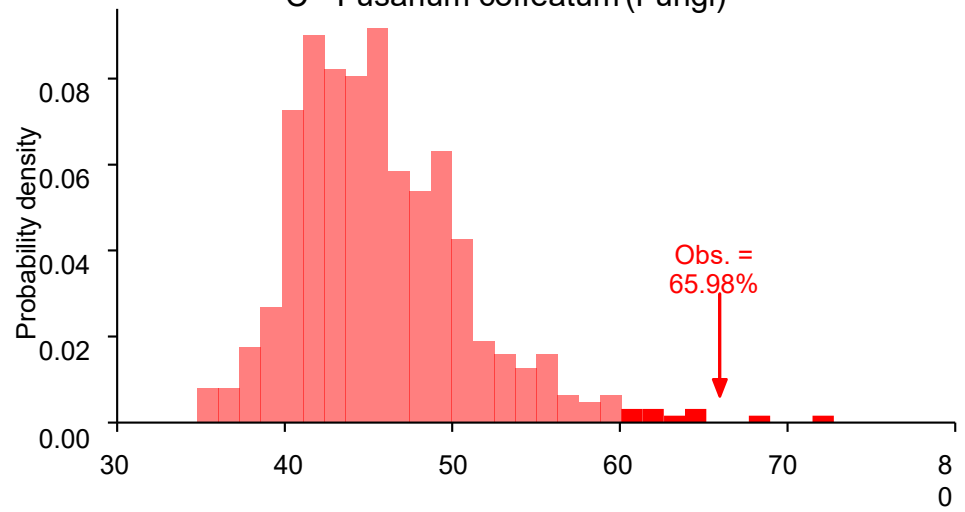
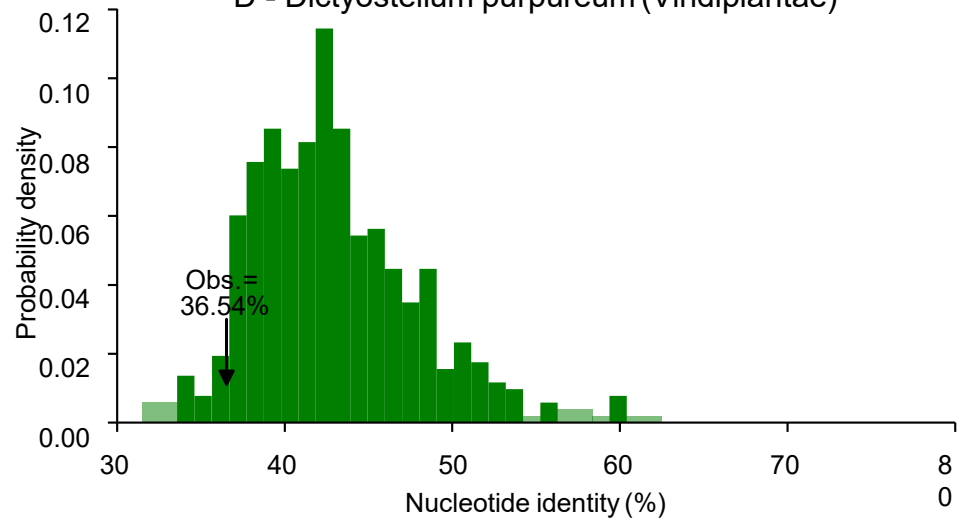
Fig. S3_16 - HGT_16 (Putative tannase)



Topology	-Ln	D(-Ln)	PvalLee
Clade seed (1, 2, 3, 4, 5, 6, 7, 8, 9, 10, 11, 12, 13, 14, 15, 16, 17, 18, 19, 20, 21, 22, 23, 24, 25, 26, 27, 28, 29, 30, 31, 32, 33, 34, 35, 36, 37, 38, 39, 40, 41, 42, 43, 44, 45, 46, 47, 48, 49, 50, 51, 52, 53, 54, 55, 56, 57, 58, 59, 60, 61, 62, 63, 64, 65, 66, 67, 68, 69, 70, 71, 72, 73, 74, 75, 76, 77, 78, 79, 80, 81, 82, 83, 84, 85, 86, 87, 88, 89, 90, 91, 92, 93, 94, 95, 96, 97, 98, 99, 100)	22106400	0	ns
Expected (1, 2, 3, 4, 5, 6, 7, 8, 9, 10, 11, 12, 13, 14, 15, 16, 17, 18, 19, 20, 21, 22, 23, 24, 25, 26, 27, 28, 29, 30, 31, 32, 33, 34, 35, 36, 37, 38, 39, 40, 41, 42, 43, 44, 45, 46, 47, 48, 49, 50, 51, 52, 53, 54, 55, 56, 57, 58, 59, 60, 61, 62, 63, 64, 65, 66, 67, 68, 69, 70, 71, 72, 73, 74, 75, 76, 77, 78, 79, 80, 81, 82, 83, 84, 85, 86, 87, 88, 89, 90, 91, 92, 93, 94, 95, 96, 97, 98, 99, 100)	22359833	2235444	<0.001
Host (1, 2, 3, 4, 5, 6, 7, 8, 9, 10, 11, 12, 13, 14, 15, 16, 17, 18, 19, 20, 21, 22, 23, 24, 25, 26, 27, 28, 29, 30, 31, 32, 33, 34, 35, 36, 37, 38, 39, 40, 41, 42, 43, 44, 45, 46, 47, 48, 49, 50, 51, 52, 53, 54, 55, 56, 57, 58, 59, 60, 61, 62, 63, 64, 65, 66, 67, 68, 69, 70, 71, 72, 73, 74, 75, 76, 77, 78, 79, 80, 81, 82, 83, 84, 85, 86, 87, 88, 89, 90, 91, 92, 93, 94, 95, 96, 97, 98, 99, 100)	22107340	33340	<0.001
Fungi (1, 2, 3, 4, 5, 6, 7, 8, 9, 10, 11, 12, 13, 14, 15, 16, 17, 18, 19, 20, 21, 22, 23, 24, 25, 26, 27, 28, 29, 30, 31, 32, 33, 34, 35, 36, 37, 38, 39, 40, 41, 42, 43, 44, 45, 46, 47, 48, 49, 50, 51, 52, 53, 54, 55, 56, 57, 58, 59, 60, 61, 62, 63, 64, 65, 66, 67, 68, 69, 70, 71, 72, 73, 74, 75, 76, 77, 78, 79, 80, 81, 82, 83, 84, 85, 86, 87, 88, 89, 90, 91, 92, 93, 94, 95, 96, 97, 98, 99, 100)	22107338	221739	<0.005

Fig. S3_17 - HGT_17 (Putative pectinesterase)

A - Observed phylogeny

C - *Fusarium coffeatum* (Fungi)D - *Dictyostelium purpureum* (Viridiplantae)

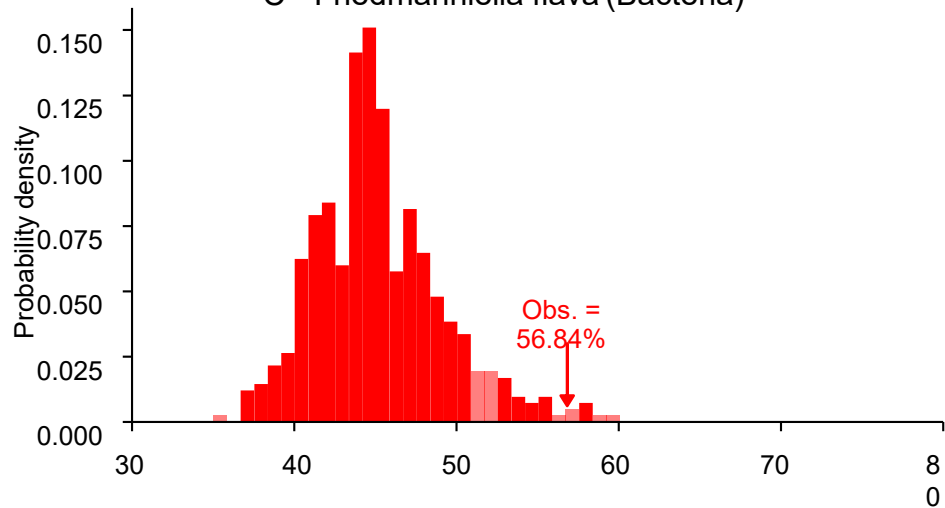
Topology	-Ln	D(-Ln)	PvalLee
Clade seed (topology)	16161616227	0	ns
EEpqrst (topology)	16161616222	1442386	<0.001
Heterokonta (topology) Fungi (Fungi) donor	17171232002	3315775	<0.001
Fungi (Fungi) donor	16161616225	140118	ns

Fig. S3_18 - HGT_18 (ATP-binding Cassette [ABC])

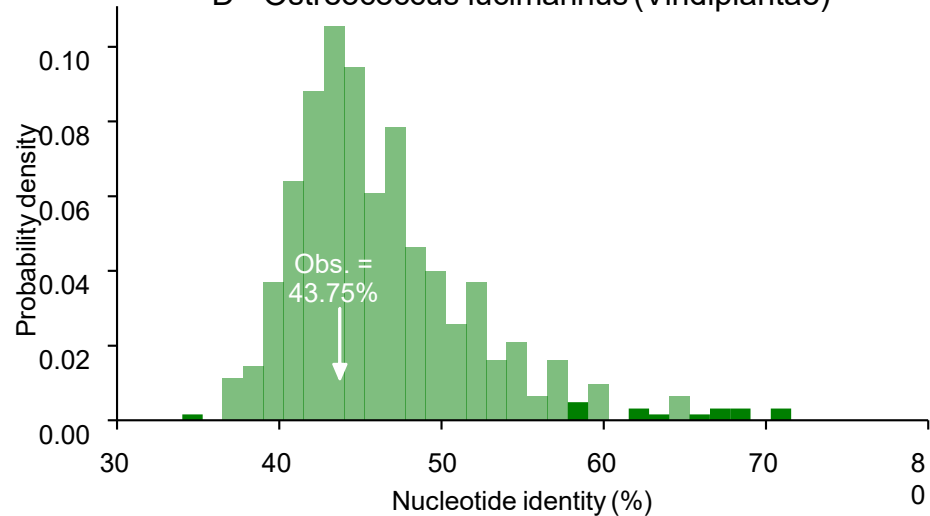
A - Observed phylogeny



C - *Friedmanniella flava* (Bacteria)



D - *Ostreococcus lucimarinus* (Viridiplantae)



Topology	-Ln	D(-Ln)	P-value
Observed topology	44837732	0	ns
Expected topology	44872284	34532	<0.005
Horizontal transfer (Bacterial to Bacterial donor)	44843888	-6.31	ns
Bacterial to eukaryotic (Horizontal transfer donor)	44878107	34532	<0.001

Fig. S3_19 - HGT_20 (Ribosomal-protein-alanine acetyltransferase)

Figure S4.

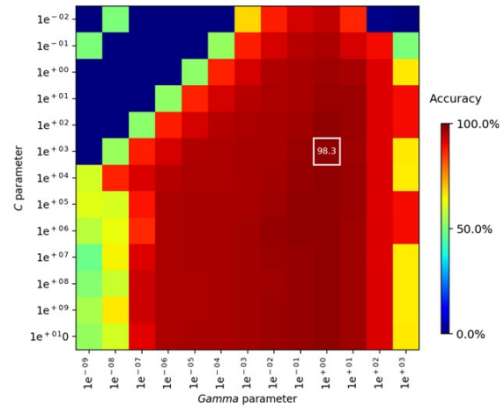


Figure S4. Identification of the radial basis function (rbf) kernel parameters (C and γ) resulting in the highest accuracy in classifying *Phytophthora*, bacteria and fungal transcripts with a Support Vector Machine (SVM) classifier based on Sequence-composition features (GC-content, codon usage). Accuracy values were obtained with a 5-fold cross-validation of the SVM classifier. The value in white represents the highest accuracy obtained.

855x481mm (38 x 38 DPI)

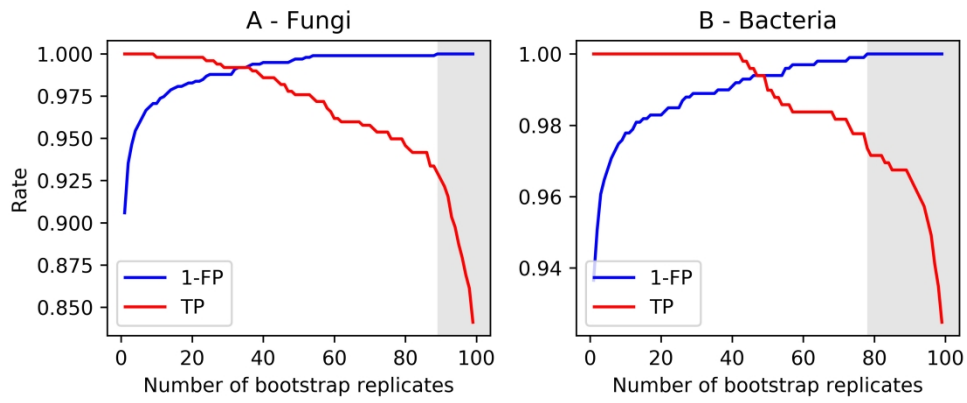


Figure S5. Relationships between the false positive rate (FP) and the true positive rate (TP) for HGT candidate discovery with a Support Vector Machine classifier and the number of bootstrap replicate datasets in which the putative HGT candidate was found. The grey area corresponds to the number of bootstrap replicates where the false positive rate reaches the null value.

452x193mm (236 x 236 DPI)

Supplementary Table 1. Full assembly and annotation statistics for 31 Phytophthora genomes.

Species	Group	Clade	Genome					K-mer size estimate	Sequence Reads
			Sequence Reads	Contigs	N50	Assembly Length			
<i>P. cactorum</i>	EMR	1	NA ^a	7,888	15,053	56,443,298	NA ^a	28,693,892	
<i>P. idaei</i>	EMR	1	NA ^a	7,163	14,461	53,468,943	NA ^a	NA ^b	
<i>P. pini</i>	USDA-D	2	29,016,981	2,131	42,987	38,730,000	53,447,651	24,861,861	
<i>P. multivora</i>	Scion	2	NA ^a	2,844	46,133	40,059,192	NA ^a	NA ^b	
<i>P. pluvialis</i>	Scion	3	NA ^a	4,340	30,816	53,616,150	NA ^a	NA ^b	
<i>P. litchii</i>	NJAU	4	17,809,306	2,543	34,546	38,200,938	58,822,528	20,209,114	
<i>P. palmivora</i>	USDA-B	4	44,740,938	24,815	6,694	107,798,747	178,336,461	21,955,557	
<i>P. megakarya</i>	USDA-B	4	29,074,100	24,073	7,093	101,609,312	170,257,105	19,683,391	
<i>P. agathidicida</i>	Scion	5	NA ^a	3,754	19,544	37,337,699	NA ^a	NA ^b	
<i>P. taxon totara</i>	Scion	5	NA ^a	4,425	30,809	55,576,372	NA ^a	NA ^b	
<i>P. parvispora</i>	OSU	7	21,793,750	9,906	6,820	46,825,958	72,690,845	12,813,391	
<i>P. pisi</i>	Fribourg	7	34,621,167	7,667	15,253	58,856,683	105,905,508	18,243,326	
<i>P. niederhauseri</i>	Fribourg	7	39,377,584	26,463	4,805	90,270,009	126,036,921	20,314,715	
<i>P. robiniae</i>	NJAU	7	34,689,250	14,865	8,754	69,938,814	107,714,597	12,626,895	
<i>P. cajani</i>	OSU	7	26,013,994	18,255	5,113	64,854,085	108,588,397	12,589,952	
<i>P. vignae</i>	OSU	7	25,708,667	10,330	8,363	56,137,732	85,443,060	12,598,323	
<i>P. melonis</i>	NJAU	7	31,728,667	11,353	15,342	73,416,743	106,514,211	22,052,362	
<i>P. pistaciae</i>	OSU	7	41,390,989	10,414	10,302	63,209,321	80,941,143	12,493,625	
<i>P. europaea</i>	OSU	7	22,034,445	8,301	11,551	58,787,065	71,680,138	12,832,217	
<i>P. uliginosa</i>	OSU	7	21,317,084	8,955	10,095	57,072,031	72,763,188	12,712,782	
<i>P. fragariae</i>	USDA-G	7	32,666,667	8,544	20,362	76,969,737	100,354,493	13,274,875	
<i>P. rubi</i>	USDA-G	7	38,666,667	9,434	17,808	74,863,594	119,201,141	13,035,132	
<i>P. pinifolia</i>	UBC	6	NA ^a	22,610	6,021	74,478,861	NA ^a	36,047,200	
<i>P. lateralis</i>	UBC	8	23,158,308	28,263	2,396	50,496,828	NA ^a	23,158,308	
<i>P. hibernalis</i>	OSU	8	26,010,981	6,587	21,408	71,256,216	86,155,007	12,973,692	
<i>P. foliorum</i>	OSU	8	16,677,112	5,320	15,800	48,973,082	56,233,540	12,894,827	
<i>P. brassicae</i>	Fribourg	8	31,477,833	12,447	12,337	72,849,437	105,501,807	20,290,544	
<i>P. syringae</i>	USDA-G	8	19,410,417	6,572	15,987	57,045,526	66,661,136	12,799,213	
<i>P. cryptogea</i>	UBC	8	NA ^a	25,944	4,730	69,446,343	NA ^a	NA ^b	
<i>P. boehmeriae</i>	NJAU	10	34,703,473	2,866	41,917	39,747,814	NA ^a	NA ^b	
<i>P. kernoviae</i>	UBC	10	21,178,252	13,710	5,225	42,698,878	NA ^a	21,178,252	

^aGenome assemblies were completed in a different study.

^bRNA was not sequenced.

Transcriptome					Annotations		
Assemble d Contigs	Assembl ed N50	Contigs after TransDecoder	N50 after TransDecoder	Assembly Length	Repeat Percent	Predicted Genes	Strain
28,465	1,890	25,690	2,595	47,486,039	19.96	18,027	P414
NA ^b	NA ^b	NA ^b	NA ^b	NA ^b	16.19	18,038	SCR371
20,548	2,695	22,766	3,818	59,507,934	7.31	14,019	Unknown
NA ^b	NA ^b	NA ^b	NA ^b	NA ^b	10.86	13,682	NZFS 3378
NA ^b	NA ^b	NA ^b	NA ^b	NA ^b	16.04	16,285	LC9-1
28,496	2,139	28,596	3,087	60,642,271	5.98	12,391	SHS3
30,410	1,745	26,805	2,443	45,279,452	29.62	37,283	sbr112.9
31,088	1,802	28,293	2,614	49,914,387	31.94	33,614	zdho120
NA ^b	NA ^b	NA ^b	NA ^b	NA ^b	5.76	12,923	NZFS 3772
NA ^b	NA ^b	NA ^b	NA ^b	NA ^b	16.56	17,619	NZFS 3642
108,991	833	65,896	1,572	70,613,891	8.75	15,642	P8494;23
44,946	885	32,997	1,179	31,197,744	16.80	18,953	Unknown
75,089	1,177	52,635	1,476	59,497,972	20.96	29,587	Unknown
38,510	1,432	33,462	2,346	52,628,916	25.58	23,128	Unknown
33,359	2,139	36,595	2,878	76,345,822	20.65	19,840	P3105;27
41,393	1,596	37,102	2,552	62,795,853	17.45	18,535	P3019;24
28,272	1,873	26,842	2,618	48,278,380	25.93	21,276	Unknown
34,064	2,320	39,208	3,366	91,860,426	18.56	19,423	P6196;25
38,785	2,066	36,606	3,233	76,609,174	23.33	17,117	P10324;31
31,138	2,115	34,305	3,184	74,176,007	24.16	17,226	P10413;26
29,266	1,848	28,012	2,725	52,169,825	30.81	20,448	CBS 209.46
34,446	1,774	31,999	2,677	57,725,263	29.48	23,476	pd0101050015038
38,654	2,461	47,683	3,693	124,451,965	33.00	23,717	CBS 122922
13,645	670	8,094	1,690	10,528,234	23.39	19,503	CBS 168.42
36,774	2,899	49,849	4,759	150,938,535	32.46	23,578	P0647;28
27,112	2,358	32,393	3,607	80,179,397	19.26	16,083	P10974;29
35,153	1,485	27,252	2,207	42,057,210	28.39	26,010	Unknown
29,481	2,735	35,799	4,253	99,905,260	21.71	18,234	PSY-09-046
NA ^b	NA ^b	NA ^b	NA ^b	NA ^b	17.65	24,936	CBS 418.71
NA ^b	NA ^b	NA ^b	NA ^b	NA ^b	7.83	13,325	Unknown
10,461	791	7,931	1,499	9,532,089	4.15	14,322	CBS 122049

Host

Strawberry

Unknown

Unknown

Idesia polycarpa

Unknown

litchi

Theobroma cacao

Unknown

*Agathis australis**Podocarpus totara*

Unknown

Strawberry

Raspberry

Unknown

Unknown

Unknown

Unknown

Unknown

Unknown

Unknown

Unknown

Unknown

Unknown

Supplementary Table 3. Over-represented GO terms for a set of 551 candidate HGT transcripts found in 35 *Phytophthora* genomes.

GO	Term	# terms in full set ¹	# terms in HGT set ²	Pr($X=k$) ³
Biological process				
GO:0034079	butanediol biosynthetic process	28	6	<0.001
GO:0009405	pathogenesis	1538	6	<0.001
GO:0055114	obsolete oxidation-reduction process	1543	4	<0.001
GO:0046210	nitric oxide catabolic process	34	1	<0.05
GO:0051301	cell division	817	2	<0.05
GO:0000462	maturation of SSU-rRNA from tricistronic rRNA transcript	431	2	<0.01
GO:0071500	cellular response to nitrosative stress	54	1	<0.05
GO:0048285	organelle fission	64	1	<0.05
GO:0009245	lipid A biosynthesis	116	1	<0.05
GO:0051409	response to nitrosative stress	102	1	<0.05
GO:0045493	xylan catabolic process	151	1	<0.05
GO:0046514	ceramide catabolic process	174	1	<0.05
GO:0016024	CDP-diacylglycerol biosynthetic process	162	1	<0.05
GO:0009072	aromatic amino acid family metabolic process	198	1	<0.05
Molecular function				
GO:0000721	(R,R)-butanediol dehydrogenase activity	28	6	<0.001
GO:0016831	carboxy-lyase activity	201	18	<0.001
GO:0016491	oxidoreductase activity	10,881	14	<0.001
GO:0008080	N-acetyltransferase activity	1,082	4	<0.001
GO:0050525	cutinase activity	110	2	<0.001
GO:0015267	channel activity	742	3	<0.001
GO:0016787	hydrolase activity	8,099	6	<0.01
GO:0003724	RNA helicase activity	505	2	<0.01
GO:0008759	UDP-3-O-[3-hydroxymyristoyl] N-acetylglucosamine deacetylase activity	61	1	<0.05
GO:0005344	oxygen transporter activity	61	1	<0.05
GO:0004838	tyrosine transaminase activity	72	1	<0.05
GO:0097573	glutathione oxidoreductase activity	82	1	<0.05
GO:0031176	endo-1,4-beta-xylanase activity	111	1	<0.05
GO:0008941	nitric oxide dioxygenase activity	109	1	<0.05
GO:0004731	purine-nucleoside phosphorylase activity	110	1	<0.05
GO:0019825	oxygen binding	118	1	<0.05
GO:0004300	enoyl-CoA hydratase activity	151	1	<0.05
GO:0010181	FMN binding	1595	2	<0.05
GO:0102121	ceramidase activity	162	1	<0.05
GO:0017040	N-acylsphingosine amidohydrolase activity	177	1	<0.05

GO:0004605	phosphatidate cytidyltransferase activity	244	1	<0.05
GO:0004318	enoyl-[acyl-carrier protein] reductase (NADH) activity	289	1	<0.05

Cellular component

GO:0005576	extracellular region	4624	6	<0.001
GO:0005835	fatty acid synthase complex	271	1	<0.05
GO:0032040	small-subunit processome	704	2	<0.05
GO:0032153	cell division site	94	1	<0.05
GO:0005730	nucleolus	2223	2	<0.05

¹Transcriptome of 35 *Phytophthora* genomes.

²551 HGT candidates.

³Probability (Q-value) of obtaining the same number of transcripts (k) or more by chance as given by a hypergeometric probability distribution.

Table S4. Putative pathogenicity functions inferred for 28 HGT candidates identified among *Phytophthora* spp.

	Ortho group	Putative function	Best hit on PHI-base (E-value) - Reference	Notes - Other reference(s)
HGT_1	OG5_134265	Endonuclease	PHI:5754, endonuclease, <i>Fusarium graminearum</i> (3.0E-024) - Yun et al. (2015)	-
HGT_2	OG5_126928_1	Xylulose reductase	PHI:2256, xylitol dehydrogenase, <i>Parastagonospora nodorum</i> (1.0E-128) - Lowe et al. (2008)	Oxidation of xylitol to xylulose; alters plant defense responses against aphids - MacWilliams et al. (2020) L-arabinose metabolism, degradation of hemicellulose - Dimarogona and Topakas (2016)
HGT_3	OG5_130201	Quinone oxidoreductase	No hit	Protection against oxidative stress in entomopathogenic fungi (Pedrini et al. 2015); Fungal protection against destructive host-produced quinones (Petrasch et al. 2019)
HGT_4	OG5_126615	Aquaporin	PHI:7047, water channel protein aquaporin, <i>Cryptococcus neoformans</i> (4.0E-012) - Meyers et al. (2017)	-
HGT_5	OG5_133138	NPP1	No hit	Necrosis-inducing <i>Phytophthora</i> protein - Seidl and Van den Ackerveken (2019)
HGT_6	OG5_177086	Phenol acid carboxylase	No hit	Upregulated expression during <i>Phytophthora cactorum</i> x strawberry interaction - Chen et al. (2011)
HGT_7	OG5_152798	Peptidase S9	No hit	Abundant in fungal plant pathogens - Muszewska et al. (2017)
HGT_8	OG5_144202	UDP-N-acetylglucosamine-peptide N-acetylglucosaminyltransferase	PHI:4921, flagellin glycosyltransferase, <i>Burkholderia cenocepacia</i> (1.0E-021) - Khodai-Kalaki et al. (2015)	-
HGT_9	OG5_140249	Alternative oxidase	No hit	-
HGT_10	OG5_139476	Dioxygenase	No hit	-

HGT_11	OG5_130394	Thioesterase	PHI:4988, sfp-type 4'-phosphopantetheinyl transferase, <i>Bipolaris maydis</i> (3.0E-005) - Zainudin et al. (2015)	-
HGT_12	OG5_135408	Endo-1,4-beta-xylanase GH10	PHI:7912, endo-beta-1,4-xylanase <i>Phytophthora parasitica</i> (1.0E-137) - Lai and Liou, (2018)	-
HGT_13	OG5_126609	4-coumarate CoA ligase	PHI:10606, long-chain-fatty-acid-Co Aligase, <i>Pseudomonas aeruginosa</i> (1.0E-032) - Pan et al. (2020)	-
HGT_14	OG5_135743	2,4-dienoyl-CoA reductase	PHI:8134, 3-Oxoacyl-[acyl-carrier-protein] reductase, <i>Salmonella enterica</i> (1.0e-014) - Kwan et al. (2018)	-
HGT_15	OG5_126928_2	Zinc-binding dehydrogenase, Polyketide synthase, enoylreductase domain	PHI:8321, gluconate 5-dehydrogenase, <i>Salmonella enterica</i> (1.0E-016) - Alves Batista et al. (2018)	-
HGT_16	OG5_135419	Putative tannase	PHI:10222, feruloyl esterase, <i>Valsa mali</i> (4.0E-030) - Xu et al. (2018)	-
HGT_17	OG5_133550	Putative pectinesterase CE8	PHI:278, pectin methylesterase, <i>Botrytis cinerea</i> (4.0E-077) - Valette-Collet et al. (2003)	-
HGT_18	OG5_223601	ATP-binding Cassette (ABC)	No hit	Putative virulence factor - Stergiopoulos et al. (2003); Zeng and Charkowski, (2021)
HGT_19	OG5_161673	Antibiotic biosynthesis monooxygenase	No hit	-
HGT_20	OG5_132142	Ribosomal-protein-alanine acetyltransferase	No hit	-
HGT_21	OG5_136477	Endoribonuclease	No hit	-
HGT_22	OG5_132299	Pectate lyase PL3	PHI :4620, pectate lyase, <i>Phytophthora capsici</i> (1.0E-029) – Fu et al. (2015)	-
HGT_23	OG5_203245	Csa-calmodulin	No hit	-

HGT_24	OG5_126661	Mannitol-1-phosphate dehydrogenase	PHI:9524, Alcohol dehydrogenase, <i>Candida albicans</i> (4.0E-021)- Song et al. (2019)	-
HGT_25	OG5_137179	hypothetical protein	No hit	-
HGT_26	OG5_129399	2-nitropropane dioxygenase	No hit	Triggers expression of type III secretion system in <i>Ralstonia solanacearum</i> to induce pathogenicity on tobacco - Zhang et al. (2017)
HGT_27	ORTHOMCL13162	hypothetical protein	No hit	-
HGT_28	OG5_126721	type I methionyl aminopeptidase	PHI:9334, effector protein, <i>Citrobacter rodentium</i> (4.0E-020) - Xia et al. (2019)	-

References

- Alves Batista DF, de Freitas Neto OC, Maria de Almeida A, Maboni G, de Carvalho TF, de Carvalho TP, Barrow PA, Berchieri AJ. 2018. Evaluation of pathogenicity of *Salmonella gallinarum* strains harbouring deletions in genes whose orthologues are conserved pseudogenes in *S. pullorum*. *PLoS ONE* **13**: e0200585.
- Chen X, Klemsdal SS, Brurberg MB. 2011. Identification and analysis of *Phytophthora cactorum* genes up-regulated during cyst germination and strawberry infection. *Current Genetics* **57**:297-315.
- Dimarogona M, Topakas E. 2016. Chapter 12 - Regulation and heterologous expression of lignocellulosic enzymes in *Aspergillus*. In: *New and future developments in microbial biotechnology and bioengineering*. Elsevier, pp 171–190.
- Fu L, Zhu C, Ding X, Yang X, Morris PF, Tyler BM, Zhang X. 2015. Characterization of cell-death-inducing members of the pectate lyase gene family in *Phytophthora capsici* and their contributions to infection of pepper. *Molecular Plant-Microbe Interactions* **28**: 766-775.
- Khodai-Kalaki M, Andrade A, Mohamed YF, Valvano M. 2015. *Burkholderia cenocepacia* lipopolysaccharide modification and flagellin glycosylation affect virulence but not innate immune recognition in plants. *mBio* **6**: e00679-15.
- Kwan G, Plagenz B, Cowles K, Pisithkul T, Amador-Noguez D, Barak JD. 2018. Few differences in metabolic network use found between *Salmonella enterica* colonization of plants and typhoidal mice. *Frontiers in Microbiology* **9**: 695.

Lai MY, Liou RF. 2018. Two genes encoding GH10 xylanases are essential for the virulence of the oomycete plant pathogen *Phytophthora parasitica*. *Current Genetics* **64**: 931–943.

Lowe RG, Lord M, Rybak K, Trengove RD, Oliver RP, Solomon PS. 2008. A metabolomic approach to dissecting osmotic stress in the wheat pathogen *Stagonospora nodorum*. *Fungal Genetics and Biology* **45**: 1479–1486.

MacWilliams JR, Dingwall S, Chesnais Q, Sugio A, Kaloshian I. 2020. AcDCXR is a cowpea aphid effector with putative roles in altering host immunity and physiology. *Frontiers in Plant Science* **11**: 605.

Meyers GL, Jung KW, Bang S, Kim J, Kim S, Hong J, Cheong E, Kim KH, Bahn YS. 2017. The water channel protein aquaporin 1 regulates cellular metabolism and competitive fitness in a global fungal pathogen *Cryptococcus neoformans*. *Environmental Microbiology Reports* **9**: 268–278.

Muszevska A, Stepniewska-Dziubinska MM, Steczkiewicz K, Pawlowska J, Dzedzic A, Ginalski K. 2017. Fungal lifestyle reflected in serine protease repertoire. *Scientific Reports* **7**: 9147.

Pan X, Fan Z, Chen L, Liu C, Bai F, Wei Y, Tian Z, Dong Y, Shi J, Chen H, Jin Y, Cheng Z, Jin S, Lin J, Wu W. 2020. PvrA is a novel regulator that contributes to *Pseudomonas aeruginosa* pathogenesis by controlling bacterial utilization of long chain fatty acids. *Nucleic Acids Research* **48**: 5967–5985.

Pedrini N, Ortiz-Urquiza A, Huarte-Bonnet C, Fan Y, Juárez MP, Keyhani NO. 2015. Tenebrionid secretions and a fungal benzoquinone oxidoreductase form competing components of an arms race between a host and pathogen. *Proceedings of the National Academy of Sciences of the United States of America* **112**: E3651–E3660.

Petrasch S, Silva CJ, Mesquida-Pesci SD, Gallegos K, van den Abeele C, Papin V, Fernandez-Acero FJ, Knapp SJ, Blanco-Ulate B. 2019. Infection strategies deployed by *Botrytis cinerea*, *Fusarium acuminatum*, and *Rhizopus stolonifer* as a function of tomato fruit ripening stage. *Frontiers in Plant Science* **10**: 223.

Seidl MF, Van den Ackerveken GV. 2019. Activity and phylogenetics of the broadly occurring family of microbial Nep1-like proteins. *Annual Review of Phytopathology* **57**: 367–386.

Song Y, Li S, Zhao Y, Zhang Y, Lv Y, Jiang Y, Wang Y, Li D, Zhang H. 2019. ADH1 promotes *Candida albicans* pathogenicity by stimulating oxidative phosphorylation. *International Journal of Medical Microbiology* **309**: 151330.

Stergiopoulos I, Zwiers LH, De Waard MA. 2003. The ABC transporter MgAtr4 is a virulence factor of *Mycosphaerella graminicola* that affects colonization of substomatal cavities in wheat leaves. *Molecular Plant-Microbe Interactions* **16**: 689–698.

Valette-Collet O, Cimerman A, Reignault P, Levis C, Boccara M. 2003. Disruption of *Botrytis cinerea* pectin methylesterase gene *bcpme1* reduces virulence on several host plants. *Molecular Plant-Microbe Interactions* **16**: 360-367.

Xia X, Liu Y, Hodgson A, Xu D, Guo W, Yu H, She W, Zhou C, Lan L, Fu K, Vallance BA, Wan F. 2019. EspF is crucial for *Citrobacter rodentium*-induced tight junction disruption and lethality in immunocompromised animals. *PLoS Pathogens* **15**: e1007898.

Xu M, Gao X, Chen J, Yin Z, Feng H, Huang L. 2018. The feruloyl esterase genes are required for full pathogenicity of the apple tree canker pathogen *Valsa mali*. *Molecular Plant Pathology* **19**: 1353-1363.

Yun Y, Liu Z, Yin Y, Jiang J, Chen Y, Xu JR, Ma Z. 2015. Functional analysis of the *Fusarium graminearum* phosphatome. *The New Phytologist* **207**:119-134.

Zainudin NA, Condon B, De Bruyne L, Van Poucke C, Bi Q, Li W, Höfte M, Turgeon BG. 2015. Virulence, Host-Selective toxin production, and development of three *Cochliobolus* phytopathogens lacking the Sfp-Type 4'-Phosphopantetheinyl transferase Ppt1. *Molecular Plant-Microbe Interactions* **28**: 1130-1141.

Zeng Y, Charkowski AO. 2021. The role of ATP-binding cassette transporters in bacterial phytopathogenesis. *Phytopathology*, **111**: 600-610.

Zhang W, Li J, Tang Y, Chen K, Shi X, Ohnishi K, Zhang Y. 2017. Involvement of NpdA, a putative 2-nitropropane dioxygenase, in the T3SS expression and full virulence in *Ralstonia solanacearum* OE1-1. *Frontiers in Microbiology* **8**: 1990.

Supplementary Table 5. Putative pathogenicity functions inferred for 28 HGT candidates identified among *Phytophthora* spp.

	Ortho group	Putative function	Best hit on PHI-base (E-value) - Reference	Notes - Other reference(s)
HGT_1	OG5_134265	Endonuclease	PHI:5754, endonuclease, <i>Fusarium graminearum</i> (3.0E-024) - Yun et al. (2015)	-
HGT_2	OG5_126928_1	Xylulose reductase	PHI:2256, xylitol dehydrogenase, <i>Parastagonospora nodorum</i> (1.0E-128) - Lowe et al. (2008)	Oxidation of xylitol to xylulose; alters plant defense responses against aphids - MacWilliams et al. (2020) L-arabinose metabolism, degradation of hemicellulose - Dimarogona and Topakas (2016)
HGT_3	OG5_130201	Quinone oxidoreductase	No hit	Protection against oxidative stress in entomopathogenic fungi (Pedrini et al. 2015); Fungal protection against destructive host-produced quinones (Petrasch et al. 2019)
HGT_4	OG5_126615	Aquaporin	PHI:7047, water channel protein aquaporin, <i>Cryptococcus neoformans</i> (4.0E-012) - Meyers et al. (2017)	-
HGT_5	OG5_133138	NPP1	No hit	Necrosis-inducing <i>Phytophthora</i> protein - Seidl and Van den Ackerveken (2019)
HGT_6	OG5_177086	Phenol acid carboxylase	No hit	Upregulated expression during <i>Phytophthora cactorum</i> x strawberry interaction - Chen et al. (2011)
HGT_7	OG5_152798	Peptidase S9	No hit	Abundant in fungal plant pathogens - Muszewska et al. (2017)
HGT_8	OG5_144202	UDP-N-acetylglucosamine-peptide N-acetylglucosaminyltransferase	PHI:4921, flagellin glycosyltransferase, <i>Burkholderia cenocepacia</i> (1.0E-021) - Khodai-Kalaki et al. (2015)	-
HGT_9	OG5_140249	Alternative oxidase	No hit	-
HGT_10	OG5_139476	Dioxygenase	No hit	-
HGT_11	OG5_130394	Thioesterase	PHI:4988, sfp-type 4'-phosphopantetheinyl transferase, <i>Bipolaris maydis</i> (3.0E-005) - Zainudin et al. (2015)	-
HGT_12	OG5_135408	Endo-1,4-beta-xylanase	PHI:7912, endo-beta-1,4-xylanase <i>Phytophthora parasitica</i> (1.0E-137) - Lai and Liou, (2018)	-
HGT_13	OG5_126609	4-coumarate CoA ligase	PHI:10606, long-chain-fatty-acid-Co Aligase, <i>Pseudomonas aeruginosa</i> (1.0E-032) - Pan et al. (2020)	-
HGT_14	OG5_135743	2,4-dienoyl-CoA reductase	PHI:8134, 3-Oxoacyl-[acyl-carrier-protein] reductase, <i>Salmonella enterica</i> (1.0e-014) - Kwan et al. (2018)	-
HGT_15	OG5_126928_2	Zinc-binding dehydrogenase, Polyketide synthase, enoylreductase domain	PHI:8321, gluconate 5-dehydrogenase, <i>Salmonella enterica</i> (1.0E-016) - Alves Batista et al. (2018)	-
HGT_16	OG5_135419	Putative tannase	PHI:10222, feruloyl esterase, <i>Valsa mali</i> (4.0E-030) - Xu et al. (2018)	-
HGT_17	OG5_133550	Putative pectinesterase	PHI:278, pectin methylesterase, <i>Botrytis cinerea</i> (4.0E-077) - Valette-Collet et al. (2003)	-
HGT_18	OG5_223601	ATP-binding Cassette (ABC)	No hit	Putative virulence factor - Stergiopoulos et al. (2003); Zeng and Charkowski, (2021)
HGT_19	OG5_161673	Antibiotic biosynthesis monooxygenase	No hit	-
HGT_20	OG5_132142	Ribosomal-protein-alanine acetyltransferase	No hit	-
HGT_21	OG5_136477	Endoribonuclease	No hit	-
HGT_22	OG5_132299	Pectate lyase	PHI :4620, pectate lyase, <i>Phytophthora capsici</i> (1.0E-029) – Fu et al. (2015)	-
HGT_23	OG5_203245	Csa-calmodulin	No hit	-
HGT_24	OG5_126661	Mannitol-1-phosphate dehydrogenase	PHI:9524, Alcohol dehydrogenase, <i>Candida albicans</i> (4.0E-021)- Song et al. (2019)	-
HGT_25	OG5_137179	hypothetical protein	No hit	-
HGT_26	OG5_129399	2-nitropropane dioxygenase	No hit	Triggers expression of type III secretion system in <i>Ralstonia solanacearum</i> to induce pathogenicity on tobacco - Zhang et al. (2017)
HGT_27	ORTHOMCL13162	hypothetical protein	No hit	-
HGT_28	OG5_126721	type I methionyl aminopeptidase	PHI:9334, effector protein, <i>Citrobacter rodentium</i> (4.0E-020) - Xia et al. (2019)	-

References

- Alves Batista DF, de Freitas Neto OC, Maria de Almeida A, Maboni G, de Carvalho TF, de Carvalho TP, Barrow PA, Berchieri AJ. 2018. Evaluation of pathogenicity of *Salmonella gallinarum* strains harbouring deletions in genes whose orthologues are conserved pseudogenes in *S. pullorum*. *PLoS ONE* **13**: e0200585.
- Chen X, Klemsdal SS, Brurberg MB. 2011. Identification and analysis of *Phytophthora cactorum* genes up-regulated during cyst germination and strawberry infection. *Current Genetics* **57**:297-315.
- Dimarogona M, Topakas E. 2016. Chapter 12 - Regulation and heterologous expression of lignocellulosic enzymes in *Aspergillus*. In: *New and future developments in microbial biotechnology and bioengineering*. Elsevier, pp 171–190.
- Fu L, Zhu C, Ding X, Yang X, Morris PF, Tyler BM, Zhang X. 2015. Characterization of cell-death-inducing members of the pectate lyase gene family in *Phytophthora capsici* and their contributions to infection of pepper. *Molecular Plant-Microbe Interactions* **28**: 766-775.
- Khodai-Kalaki M, Andrade A, Mohamed YF, Valvano M. 2015. *Burkholderia cenocepacia* lipopolysaccharide modification and flagellin glycosylation affect virulence but not innate immune recognition in plants. *mBio* **6**: e00679-15.
- Kwan G, Plagenz B, Cowles K, Pisithkul T, Amador-Nogues D, Barak JD. 2018. Few differences in metabolic network use found between *Salmonella enterica* colonization of plants and typhoidal mice. *Frontiers in Microbiology* **9**: 695.
- Lai MY, Liou RF. 2018. Two genes encoding GH10 xylanases are essential for the virulence of the oomycete plant pathogen *Phytophthora parasitica*. *Current Genetics* **64**: 931–943.
- Lowe RG, Lord M, Rybak K, Trengove RD, Oliver RP, Solomon PS. 2008. A metabolomic approach to dissecting osmotic stress in the wheat pathogen *Stagonospora nodorum*. *Fungal Genetics and Biology* **45**: 1479-1486.
- MacWilliams JR, Dingwall S, Chesnais Q, Sugio A, Kaloshian I. 2020. AcDCXR is a cowpea aphid effector with putative roles in altering host immunity and physiology. *Frontiers in Plant Science* **11**: 605.
- Meyers GL, Jung KW, Bang S, Kim J, Kim S, Hong J, Cheong E, Kim KH, Bahn YS. 2017. The water channel protein aquaporin 1 regulates cellular metabolism and competitive fitness in a global fungal pathogen *Cryptococcus neoformans*. *Environmental Microbiology Reports* **9**: 268-278.
- Muszevska A, Stepniewska-Dziubinska MM, Steczkiewicz K, Pawlowska J, Dziedzic A, Ginalski K. 2017. Fungal lifestyle reflected in serine protease repertoire. *Scientific Reports* **7**: 9147.
- Pan X, Fan Z, Chen L, Liu C, Bai F, Wei Y, Tian Z, Dong Y, Shi J, Chen H, Jin Y, Cheng Z, Jin S, Lin J, Wu W. 2020. PvrA is a novel regulator that contributes to *Pseudomonas aeruginosa* pathogenesis by controlling bacterial utilization of long chain fatty acids. *Nucleic Acids Research* **48**: 5967–5985.
- Pedrini N, Ortiz-Urquiza A, Huarte-Bonnet C, Fan Y, Juárez MP, Keyhani NO. 2015. Tenebrionid secretions and a fungal benzoquinone oxidoreductase form competing components of an arms race between a host and pathogen. *Proceedings of the National Academy of Sciences of the United States of America* **112**: E3651–E3660.
- Petrasch S, Silva CJ, Mesquida-Pesci SD, Gallegos K, van den Abeele C, Papin V, Fernandez-Acero FJ, Knapp SJ, Blanco-Ulate B. 2019. Infection strategies deployed by *Botrytis cinerea*, *Fusarium acuminatum*, and *Rhizopus stolonifer* as a function of tomato fruit ripening stage. *Frontiers in Plant Science* **10**: 223.
- Seidl MF, Van den Ackerveken GV. 2019. Activity and phylogenetics of the broadly occurring family of microbial Nep1-like proteins. *Annual Review of Phytopathology* **57**: 367–386.
- Song Y, Li S, Zhao Y, Zhang Y, Lv Y, Jiang Y, Wang Y, Li D, Zhang H. 2019. ADH1 promotes *Candida albicans* pathogenicity by stimulating oxidative phosphorylation. *International Journal of Medical Microbiology* **309**: 151330.
- Stergiopoulos I, Zwiers LH, De Waard MA. 2003. The ABC transporter MgAtr4 is a virulence factor of *Mycosphaerella graminicola* that affects colonization of substomatal cavities in wheat leaves. *Molecular Plant-Microbe Interactions* **16**: 689-698.
- Valette-Collet O, Cimerman A, Reignault P, Levis C, Boccara M. 2003. Disruption of *Botrytis cinerea* pectin methylesterase gene bcpme1 reduces virulence on several host plants. *Molecular Plant-Microbe Interactions* **16**: 360-367.
- Xia X, Liu Y, Hodgson A, Xu D, Guo W, Yu H, She W, Zhou C, Lan L, Fu K, Vallance BA, Wan F. 2019. EspF is crucial for *Citrobacter rodentium*-induced tight junction disruption and lethality in immunocompromised animals. *PLoS Pathogens* **15**: e1007898.
- Xu M, Gao X, Chen J, Yin Z, Feng H, Huang L. 2018. The feruloyl esterase genes are required for full pathogenicity of the apple tree canker pathogen *Valsa mali*. *Molecular Plant Pathology* **19**: 1353-1363.
- Yun Y, Liu Z, Yin Y, Jiang J, Chen Y, Xu JR, Ma Z. 2015. Functional analysis of the *Fusarium graminearum* phosphatome. *The New Phytologist* **207**:119-134.
- Zainudin NA, Condon B, De Bruyne L, Van Poucke C, Bi Q, Li W, Höfte M, Turgeon BG. 2015. Virulence, Host-Selective toxin production, and development of three *Cochliobolus* phytopathogens lacking the Sfp-Type 4'-Phosphopantetheinyl transferase Ppt1. *Molecular Plant-Microbe Interactions* **28**: 1130-1141.
- Zeng Y, Charkowski AO. 2021. The role of ATP-binding cassette transporters in bacterial phytopathogenesis. *Phytopathology*, **111**: 600-610.
- Zhang W, Li J, Tang Y, Chen K, Shi X, Ohnishi K, Zhang Y. 2017. Involvement of NpdA, a putative 2-nitropropane dioxygenase, in the T3SS expression and full virulence in *Ralstonia solanacearum* OE1-1. *Frontiers in Microbiology* **8**: 1990.